Information theory approaches in Sun-Earth's relations

Simon Wing
The Johns Hopkins University

Outline

1. Information theory: mutual information, conditional mutual information, and transfer entropy

2. Three applications

   2.1 Radiation belt dynamics

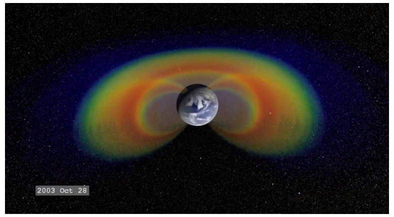

   2.2 Solar dynamo

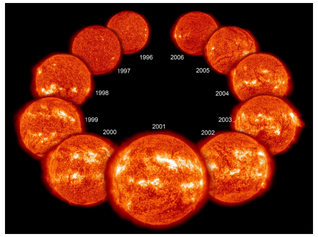

   2.3 Radio waves at Saturn

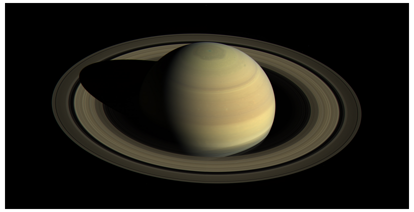

3. Summary

Dependence between two variables

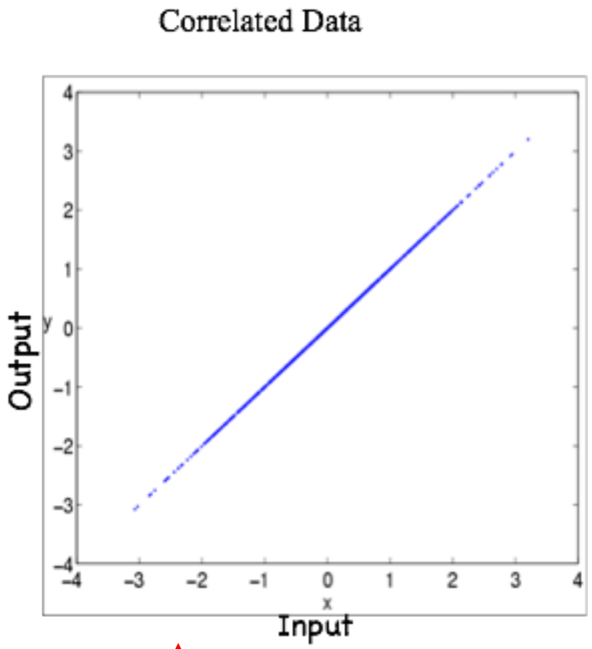

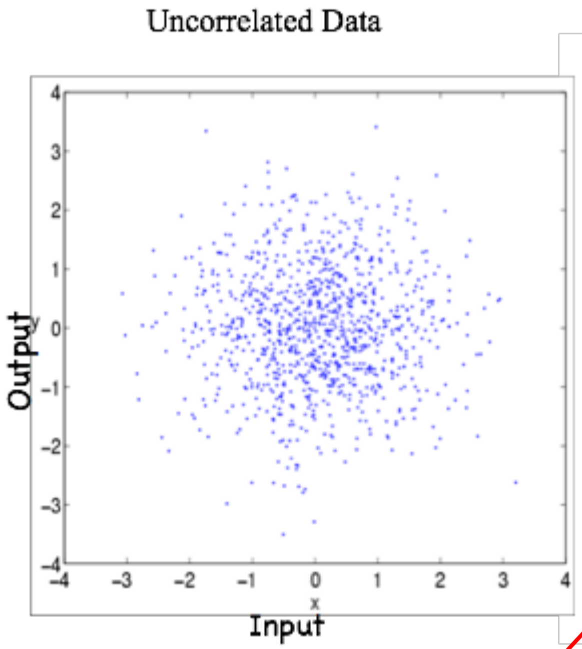

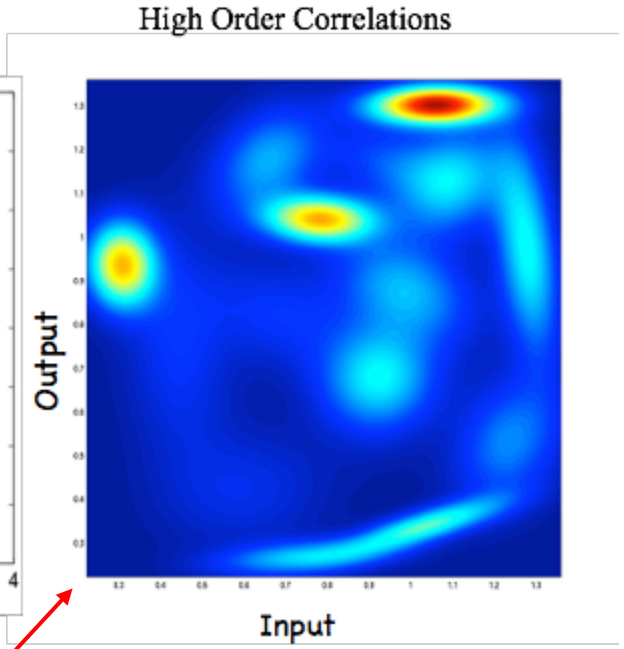

standard correlational analysis can characterize the relationship

standard correlational analysis would be inadequate

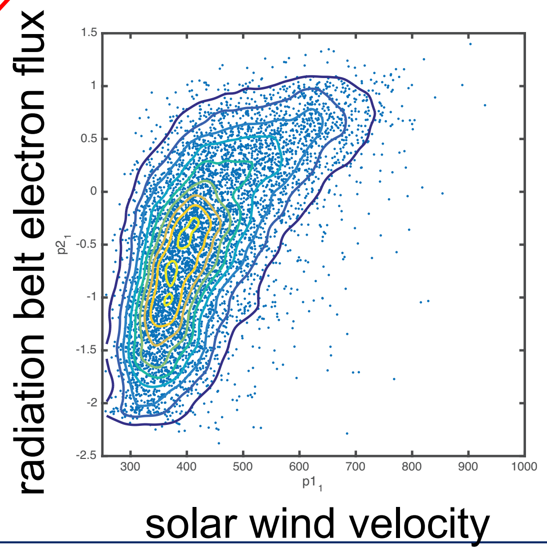

Information theory

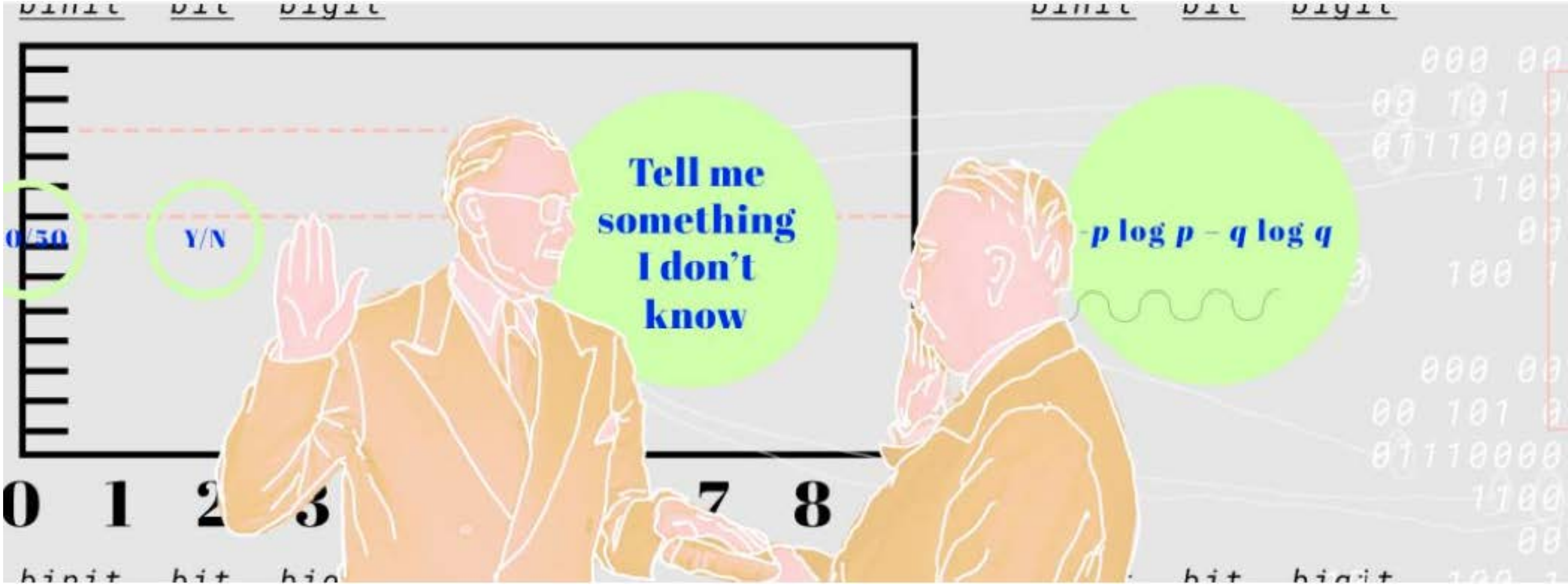

mutual information

Suppose that two variables x and y are binned so that they take on discrete values $\hat{x}$ and $\hat{y}$

$$x \in \{\hat{x}_1, \hat{x}_2, \cdots, \hat{x}_n\} \equiv \aleph_1; \;\; y \in \{\hat{y}_1, \hat{y}_2, \cdots, \hat{y}_m\} \equiv \aleph_2$$

The variables may be thought of as letters in alphabets $\aleph_1$ and $\aleph_2$, which have n and m letters

The entropy associated with each of the variables is defined as

$$H(x) = -\sum_{\aleph_1} p(\hat{x}) \log p(\hat{x})$$

$$H(y) = -\sum_{\aleph_2} p(\hat{y}) \log p(\hat{y})$$

where p($\hat{x}$) is the probability of finding the word $\hat{x}$ in the set of x-data and p($\hat{y}$) is the probability

of finding word $\hat{y}$ in the set of *y*-data

entropy gives a measure of the amount of information in a variable/set
(measure of disorder/uncertainty)

Shannon entropy

(Luis Serrano)

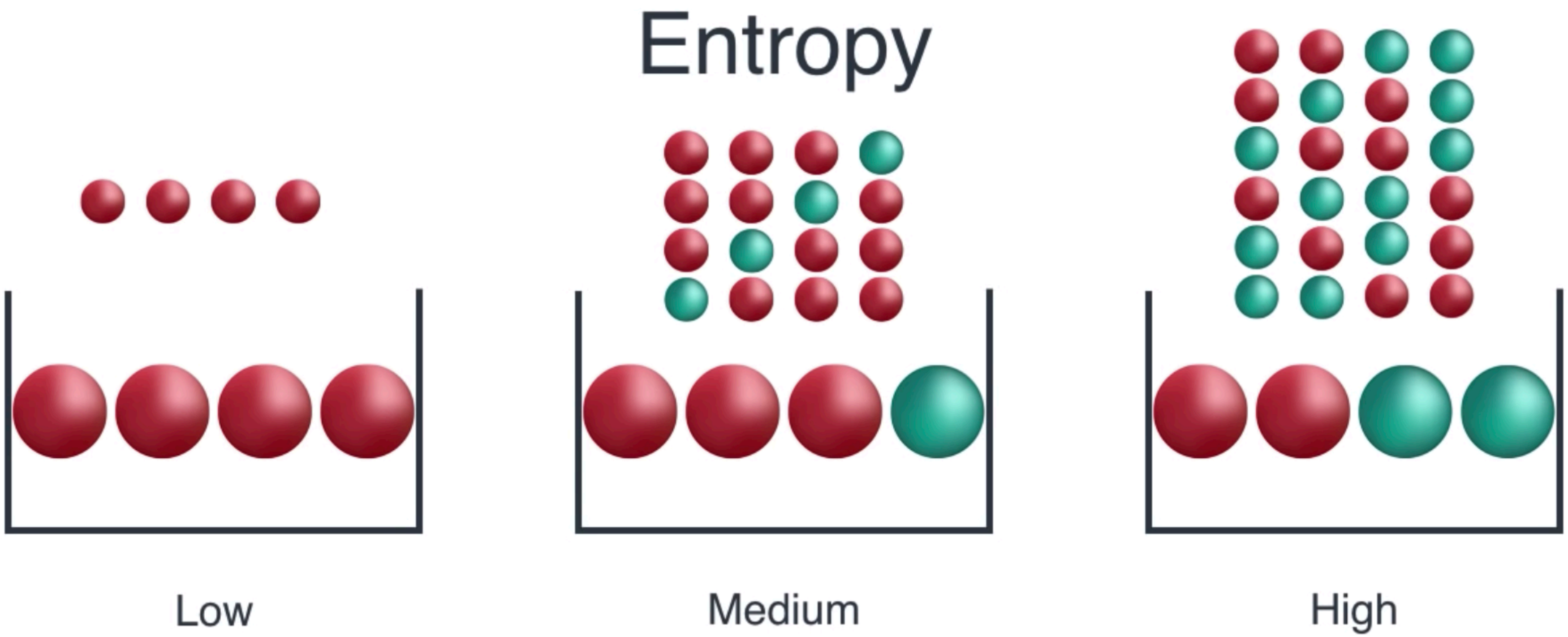

mutual information

The joint entropy is defined by

$$H(x,y) = -\sum_{\aleph_1 \aleph_2} p(\hat{x},\hat{y}) \log p(\hat{x},\hat{y})$$

where $p(\hat{x},\hat{y})$ is the probability of finding the word combination $(\hat{x},\hat{y})$ in the set of (x, y) data

The mutual information: MI (x, y) = H (x) + H (y) − H (x, y)

MI is useful to identify nonlinear dependence between two variables [Tsonis, 2001]

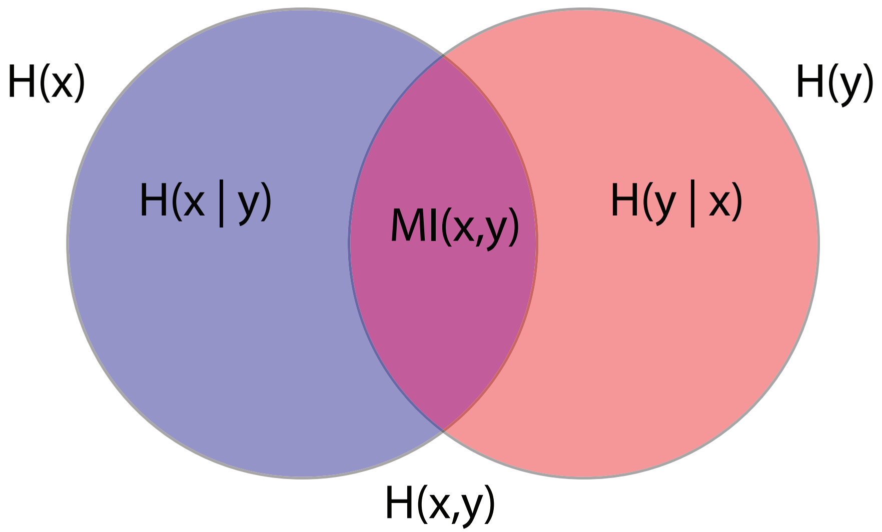

MI(x,y) = information that x and y share

MI(x, y) = 0 iff x and y are independent

MI(x,y) = H(x) = H(y) if knowing x determines y

Mutual Information is computed on pairs of attributes or variables

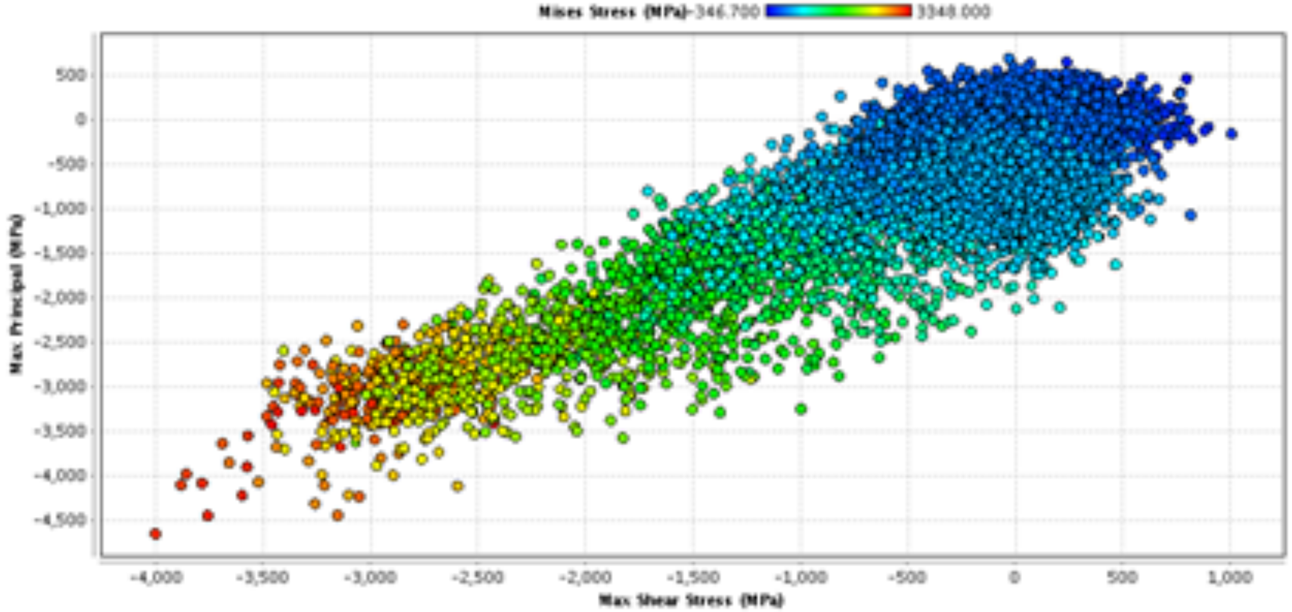

Mutual Information calculates that probability of knowing the y-value when the x-value is given.

Mutual Information Example

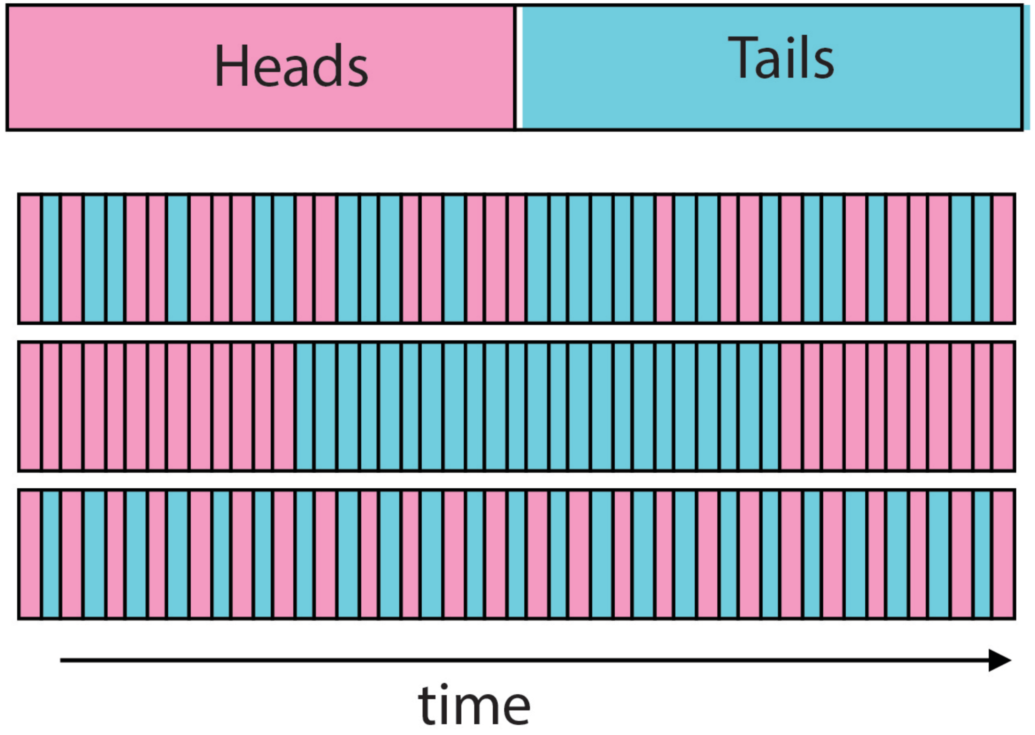

P_h	P_t	P_{hh}	P_{ht}	P_{th}	P_{tt}	MI
1/2	1/2	10/46	12/46	12/46	12/46	.004
1/2	1/2	22/46	1/46	1/46	22/46	0.82
1/2	1/2	0	1/2	1/2	0	1.0

Same distributions, different mutual information!

Mutual information vs. Pearson and Spearman correlation

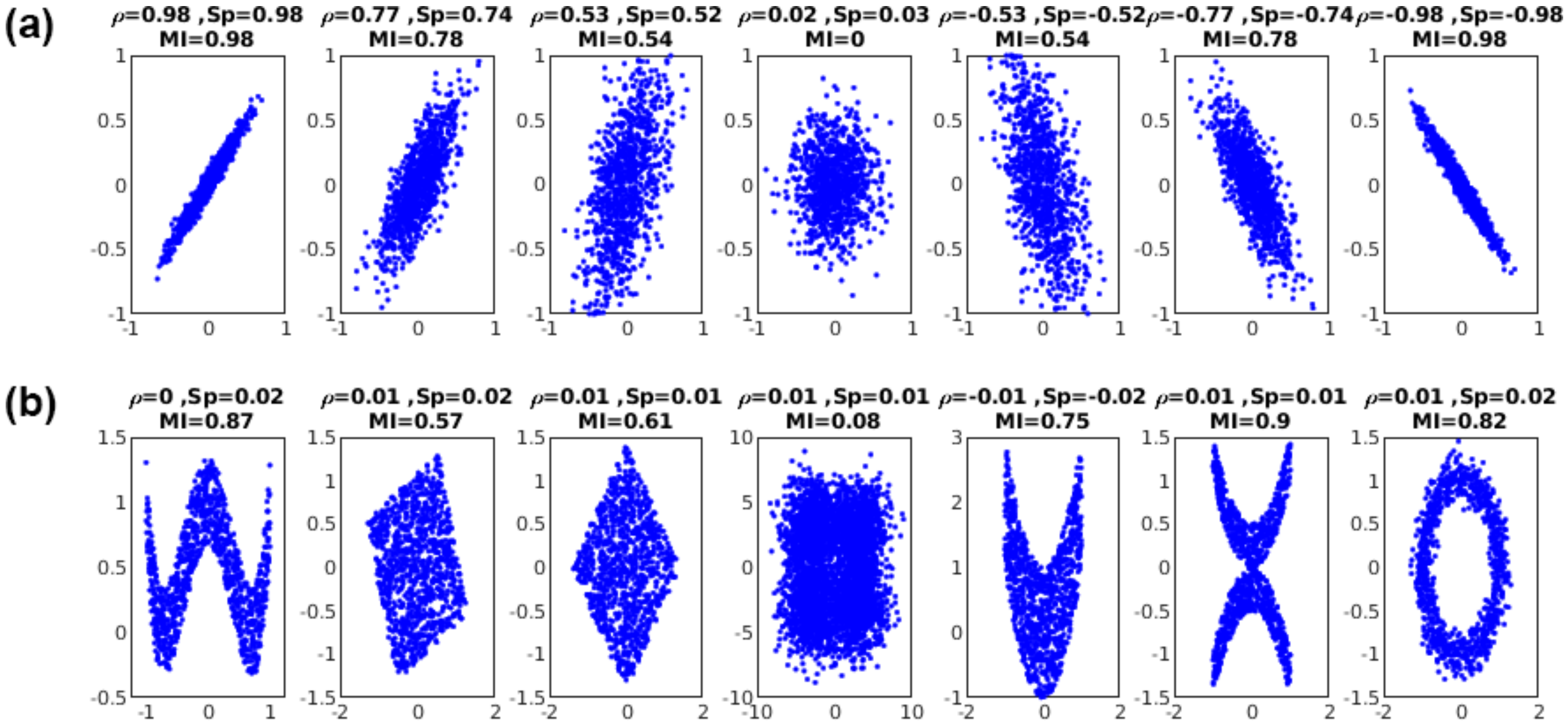

P = pearson correlation (linear relationship)
Sp = Spearman correlation (monotonic relationship)
MI = mutual information (linear and nonlinear relationship)

conditional mutual information

conditional mutual information (CMI) [Wyner, 1978] :

$$\mathrm{CMI}(x,\, y \mid z) = \sum_{\aleph_1\aleph_2\aleph_3} p(\hat{x}, \hat{y}, \hat{z}) \log \frac{p(\hat{x},\ \hat{y} \mid \hat{z})}{p(\hat{x} \mid \hat{z})\, p(\hat{y} \mid \hat{z})} = \mathrm{H}(x,z) + \mathrm{H}(y,z) - \mathrm{H}(x,y,z) - \mathrm{H}(z)$$

CMI(x, y | z) determines the mutual information between *x* and *y* given that *z* is known

if *z* is unrelated or random, CMI(*x*,*y* |*z*) = MI(*x*,*y*)

if *x* or *y* is known based on *z*, then CMI(*x*,*y* |*z*) = 0

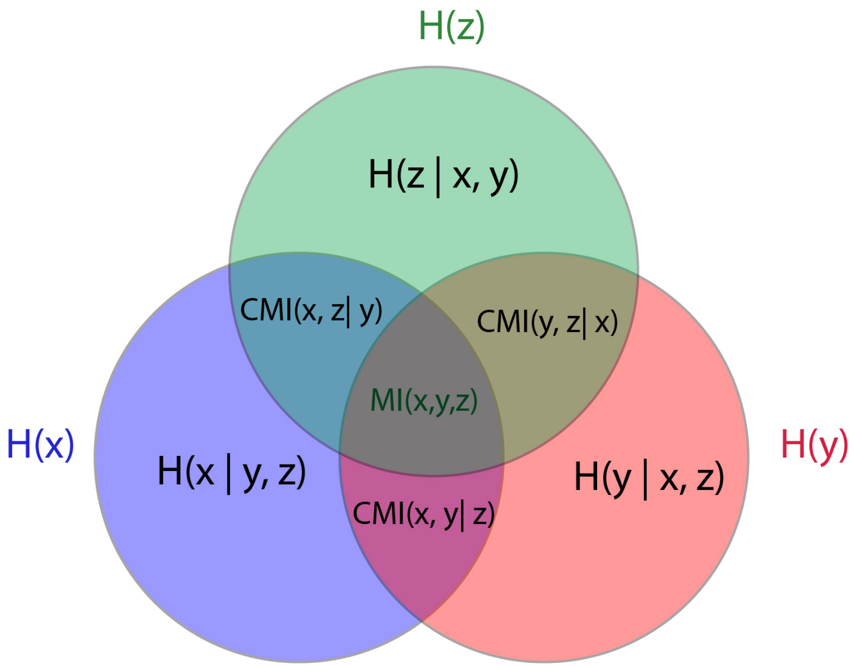

An example of CMI: RB electron response to Vsw, nsw, and solar wind pdyn

(a)

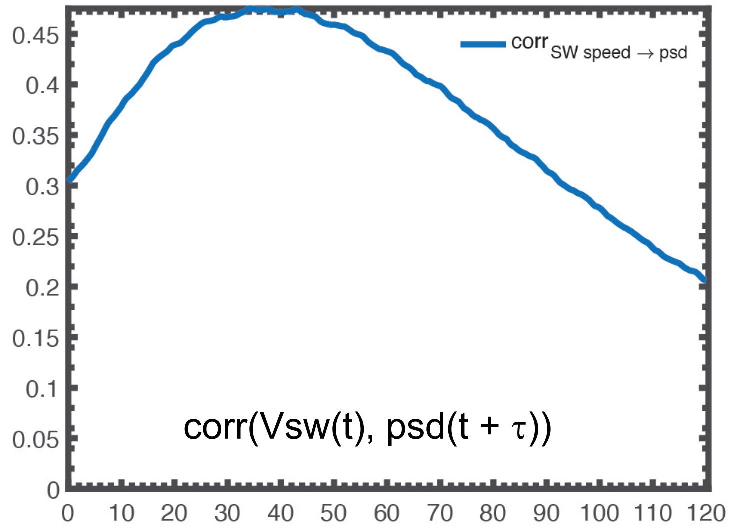

(b)

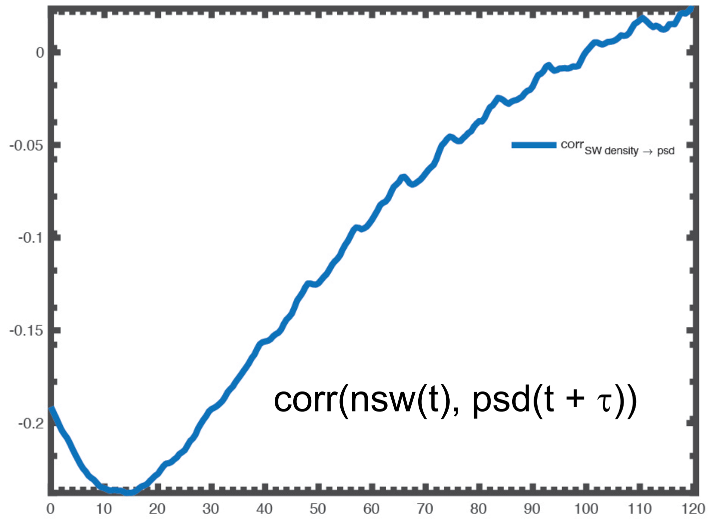

RBSP MagEIS data
2013–2018
~1 MeV electrons

(c)

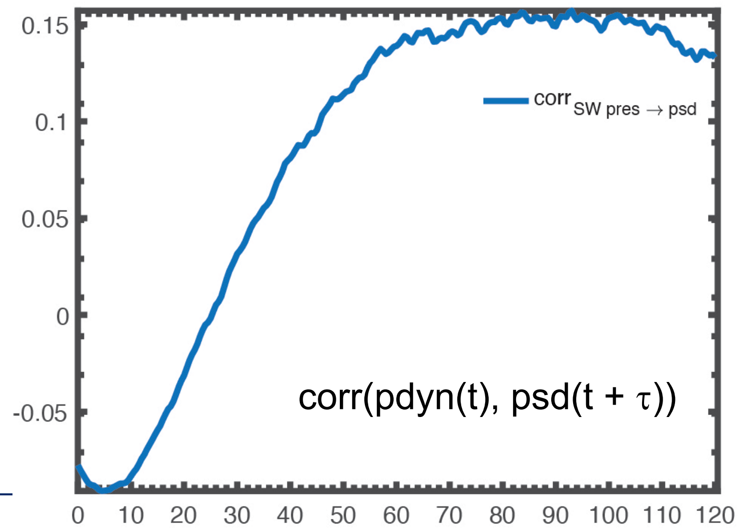

(d)

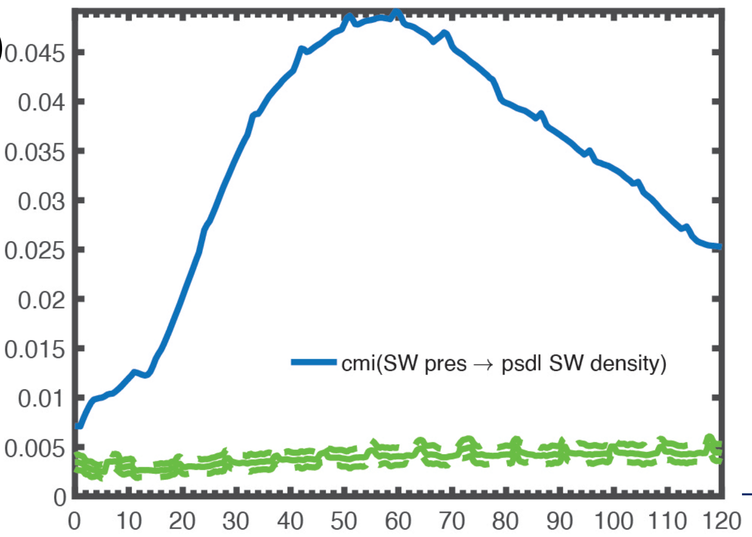

SW dynamic pres ~ nV^2

transfer entropy

A common method to establish causal-relationships between two time series, e.g., $[x_t]$ and $[y_t]$, is to use a time-shifted correlation function

$$r(\tau) = \frac{\langle x_t \, y_{t+\tau} \rangle - \langle x \rangle \langle y \rangle}{\sqrt{\langle x^2 \rangle - \langle x \rangle^2} \, \sqrt{\langle y^2 \rangle - \langle y \rangle^2}}$$

where r = correlation coefficient and τ = lag time

The results may not be clear if x and y have multiple peaks

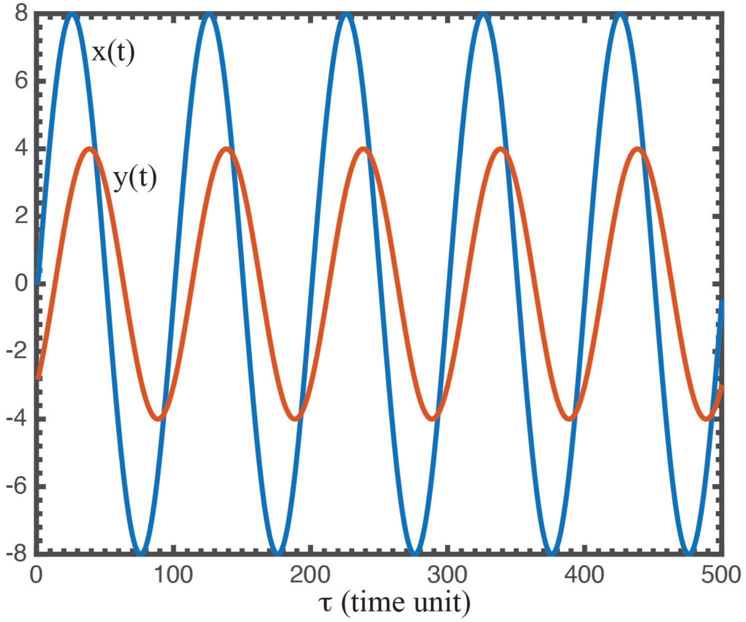

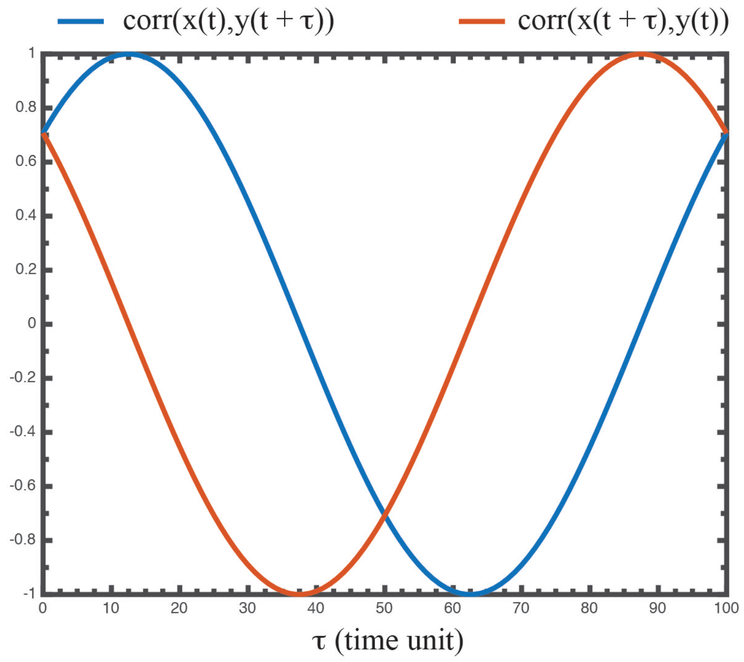

transfer entropy

A better alternative is to use transfer entropy [Schreiber, 2000]

$$TE_{x\to y}(\tau) = \sum_t p(y_{t+\tau}, yp_t,\ x_t)\ \log\left(\frac{p(y_{t+\tau}\mid yp_t,\ \ x_t)}{p(y_{t+\tau}\mid yp_t)}\right)$$

$yp_t = [y_t,\ y_{t-\Delta}, \cdots, y_{t-k\Delta}]$, $k+1$ = dimensionality of the system, and Δ = first minimum in MI

TE($x \rightarrow y$) gives a measure of how much additional information x provides in predicting the future of y beyond the degree to which y already predicts its own future

TE can be considered a special case of CMI

$$TE_{x\to y}(\tau) = CMI(y(t+\ \tau), x(t)|yp(t))$$

if no information flow from x to y, TE($x \rightarrow y$) = 0

unlike correlation, TE($x \rightarrow y$) ≠ TE($y \rightarrow x$)

TE reduces to Granger causality in a linear system

Granger causality and transfer entropy

Granger causality principles (Granger, 1969; 1980):

- The cause occurs prior to its effect.
- The cause has *unique* information about the future values of its effect.

Relationship to transfer entropy

- X (Granger) causes Y if, in an appropriate statistical sense, X assists in predicting the future of Y beyond the degree to which Y already predicts its own future (Granger, 1969; Barrett et al., 2009)
- Transfer entropy reduces to Granger causality in a linear system
- Granger causality is pragmatic, well defined, and has delivered many insights into the functional connectivity of systems in a variety of fields (Ding et al., 2006, Set and Edelman, 2007, Cadotte et al., 2008).

Transfer entropy

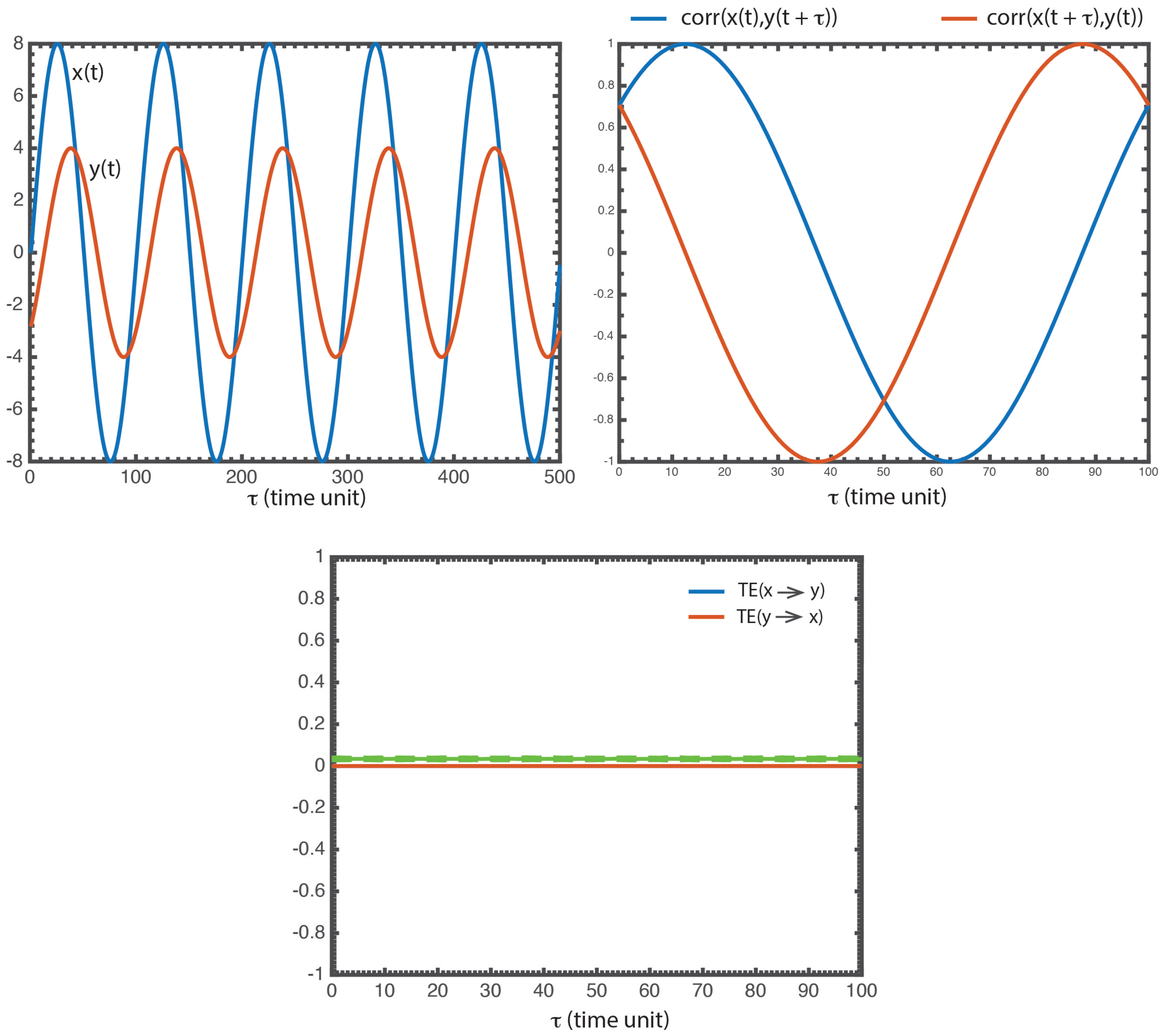

Radiation belt dynamics

1. Radiation belt dynamics

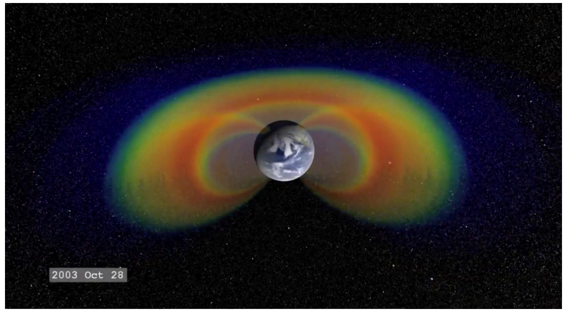

2. Solar dynamo

3. Radio waves at Saturn

Magnetosphere

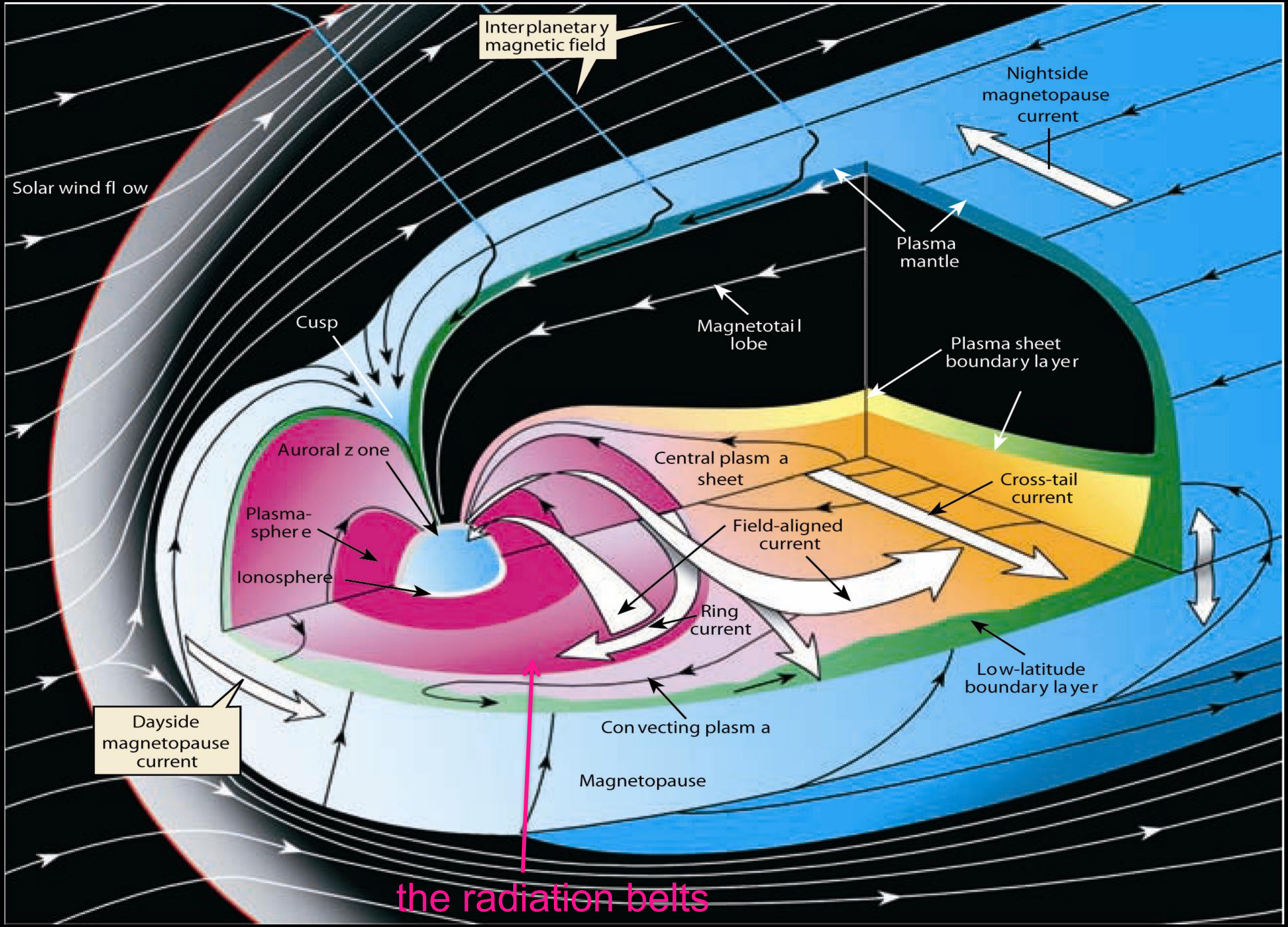

- radiation belts are highly variable
- to a large extent, solar wind controls the radiation belt variability
- it is not always clear which solar wind parameter plays the most dominant role

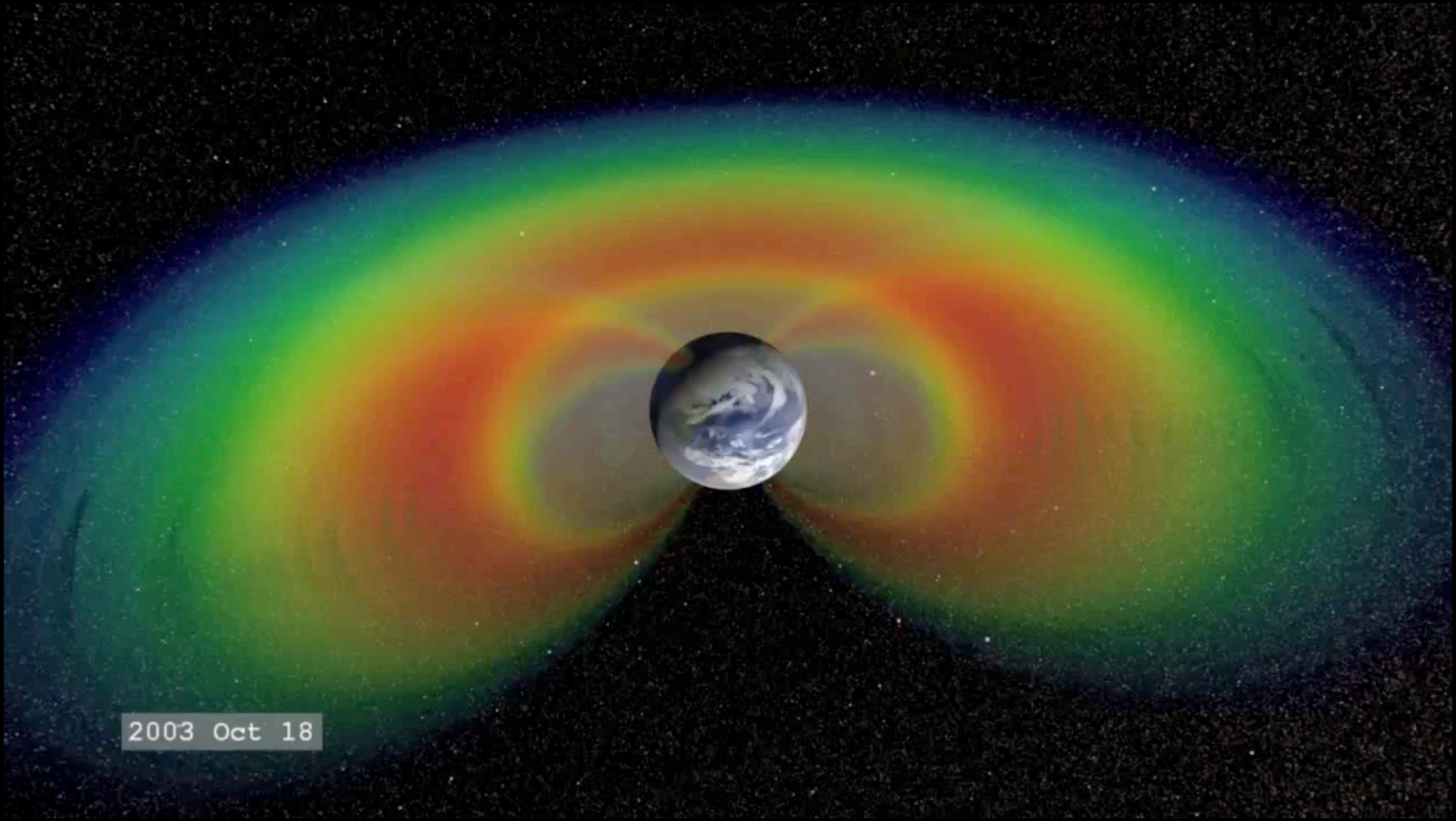

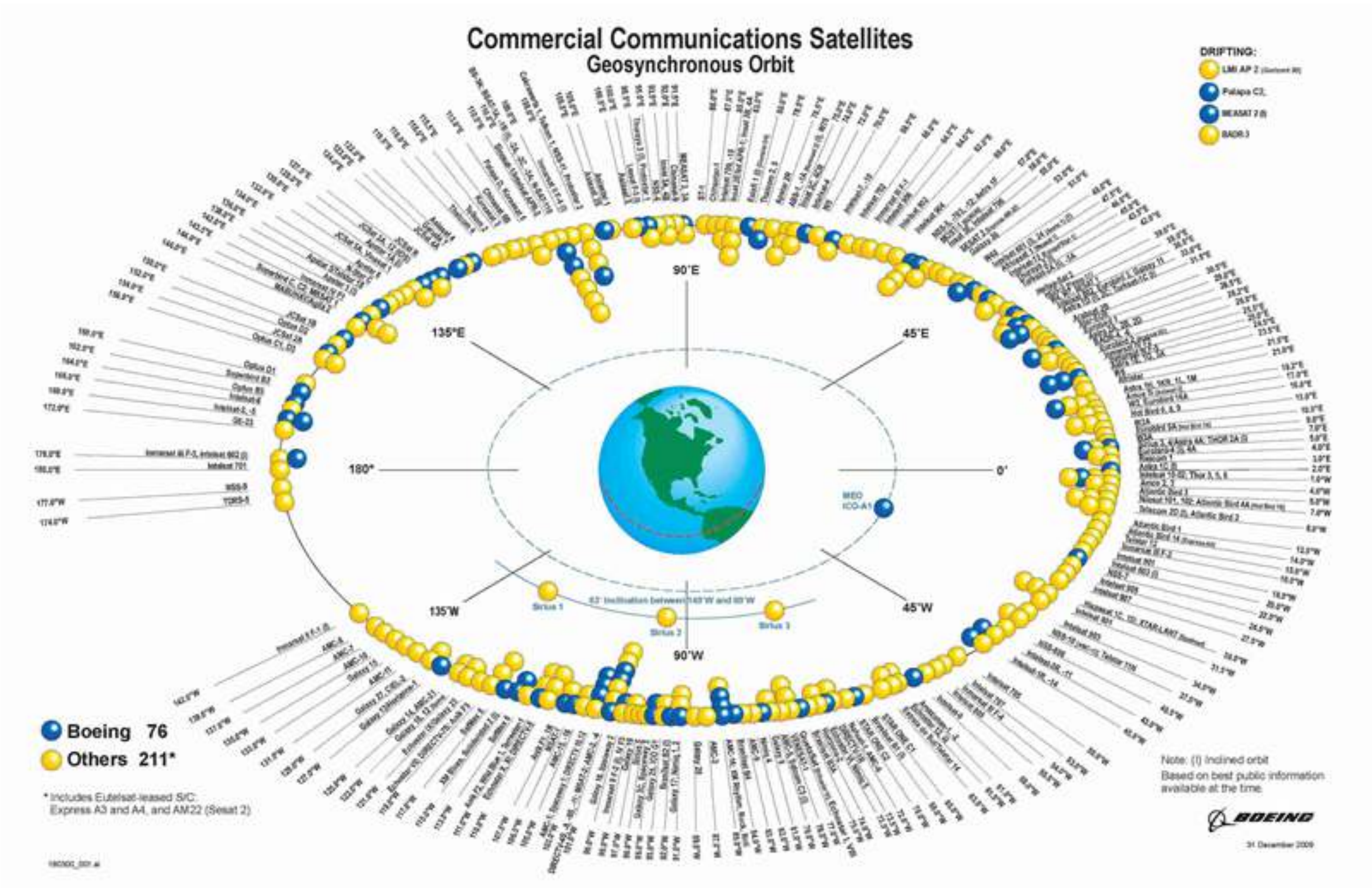

Commercial Communications Satellites
Geosynchronous Orbit
DRIFTING:
90°E
135°E
45°E
180°
0°
135°W
90°W
45°W
Sirius 1
Sirius 2
Sirius 3
Boeing 76
Others 211*
* Includes Eutelsat-leased S/C:
Express A3 and A4, and AM22 (Sesat 2)
Note: (I) Inclined orbit
Based on best public information available at the time.
BOEING

Space weather risks at geosynchronous orbit

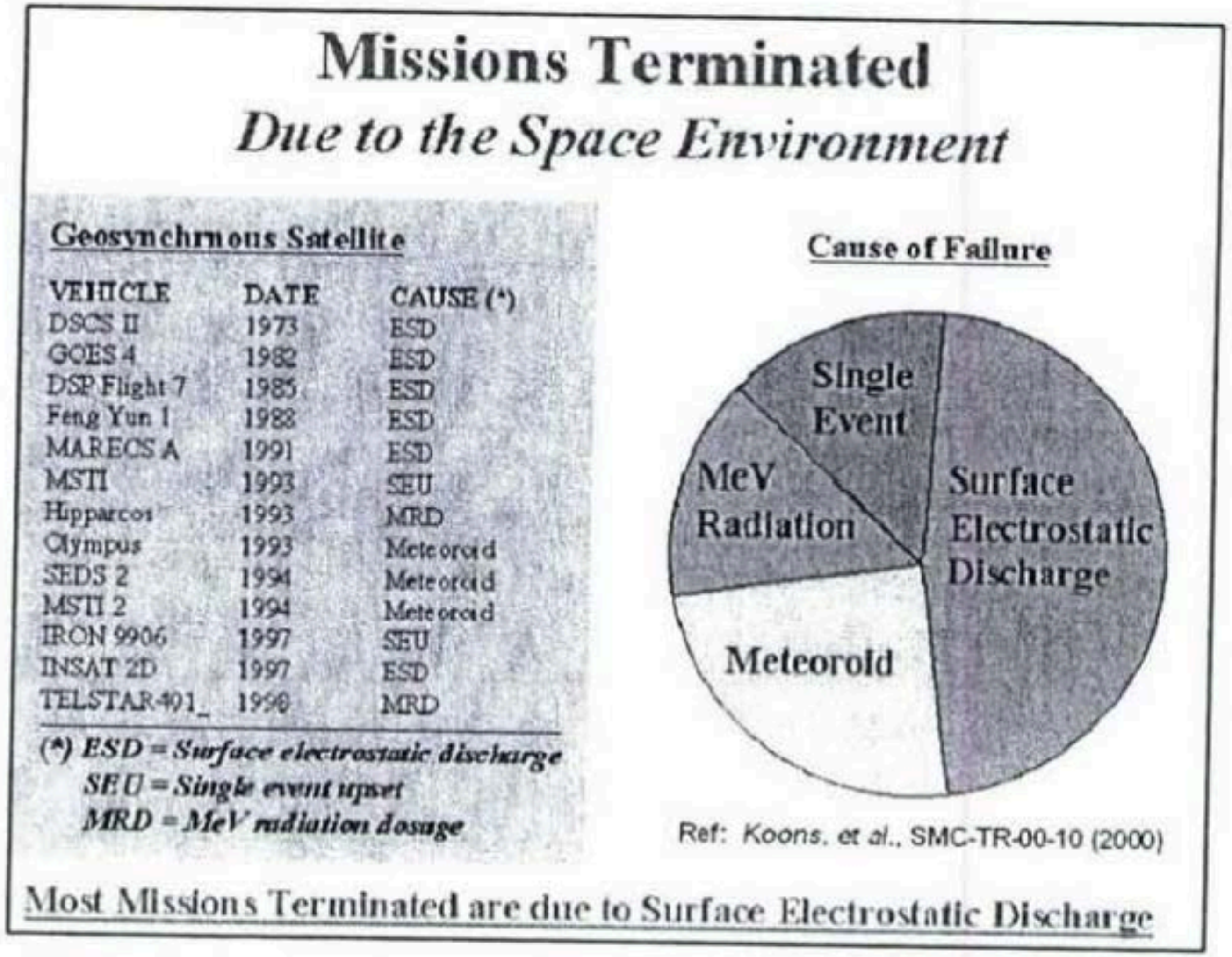

Missions Terminated
Due to the Space Environment

Geosynchronous Satellite

VEHICLE	DATE	CAUSE (*)
DSCS II	1973	ESD
GOES 4	1982	ESD
DSP Flight 7	1985	ESD
Feng Yun 1	1988	ESD
MARECS A	1991	ESD
MSTI	1993	SEU
Hipparcos	1993	MRD
Olympus	1993	Meteoroid
SEDS 2	1994	Meteoroid
MSTI 2	1994	Meteoroid
IRON 9906	1997	SEU
INSAT 2D	1997	ESD
TELSTAR 401	1998	MRD

(*) *ESD = Surface electrostatic discharge*
SEU = Single event upset
MRD = MeV radiation dosage

Ref: Koons, et al., SMC-TR-00-10 (2000)

Most Missions Terminated are due to Surface Electrostatic Discharge

- many geosynchronous satellites have terminated/died

Data set

- LANL geosynchronous satellite data 1989 – 2009
  - electrons with energy range 1.8–3.5 MeV
  - daily resolution: diurnal, MLT, lat-long dependences are reduced
  - Reeves et al. [2011] (ftp://ftop.agu.org/apend/ja/2010ja0157535)

- OMNI solar wind data at daily and hourly resolution
  - NASA OMNIweb (http://omniweb.gsfc.nasa.gov)

- Merged LANL and OMNI data set has 6438 data points

radiation belt electron flux vs. V_{sw}

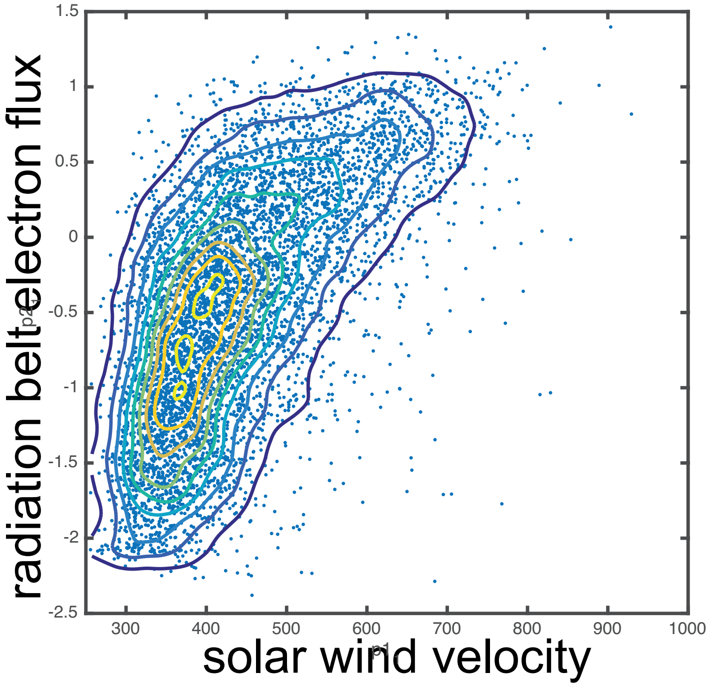

- solar wind – radiation belt system is nonlinear (linear correlational analysis would be inadequate)

RB MeV J_e vs. V_{sw}

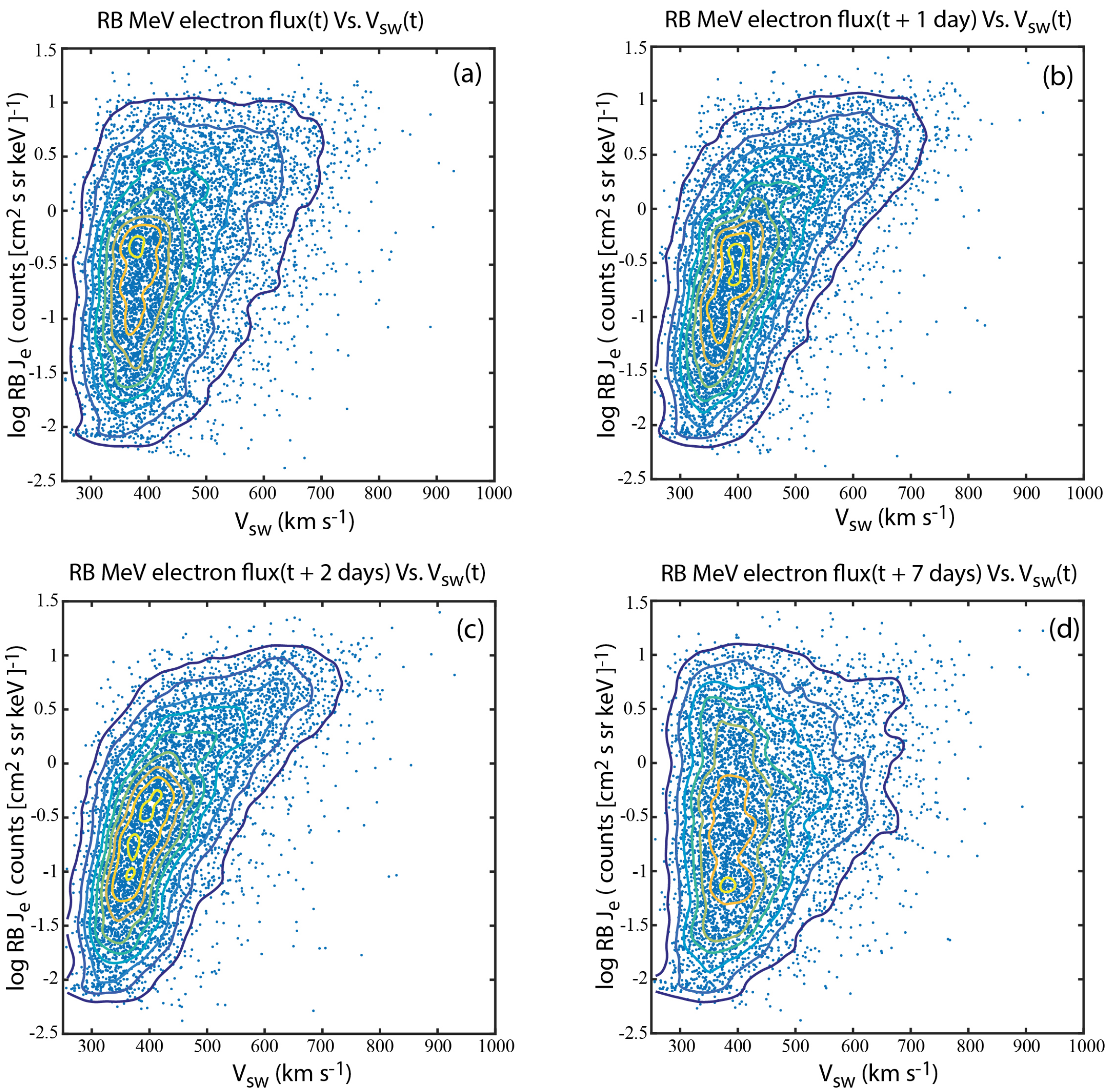

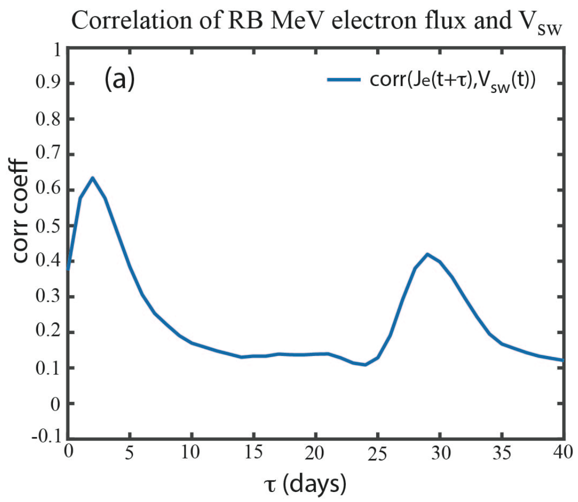

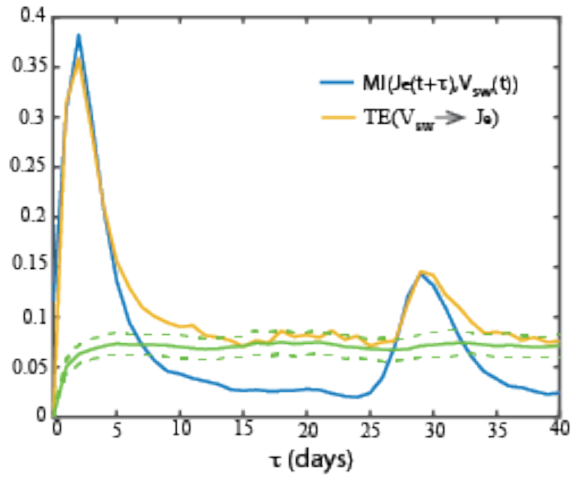

Transfer of information from $V_{sw} \rightarrow$ RB J_e peaks at τ = 2 days

J_e = electron flux

RB MeV J_e vs. n_{sw}

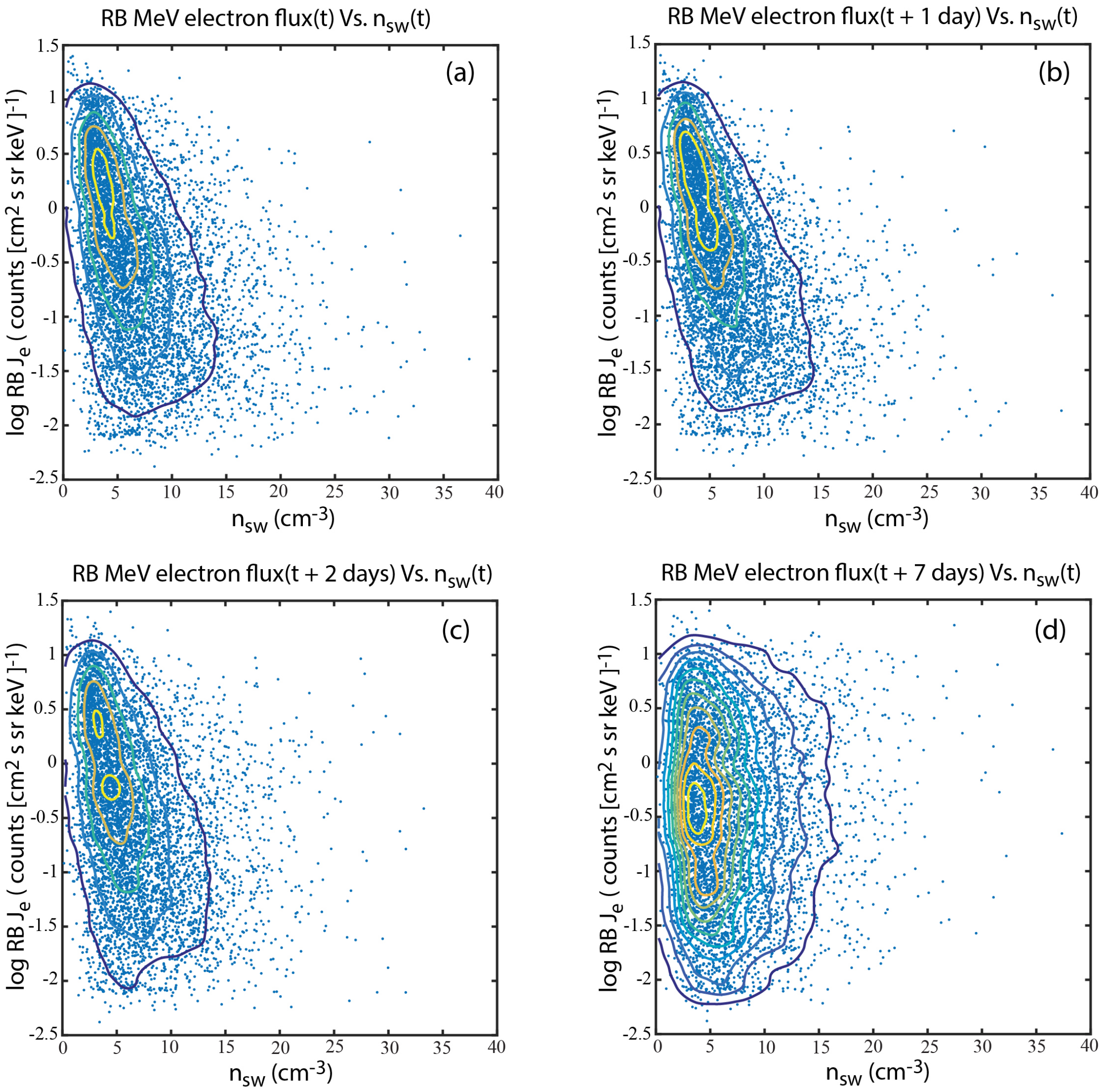

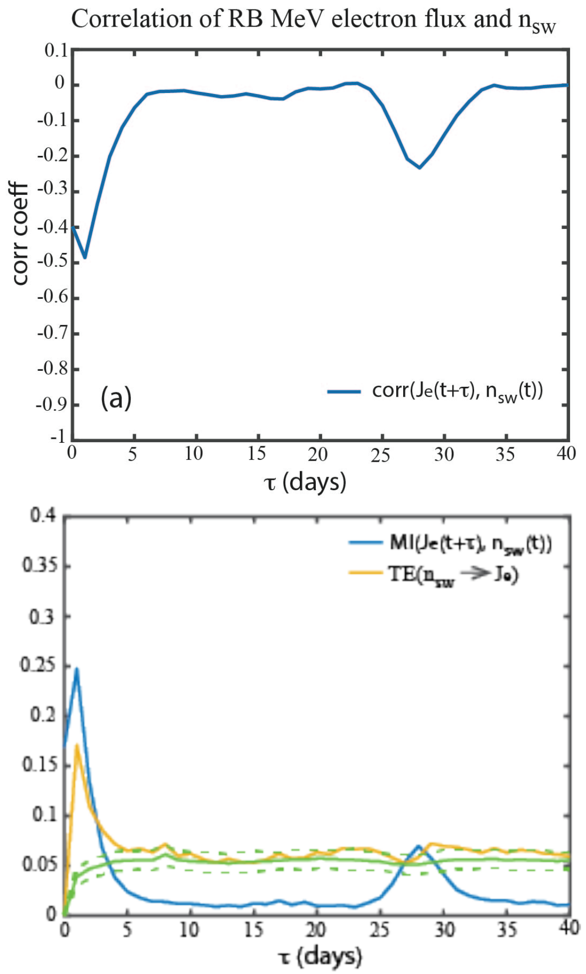

Transfer of information from $n_{sw} \rightarrow$ RB J_e peaks at τ = 1 day

n_{sw} vs. V_{sw}

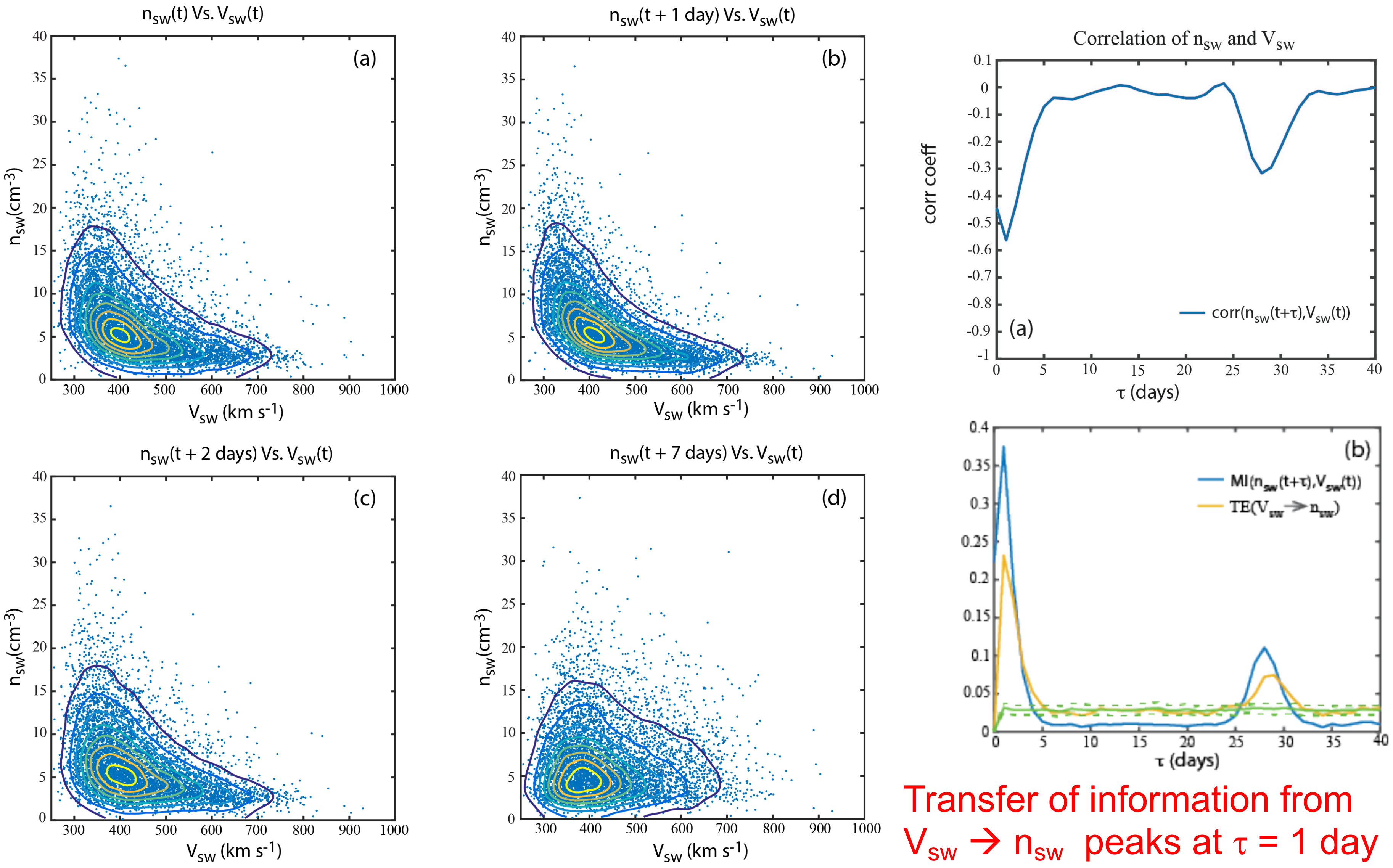

Transfer of information from $V_{sw} \rightarrow n_{sw}$ peaks at τ = 1 day

Summary

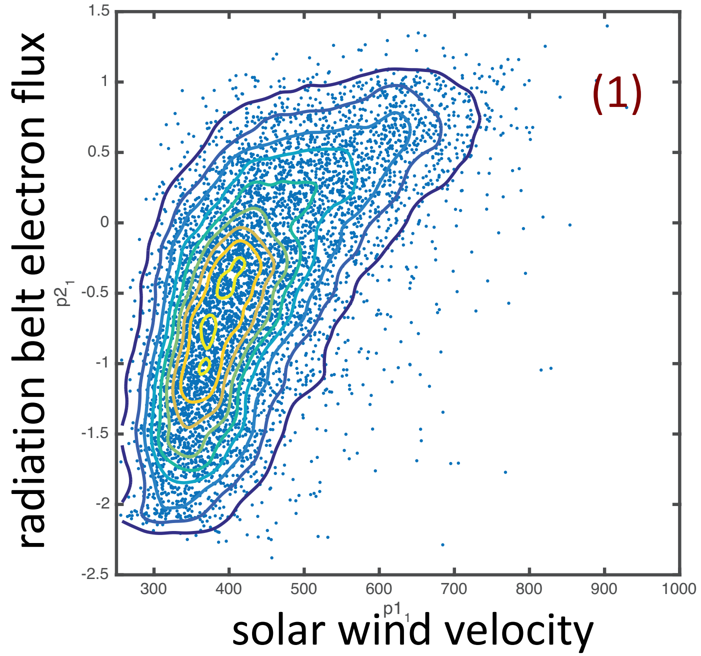

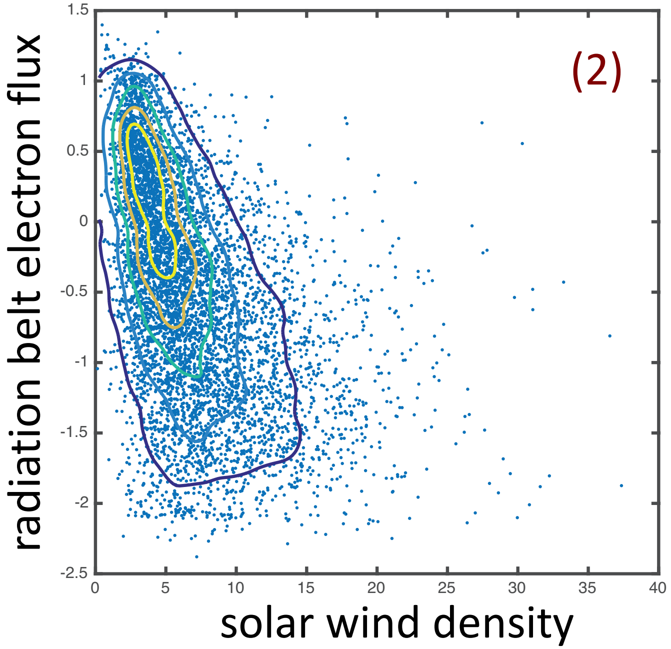

Wing et al., 2016

LANL daily resolution data 1989-2009
1.8-3.5 MeV

OMNI solar wind data

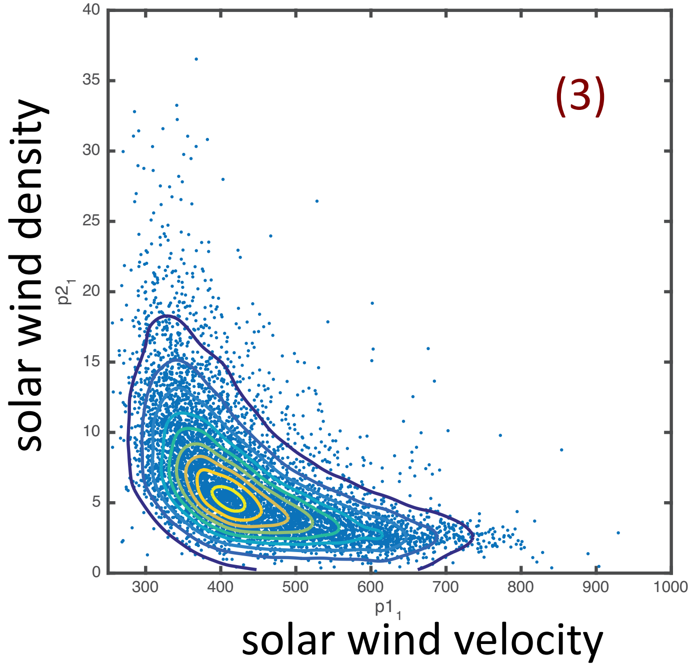

1. corr(V_{sw} (t),RB Je (t+τ), τ_{max} = 2 days, corr > 0
2. corr(n_{sw} (t), RB Je(t+ τ), τ_{max} = 1 day, corr < 0
3. But, corr(V_{sw}n(t), n_{sw}(t +τ)), τ_{max} = 1 day, corr < 0

- Is (1) or (2) just a coincidence?
- Is it possible that V_{sw} and n_{sw} can independently exert influence on radiation belt? If that is the case, how do we separate the effect of V_{sw} from n_{sw}?

Input-Output problem

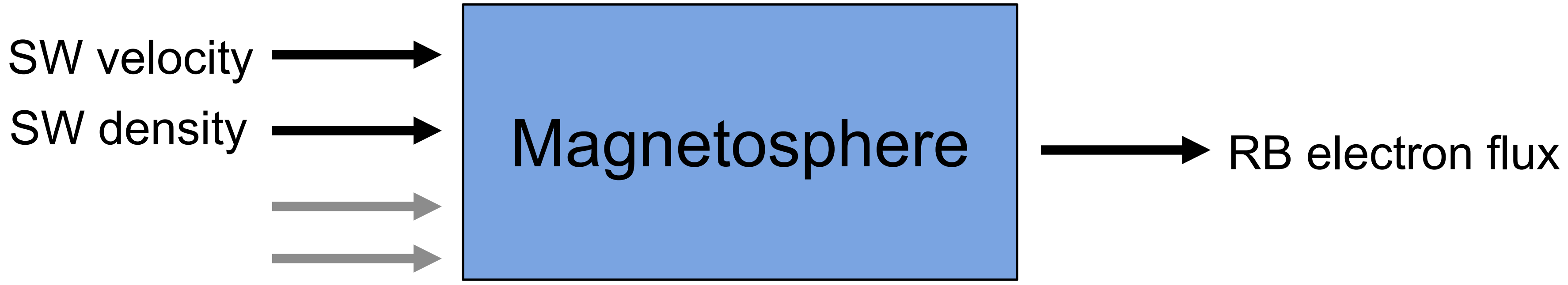

CMI can separate the effect of V_{sw} from n_{sw} and vice versa

Wing et al., 2016

peak at τ = 0 day

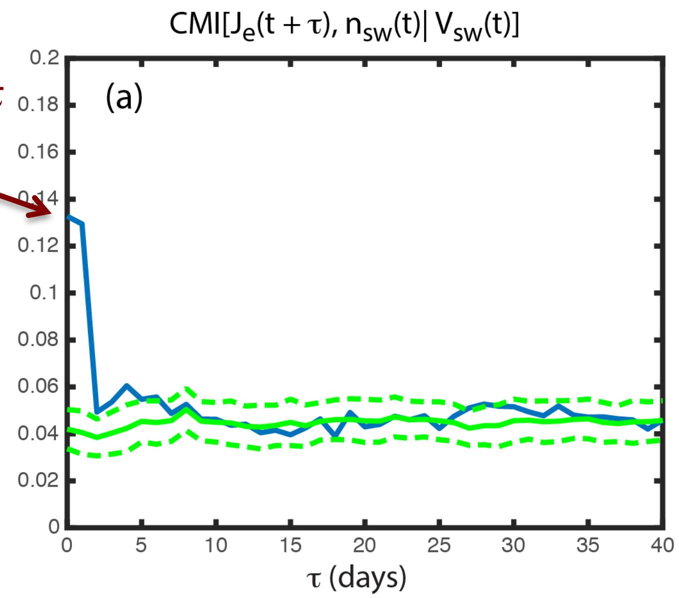

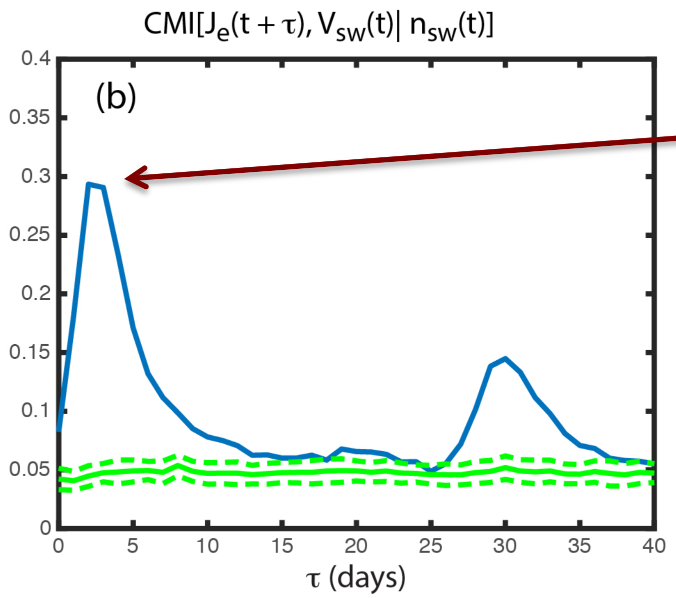

broad peak at τ = 2-3 days

LANL daily resolution data 1989-2009 1.8-3.5 MeV

OMNI solar wind data

peak at τ = 1 day

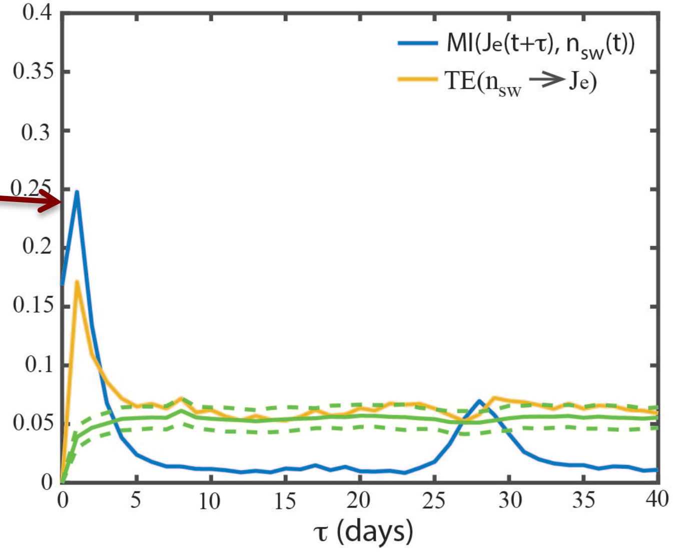

narrow peak at τ = 2 days

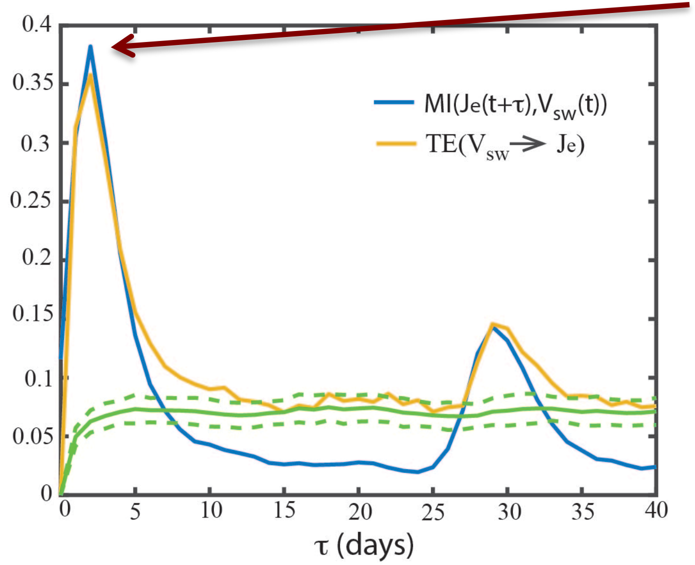

CMI can separate the effect of V_{sw} from n_{sw} and vice versa

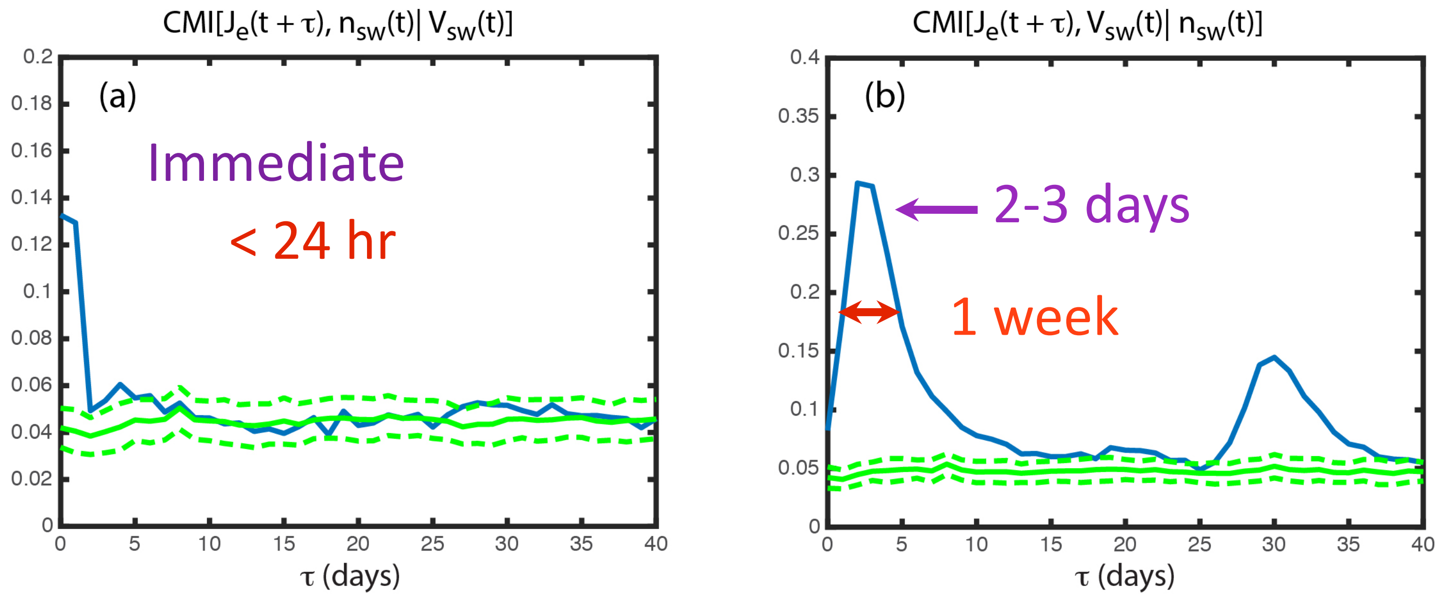

V_{sw} transfers ~2.7 times more information to RB electrons than n_{sw} does

CMI[Je(t + 0), n_{sw}(t) | V_{sw}(t)] –
CMI[Je(t + 0), sur[n_{sw}(t)] | V_{sw}(t)] = 0.09

"magnetopause shadowing" [Li et al., 2001, Shprits et al., 2006, Ukhorskiy et al., 2006]

CMI[Je(t + 2), V_{sw}(t) | n_{sw}(t)] –
CMI[Je(t + 2), sur[V_{sw}(t)] | n_{sw}(t)] = 0.25

- acceleration caused by ULF waves generated at magnetopause by KHI [Reeves et al., 2007]
- "local acceleration" caused by VLF waves during particle injections [Summers et al., 1998; Horne et al., 2005]

Magnetosphere

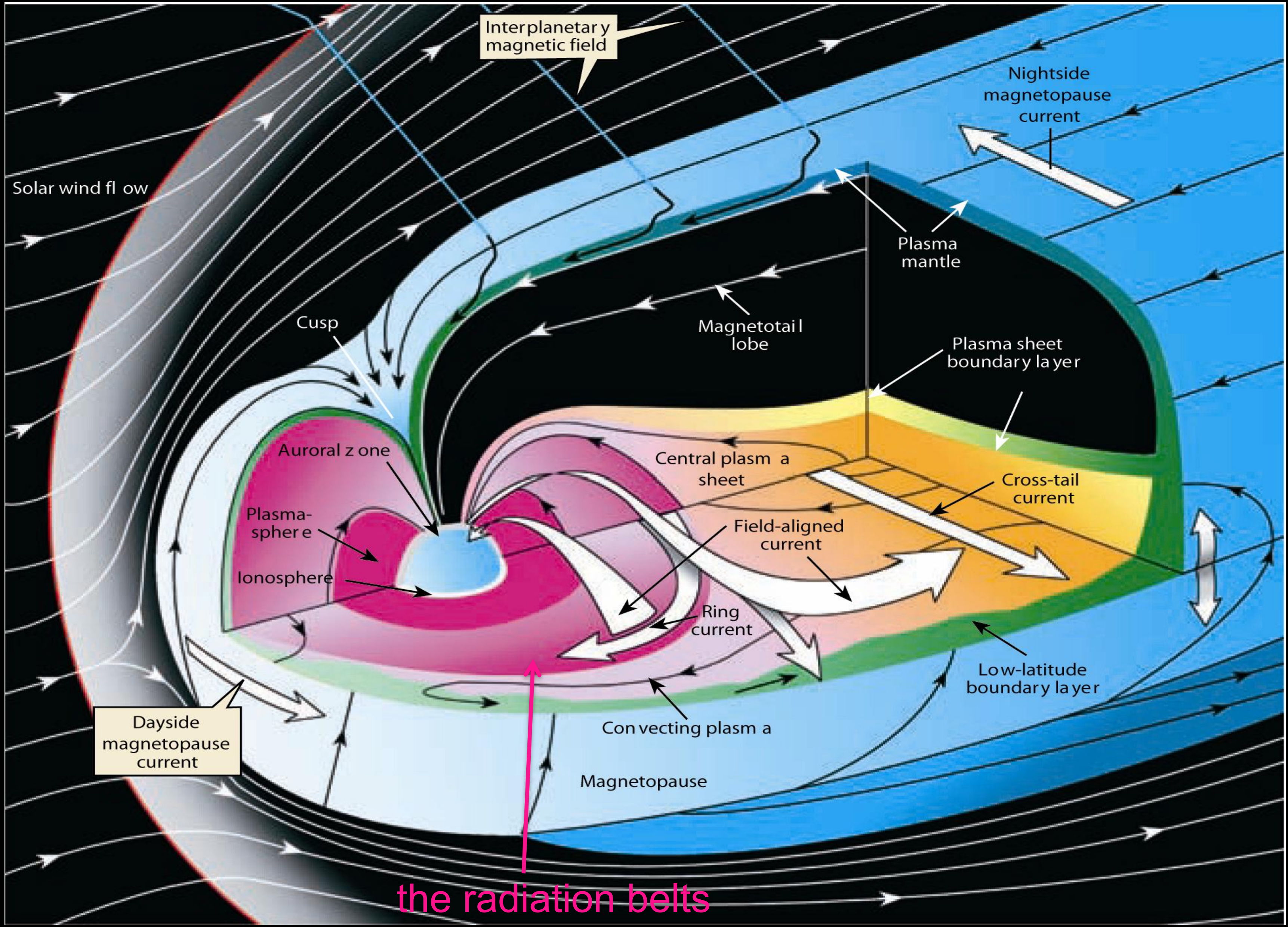

The triangle distribution is well ordered by Transfer Entropy(TE)

RB MeV J_e(t + 2 days) vs. V_{sw}(t)

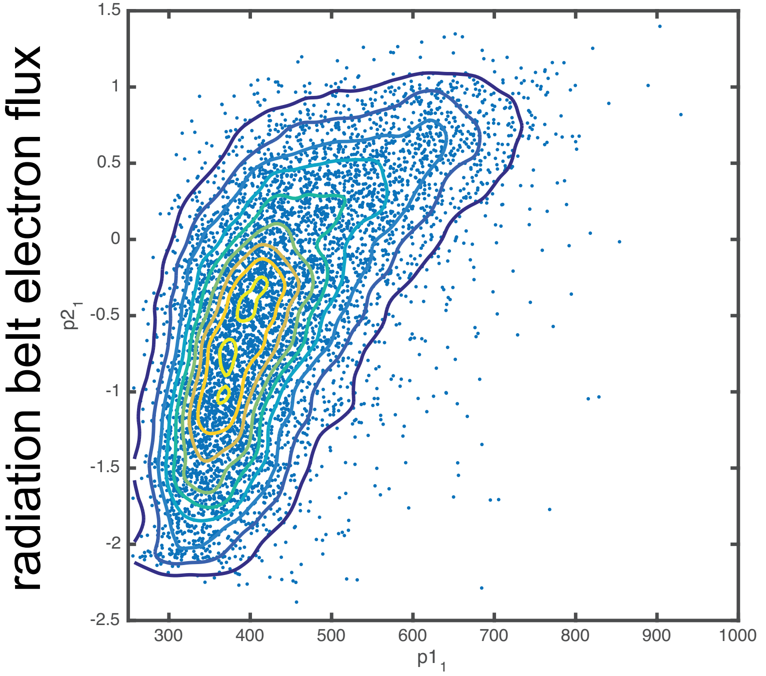

solar wind velocity

- Triangle distribution problem was first posed by Reeves et al. [2011]
- why is there such a huge variability when solar wind velocity is low?

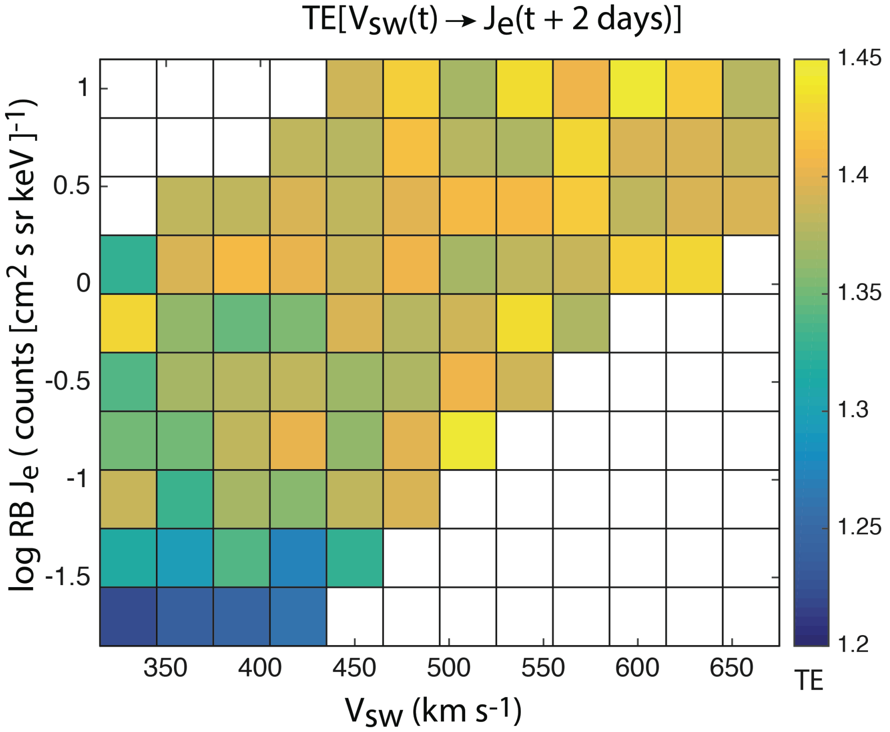

High RB Je corresponds to high TE and vice versa

RB Je lags both Vsw and nsw by 2 days

But, from the CMI analysis, RB Je response to nsw should have **0 day** lag

solar wind density effect on the triangle distribution

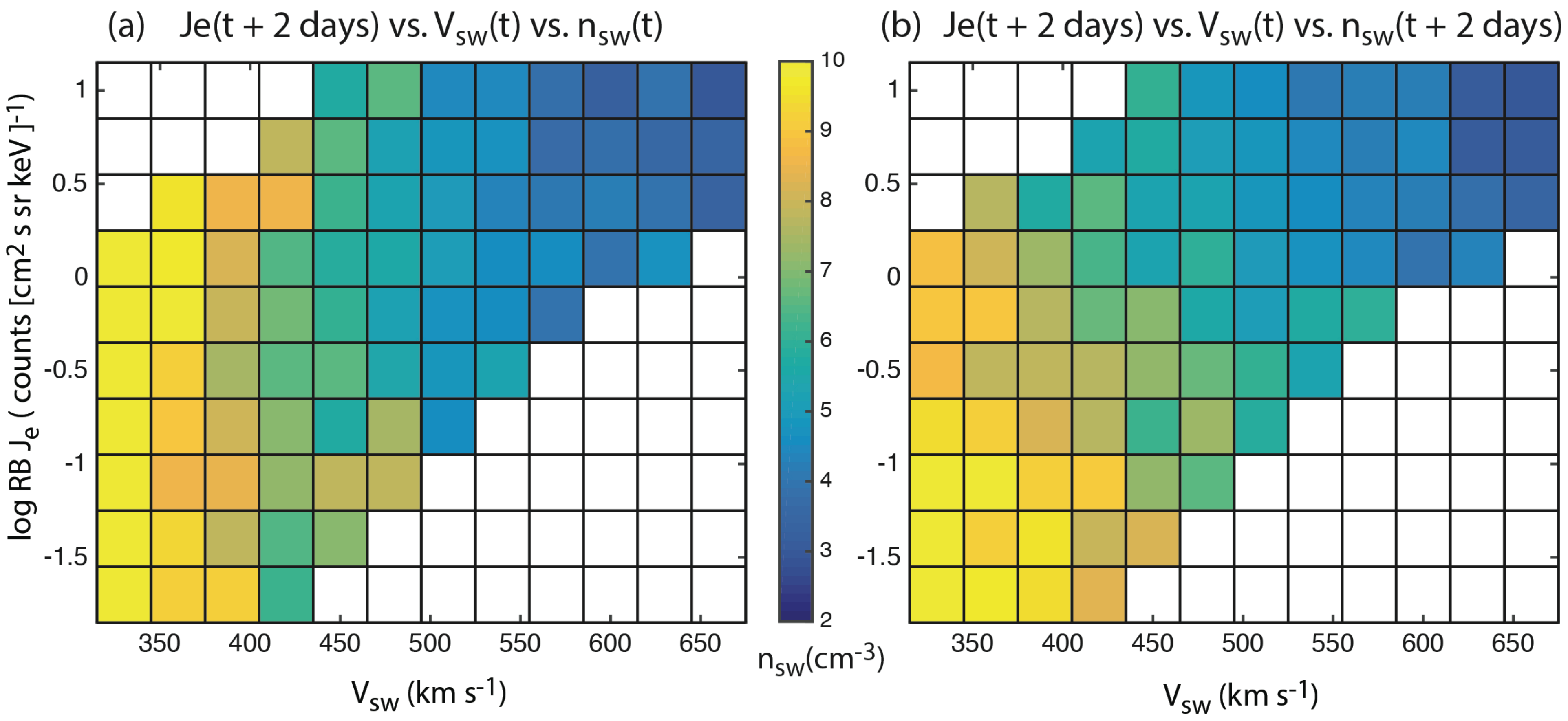

density gradient in the X direction

because n_{sw} anticorrelates with V_{sw}

density gradient in the X and Y directions

high n_{sw} (or Pdyn) → low RB J_e
and vice versa

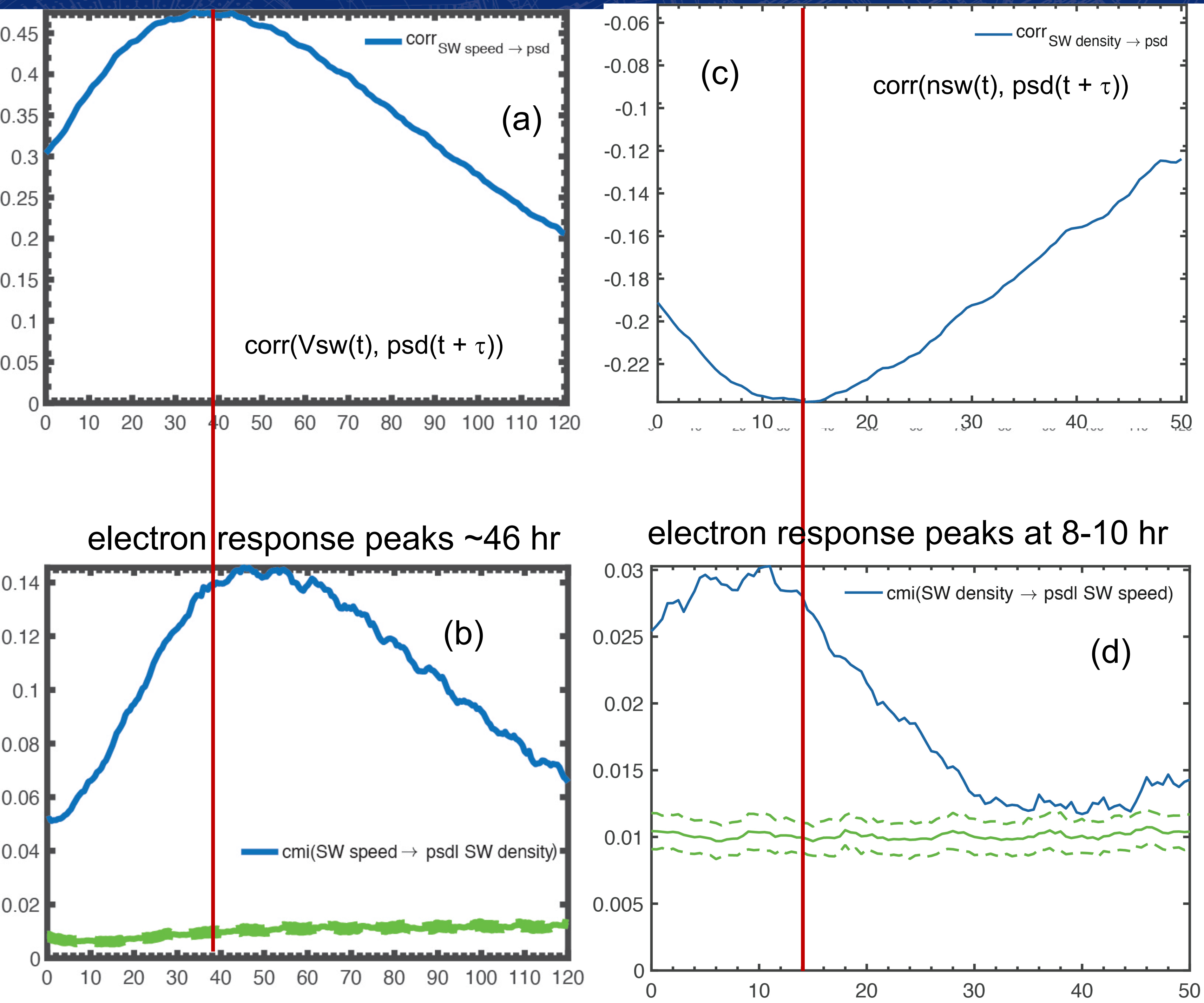

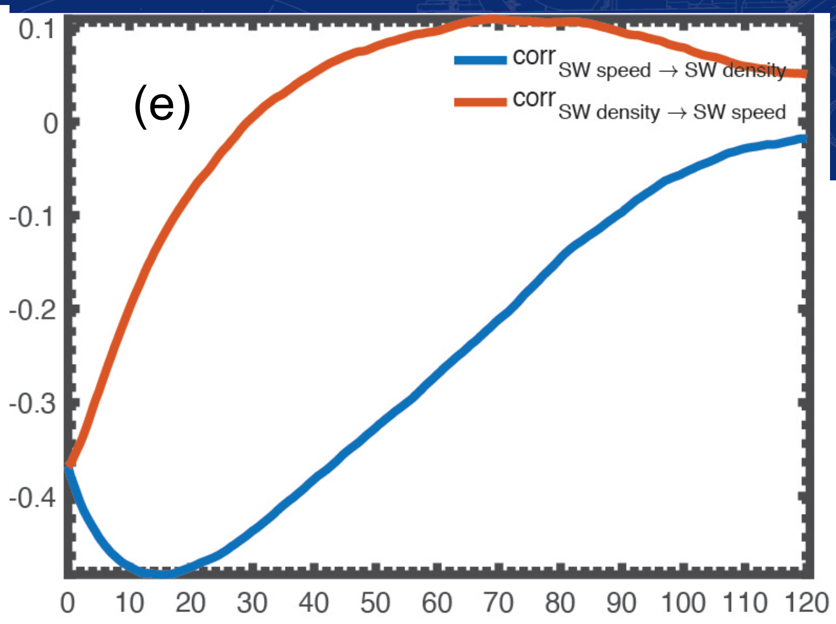

RBSP MagEIS data 2013–2018
electron μ = 700 MeV/G, I = 0.11Re G$^{0.5}$
(~1 MeV)
30 min boxcar average

OMNI solar wind data

Ranking of solar wind parameters based on information transfer to RB J_e, given V_{sw}

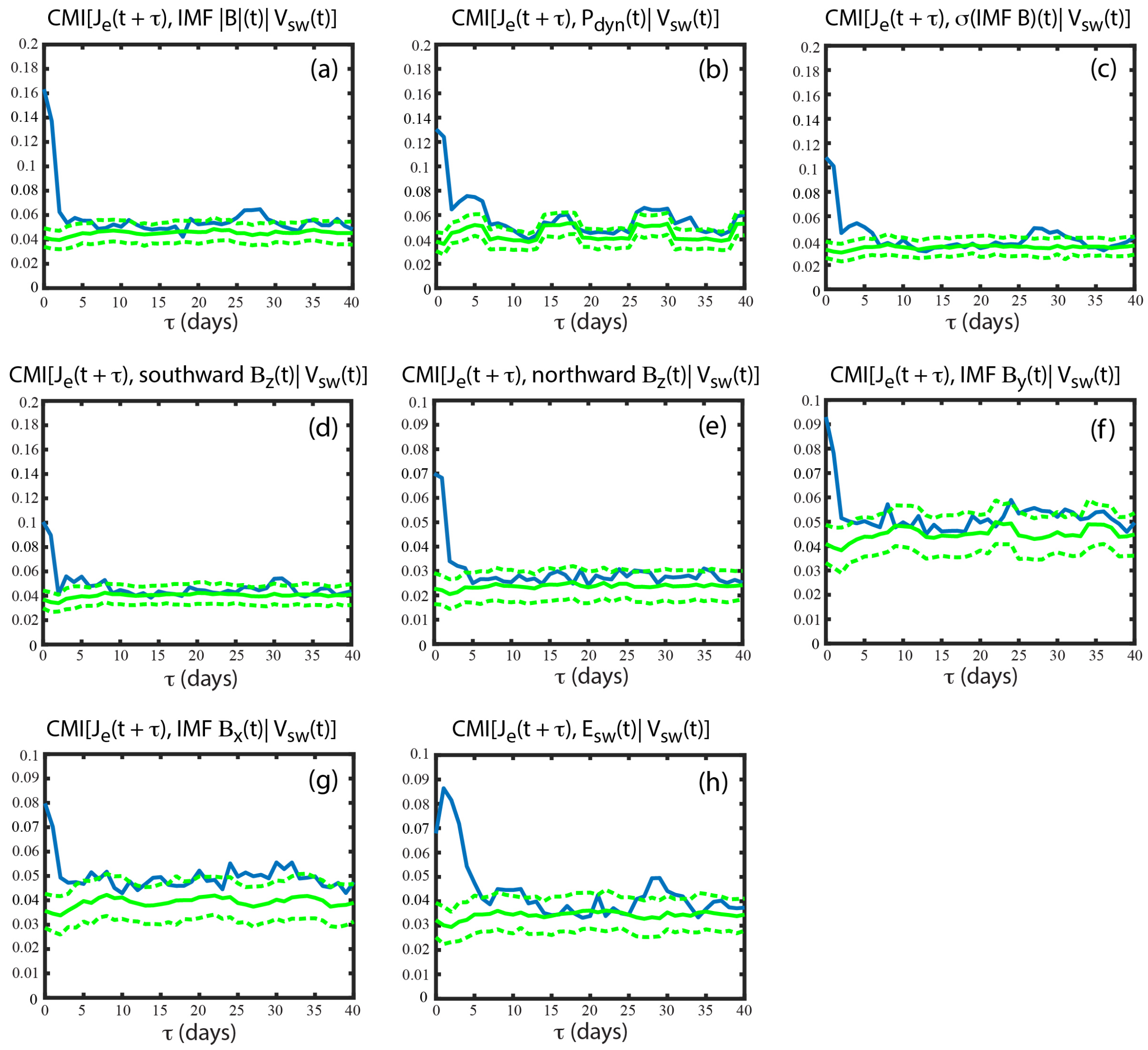

solar wind and magnetospheric parameters ranked by information transfer to PSD given Vsw

rank	solar wind and magnetospheric parameters	peak information transfer (it_{max})	τ (hours)
1	V_{sw}	0.13	46
2	SymH	0.035	30-70 (broad peak)
3	IMF |B|	0.033	6
4	P_{dyn}	0.024	7-10
5	AL	0.022	56
6	n_{sw}	0.020	11
7	IMF $B_z < 0$	0.018	4
8	IMF B_y	0.016	0
9	IMF $B_z > 0$	0.015	10
10	E_{sw}	0.014	46
11	σ (IMF B)	0.0051	4

Improving models with information theory

1. selecting input parameters based on information transfer
2. detecting changes in system dynamics with windowed TE
3. providing prediction horizon

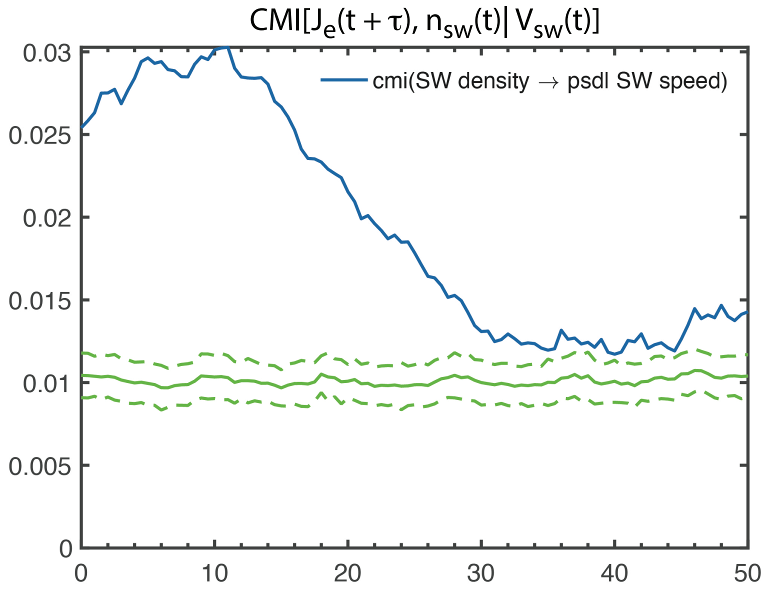

prediction horizon ~30 hr

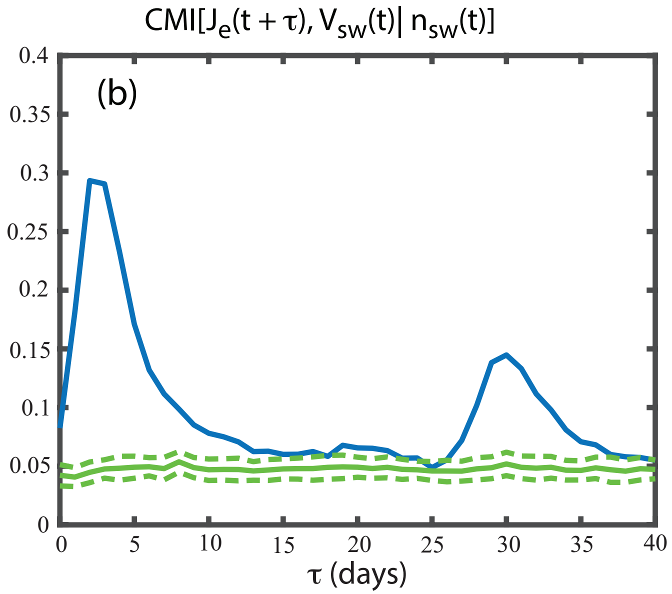

prediction horizon ~10 days

Windowed TE can detect changes in system dynamics

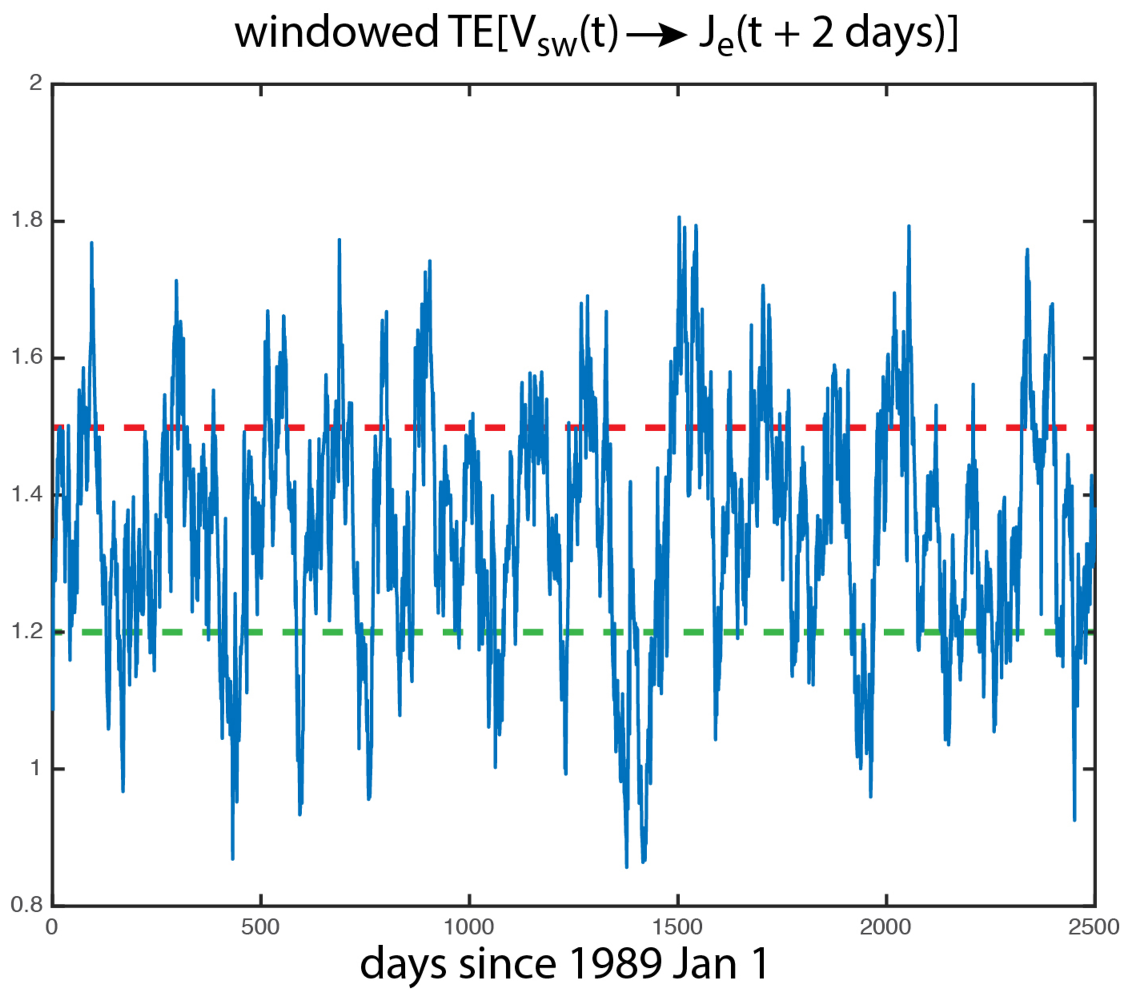

use information theory and NN to model RB electron PSD

use information theory and NN to predict RB electrons

Information theory

- relevant input parameters
- response lag times
- noise
- prediction horizon

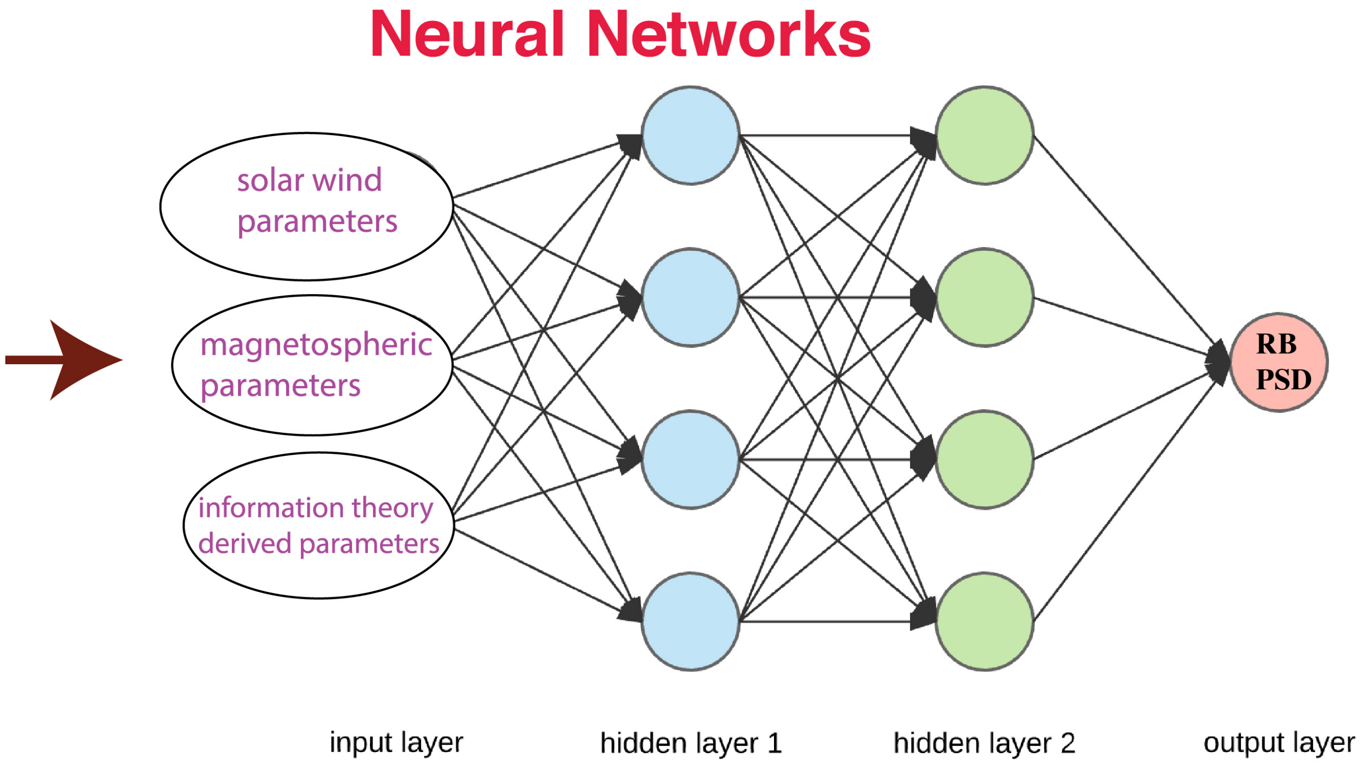

Work in progress

Preliminary NN model results

input parameters: Vsw (t=0-48 hr), nsw(t=0-12 hr), IMF Bz(t=0-4 hr), IMF By(t=0-4 hr), AL(t=0-48 hr), Symh(t=0-48 hr), L*(t= 0 hr)

output parameter: PSD(t=0)

data: RBSP 2013-2018, μ = 700 MeV/G, I = 0.11 Re $G^{0.5}$

work in progress!

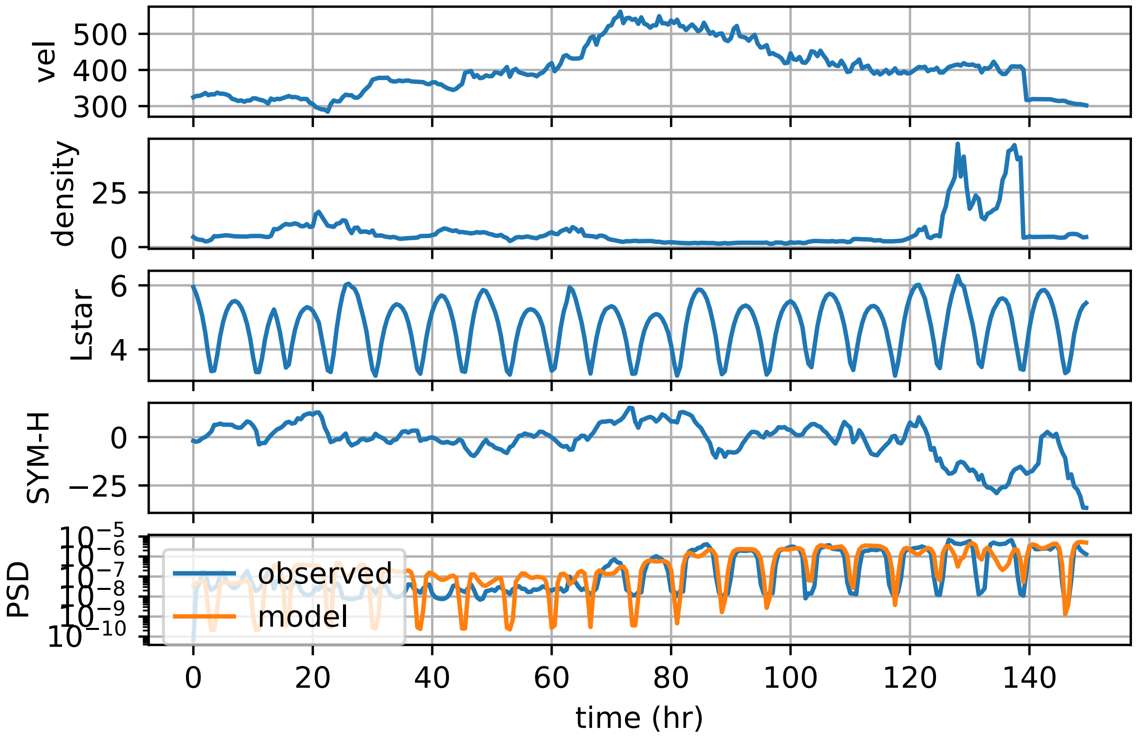

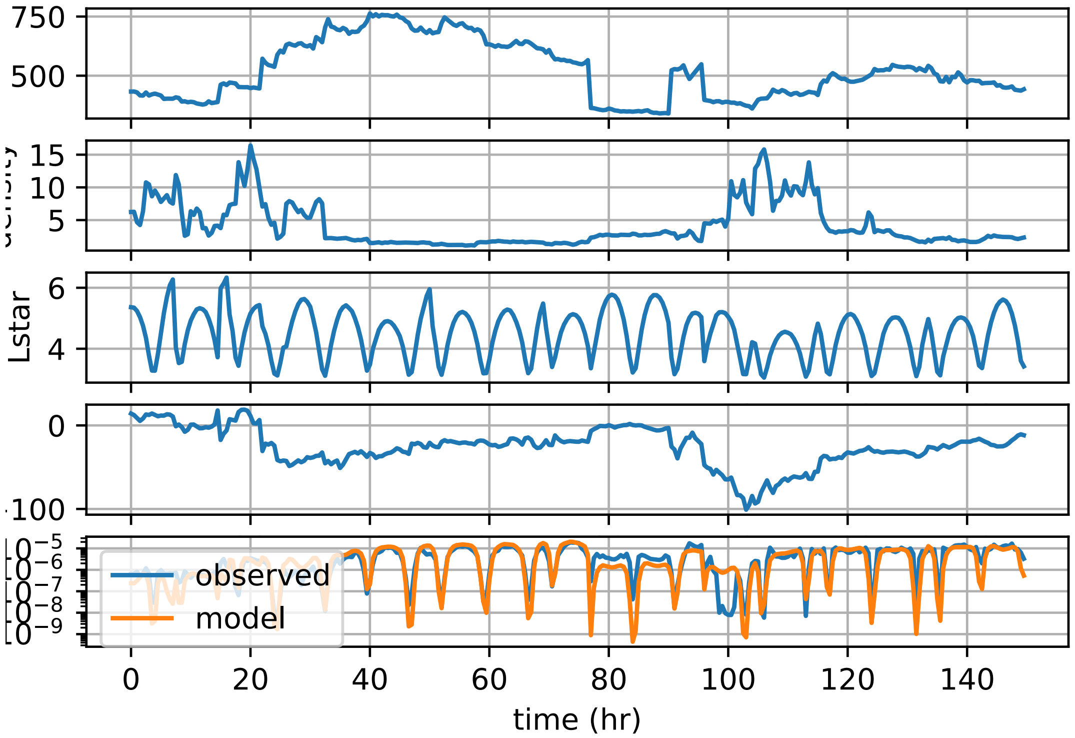

The importance of SYM-H and AL in predicting RB PSD

without AL and SYM-H as input parameters

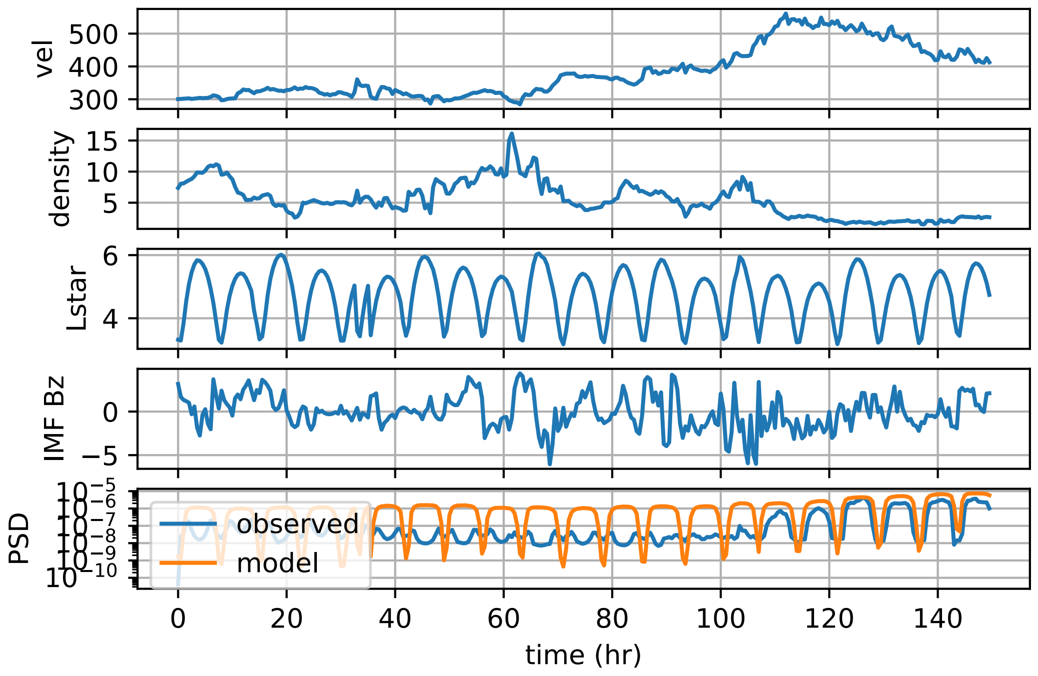

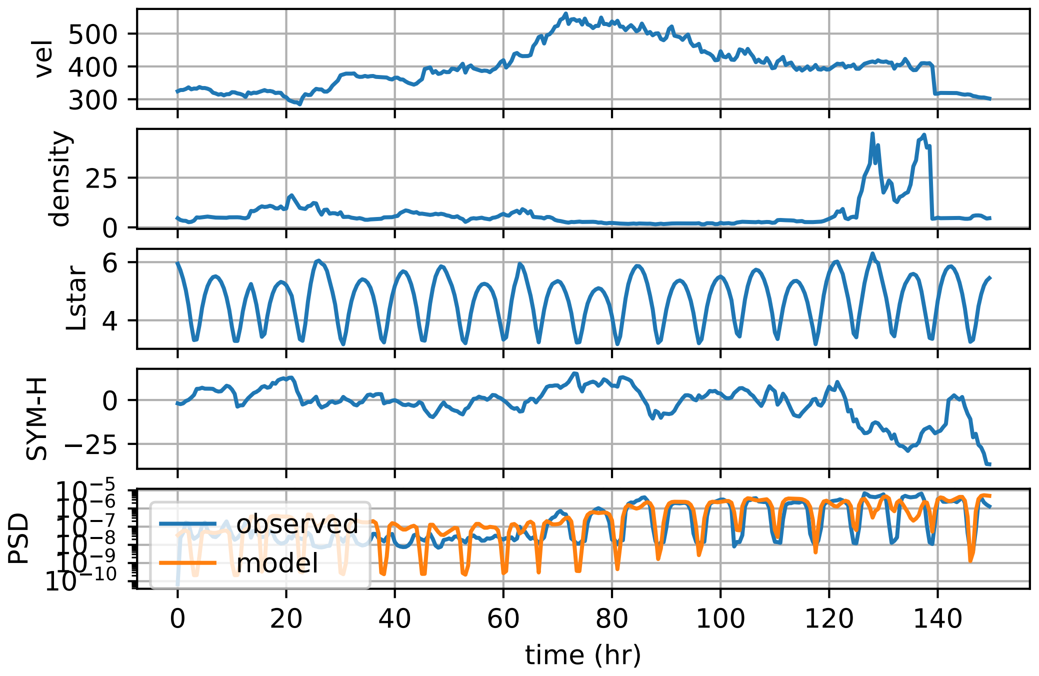

Summary

1. Information theory can help modeling by identifying
   - Relevant drivers of the radiation belt electrons
   - Response lag time
   - Prediction horizon (how far ahead can we predict?)
2. For ~1 MeV RB electrons (μ = 700 $\pm$ 25% MeV/G, I = 0.11 $\pm$ 25% Re $G^{0.5}$):
   - V_{sw} does not affect PSD at L* < 3.5
   - n_{sw} does not affect PSD at L* < 4.5
3. AL and Sym-H provide additional information to RB electrons beyond what Vsw provides
4. We rank solar wind and magnetospheric drivers of RB electrons based on CMI
5. We use NN to model RB electron PSD: PE = 0.66 (preliminary result)

Radiation belt dynamics

1. Radiation belt dynamics

2. Solar dynamo

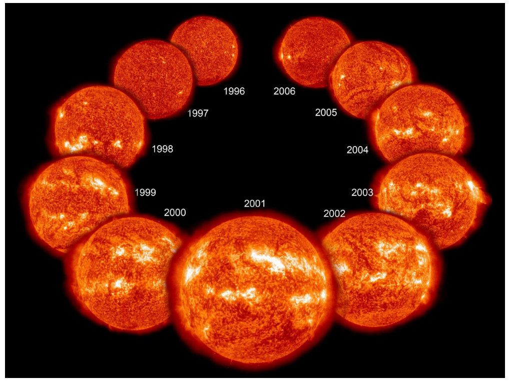

3. Radio waves at Saturn

Sunspots

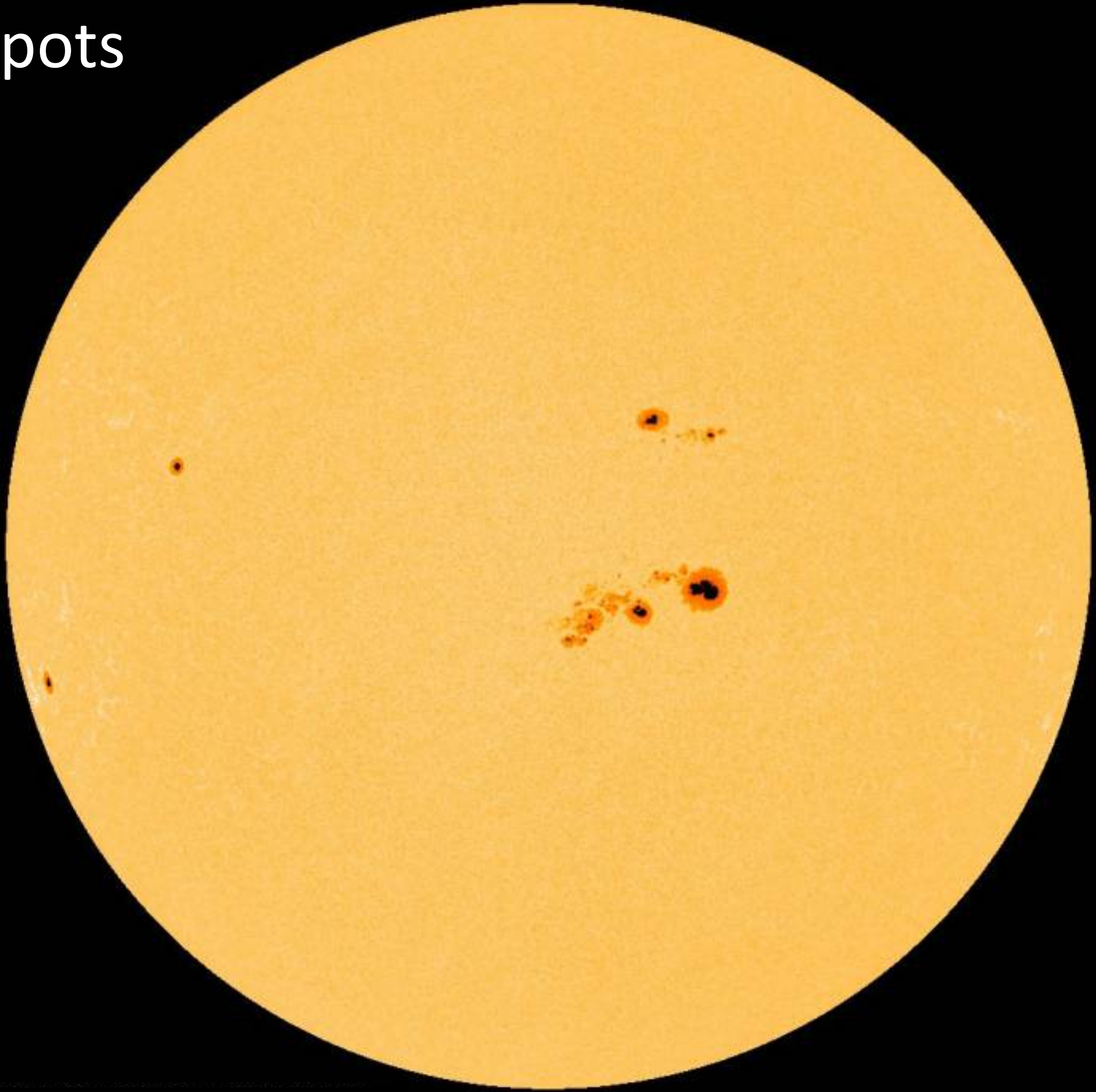

Solar cycle

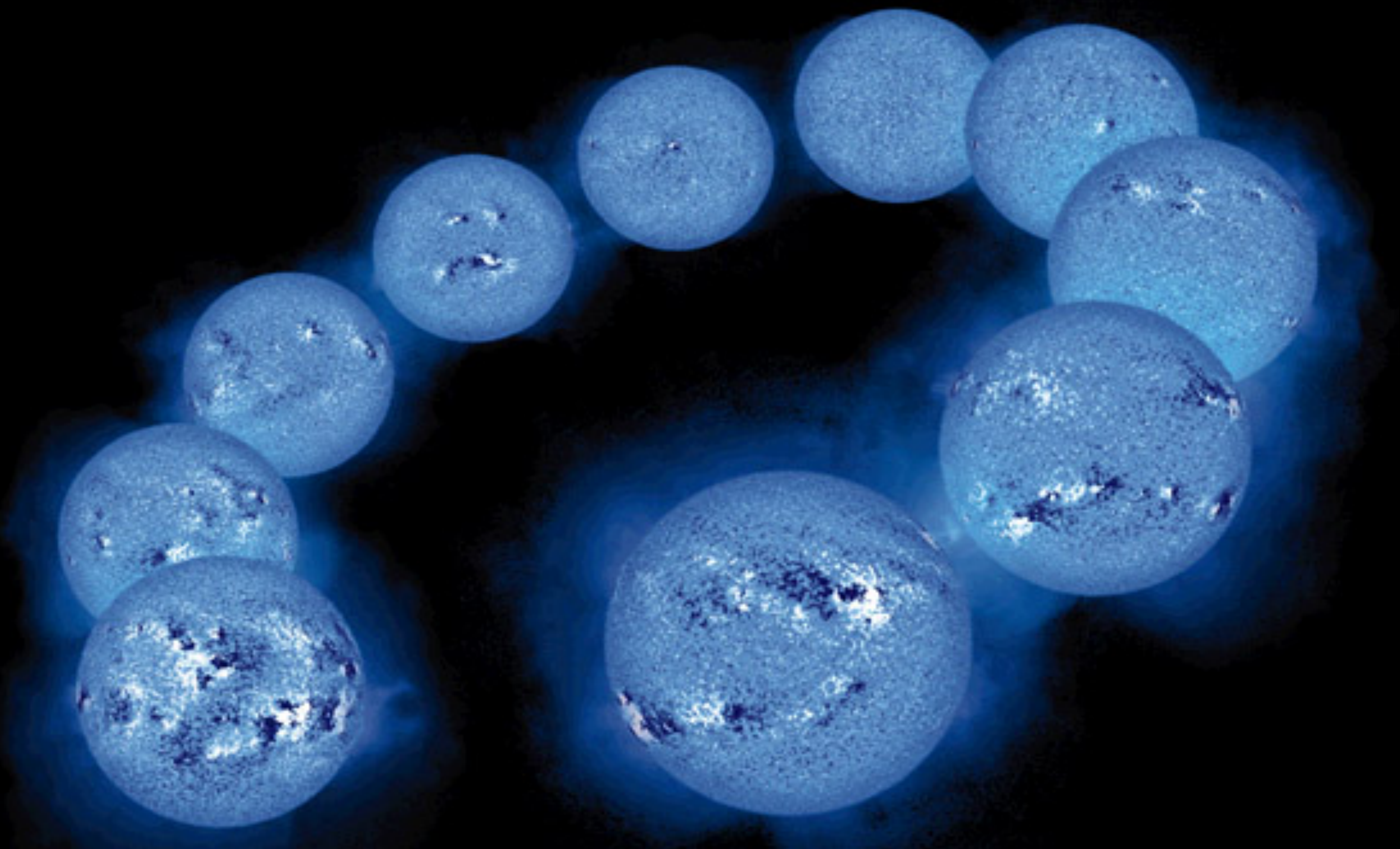

Introduction and motivation

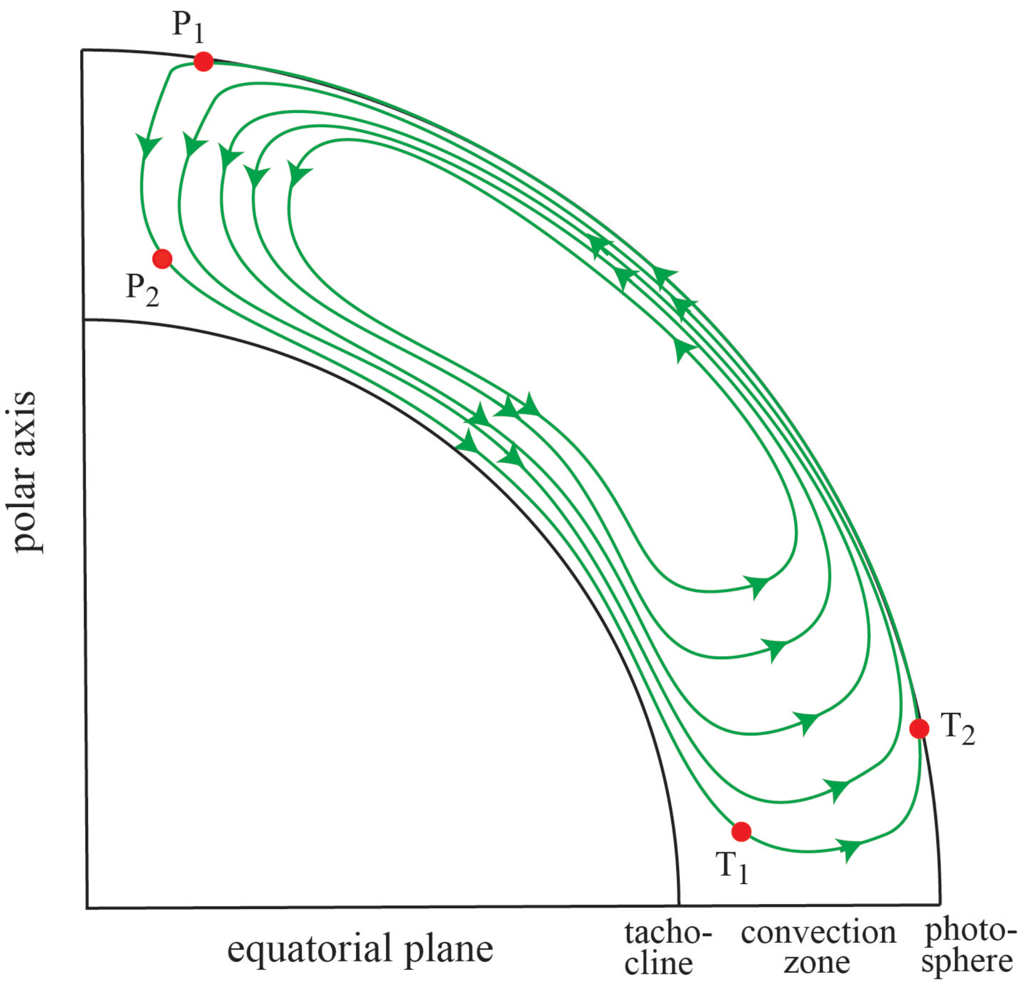

Babcock-Leighton type model
[Babcock, 1961; Leighton, 1964; 1969]

- The roles of solar parameters in the the solar dynamo are not fully understood
- It is still a challenge to predict SSN

Model predictions of SSN at solar max for solar cycle 24

Pesnell [2016]

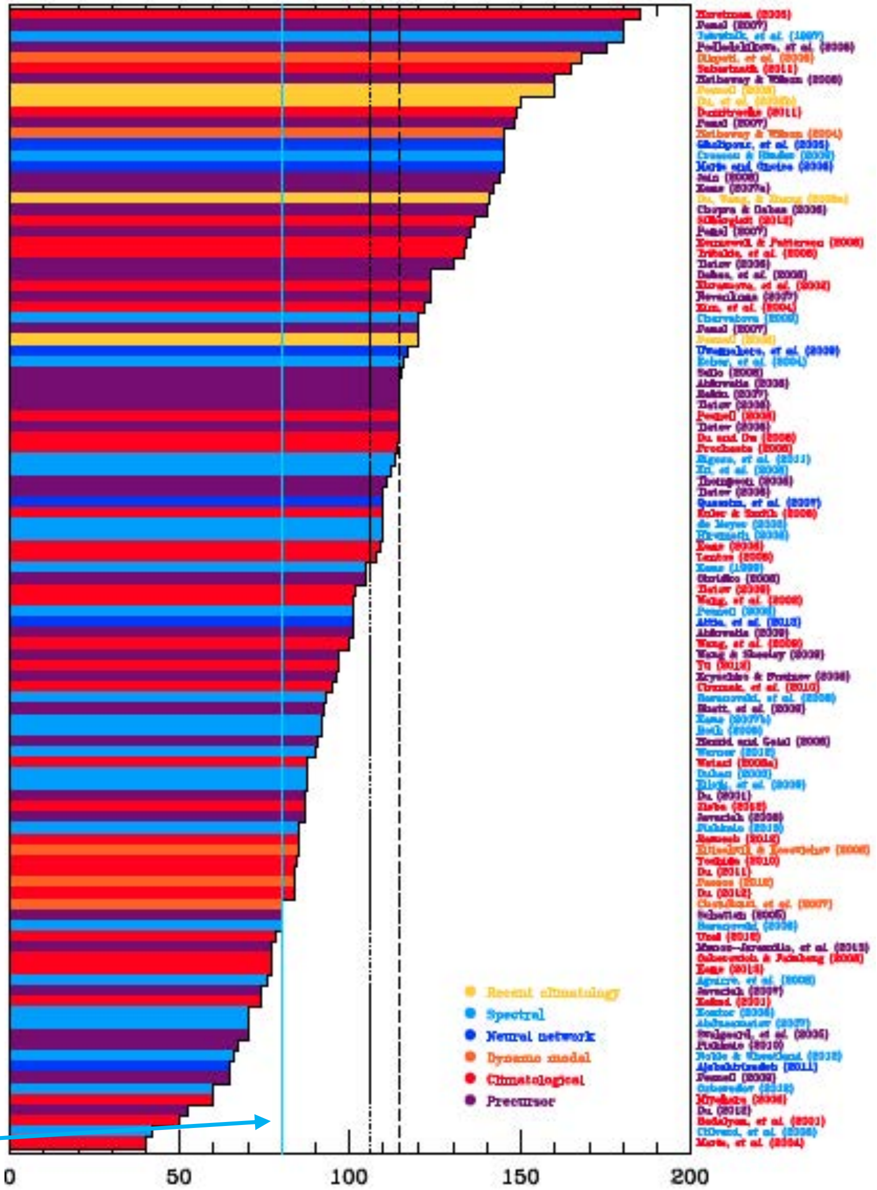

observed International SSN from SIDC

It is still a challenge to predict sunspot number (SSN)

Data set

- SSN 1749–2016 – SILSO website in Belgium
- sunspot area1874–2016 – NASA MSFC website
- meridional flow 1986–2012 – MWO [Ulrich, 2010] (from R. Ulrich)
- polar faculae 1906–2014 – MWO, WSO, SOHO [Munoz-Jaramillo et al., 2012] at Solar Polar Fields Dataverse website
- polar field 1967–2015 – MWO, SWO [Ulrich, 1992; Wang and Sheeley, 1995] (from Y.-M. Wang)
- axial dipole strength 1967–2015 – MWO, WSO [Wang and Sheeley, 1995; 2009] (from Y.-M. Wang)
- aa index 1868–2010 – NOAA NCEI website

All data are evaluated (averaged, interpolated) at monthly resolution

SSN and aa index

Hathaway et al. [1999]

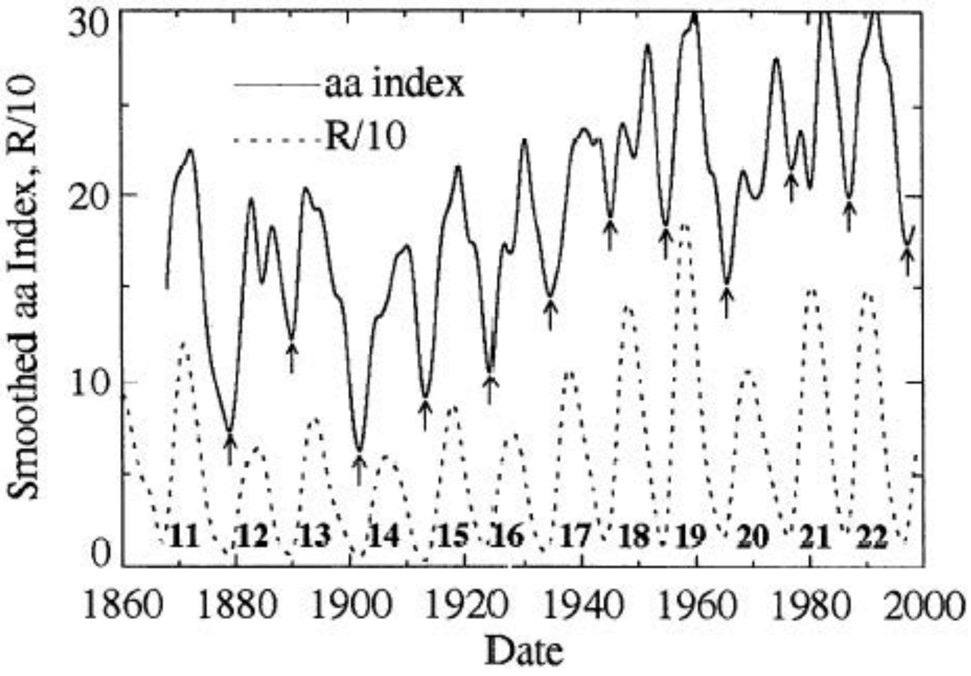

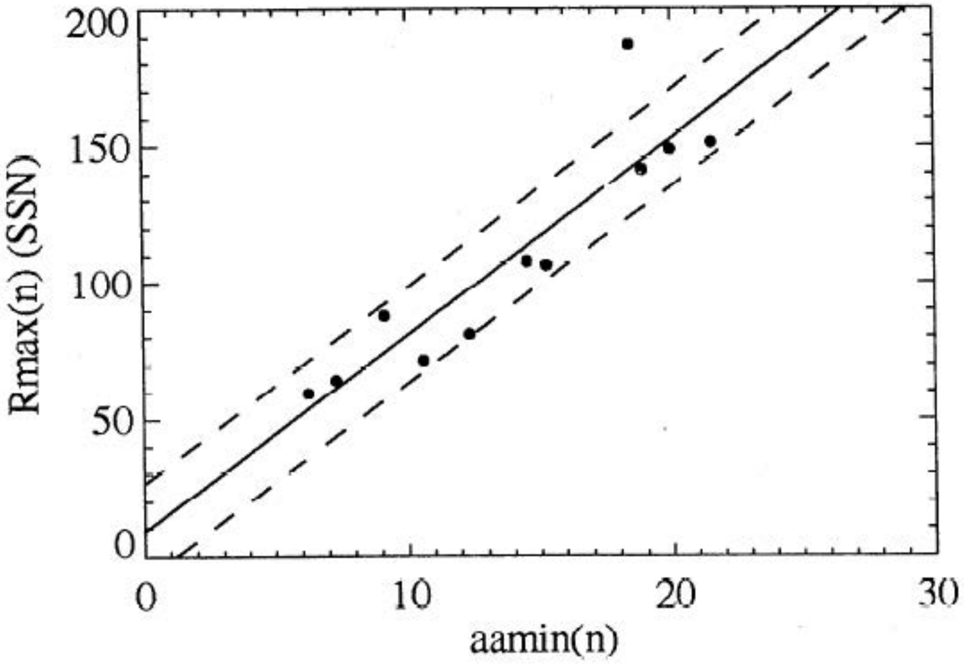

Both, SSN and aa index exhibit cyclical variations

SSN→ aa index

aa index→ SSN [e.g., Ohl, 1966; Hathaway et al., 1999; Schatten and Pesnell, 1993; Wang and Sheeley, 2009]

Babcock-Leighton type model of solar dynamo

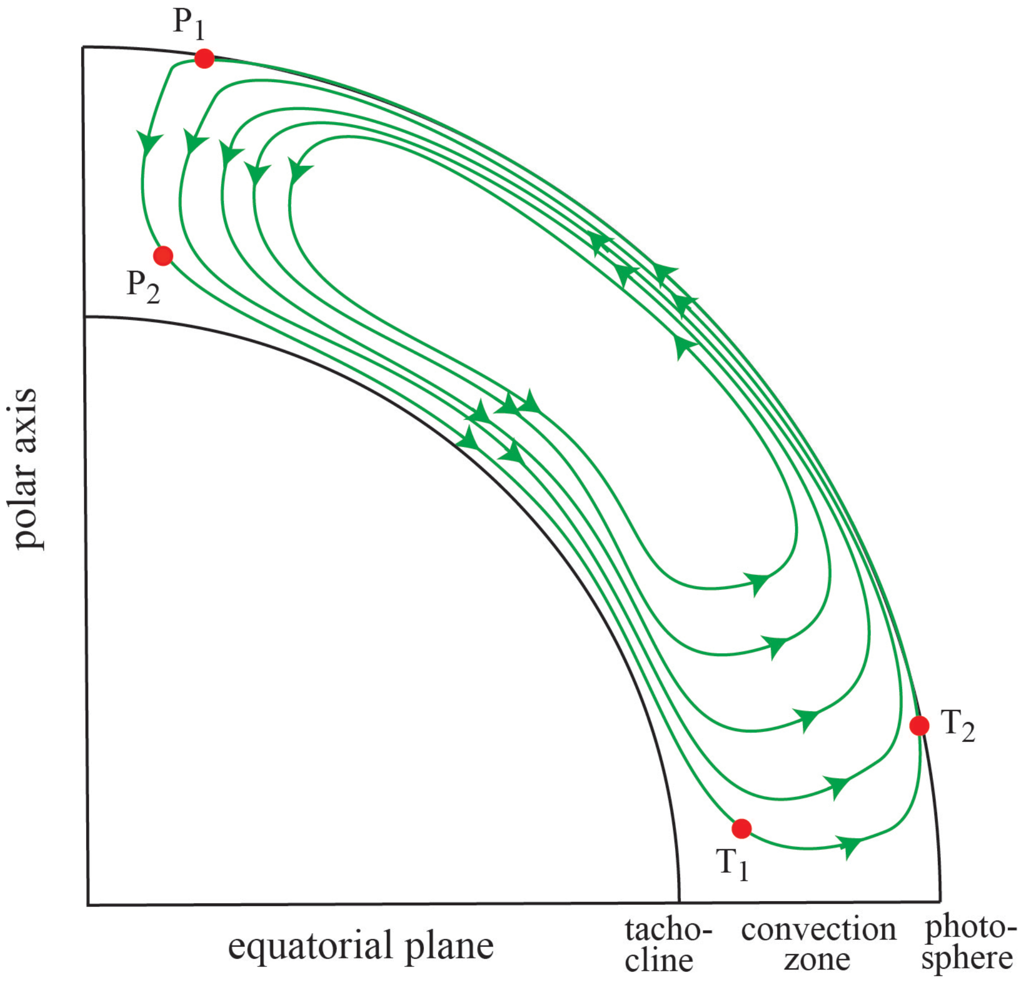

[Babcock, 1961; Leighton, 1964; 1969]

SSN and aa index

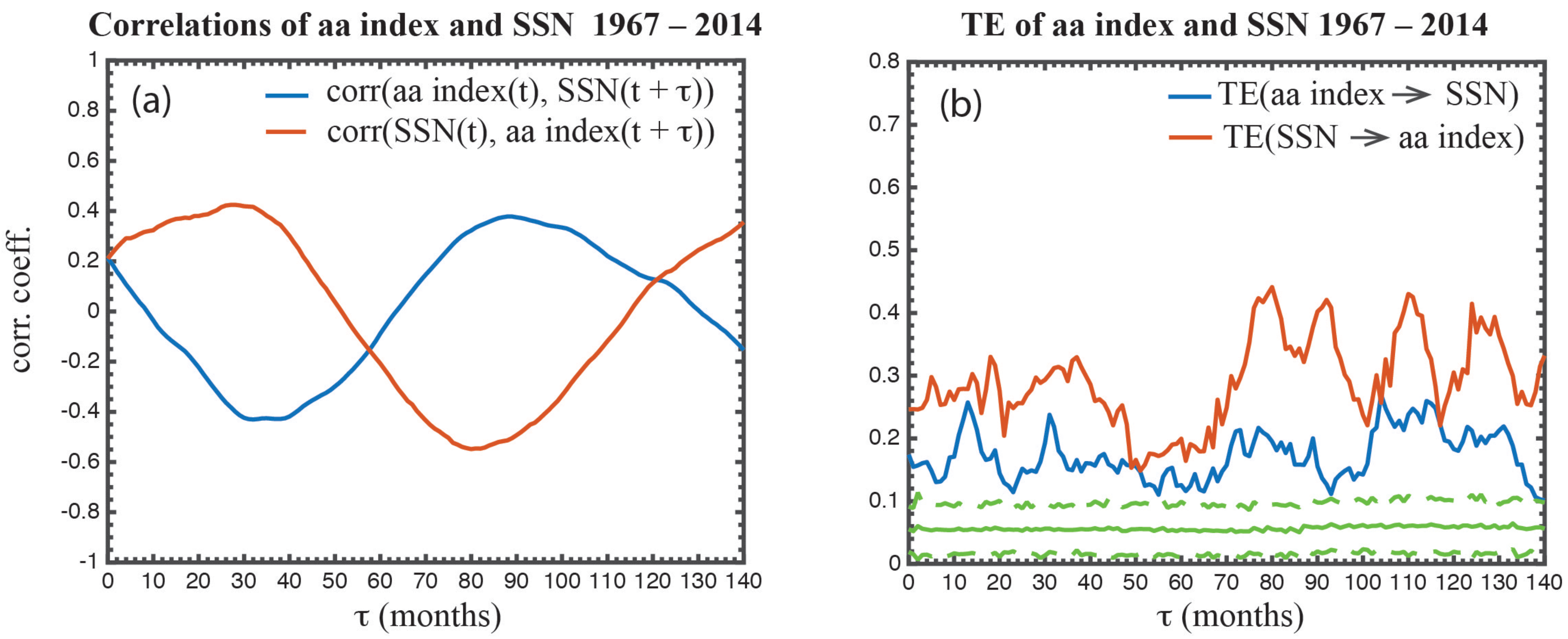

- peak |corr(aa index(t), SSN(t + τ))| ~ peak |corr(SSN(t), aa index(t + τ))|
- **But,** TE(SSN→aa index) > TE(aa index → SSN)
- more information is transferred from SSN to aa index than the other way around; aa index is a poor proxy for the solar polar field – this information cannot be obtained from correlational analysis

SSN and solar polar field

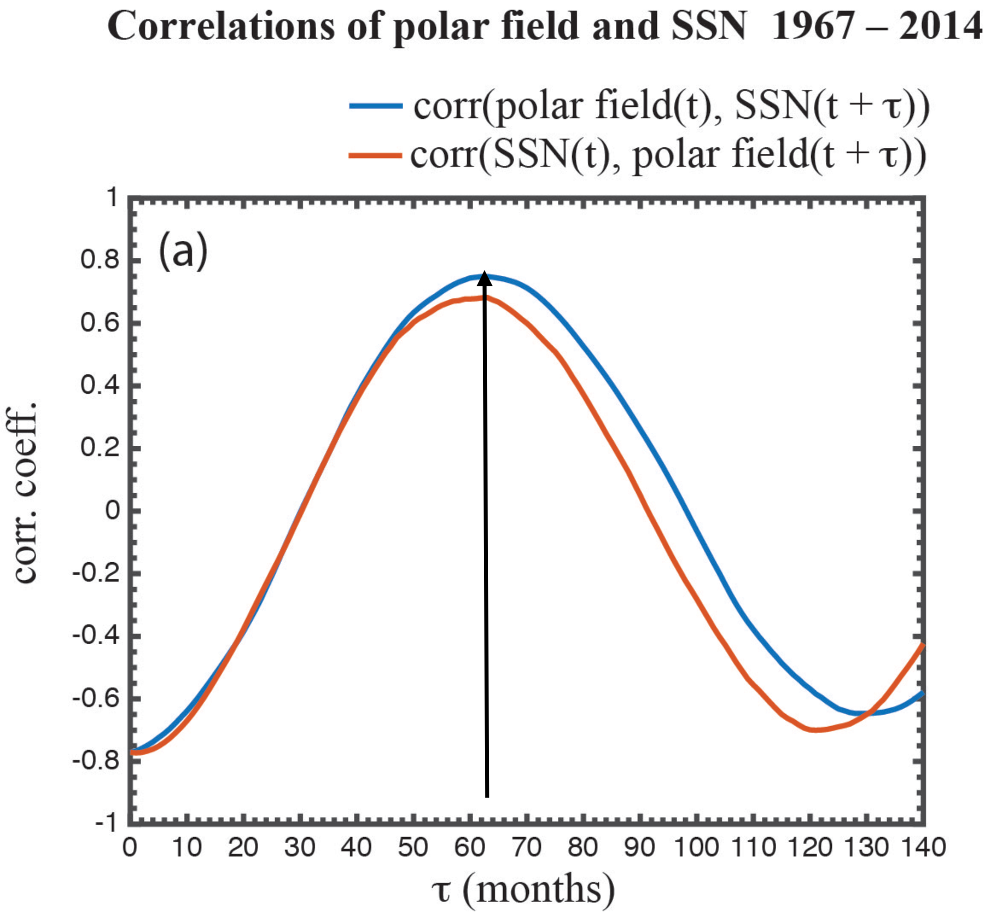

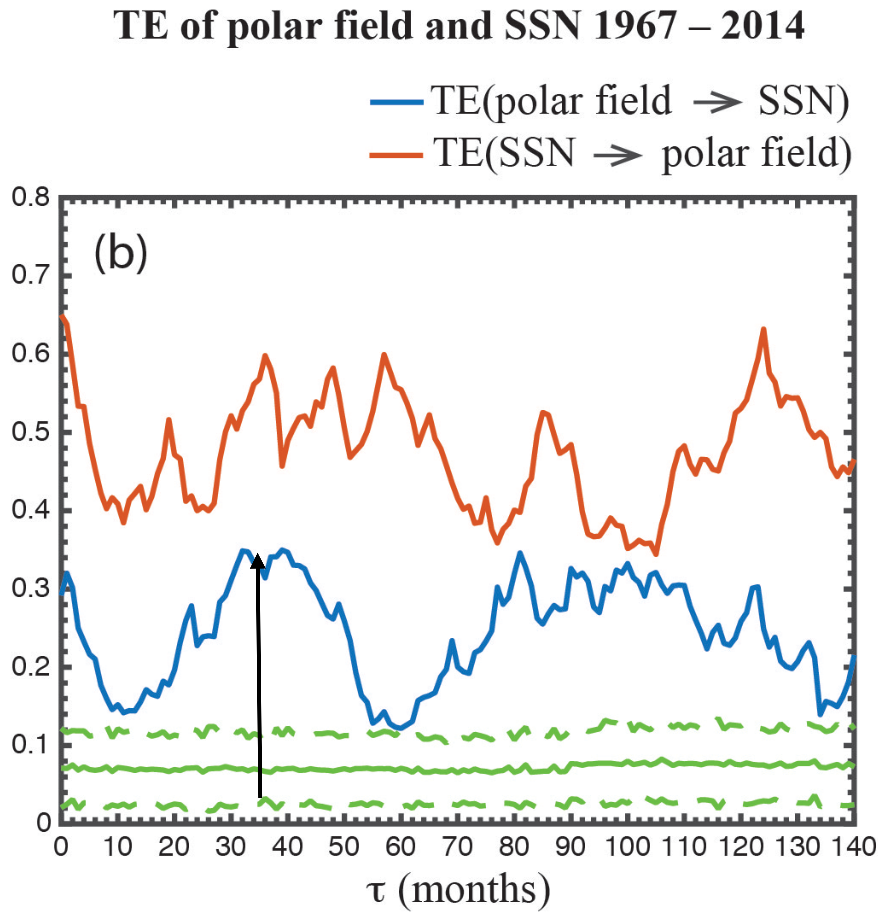

- TE(polar field → SSN) peaks around τ ~30–40 months, not 66 months assumed in some models
- peak significance = (peak TE – mean(noise))/σ(noise) = 19 σ
- TE(SSN→ polar field) is significant [Upton and Hathaway, 2014]

Introduction and motivation

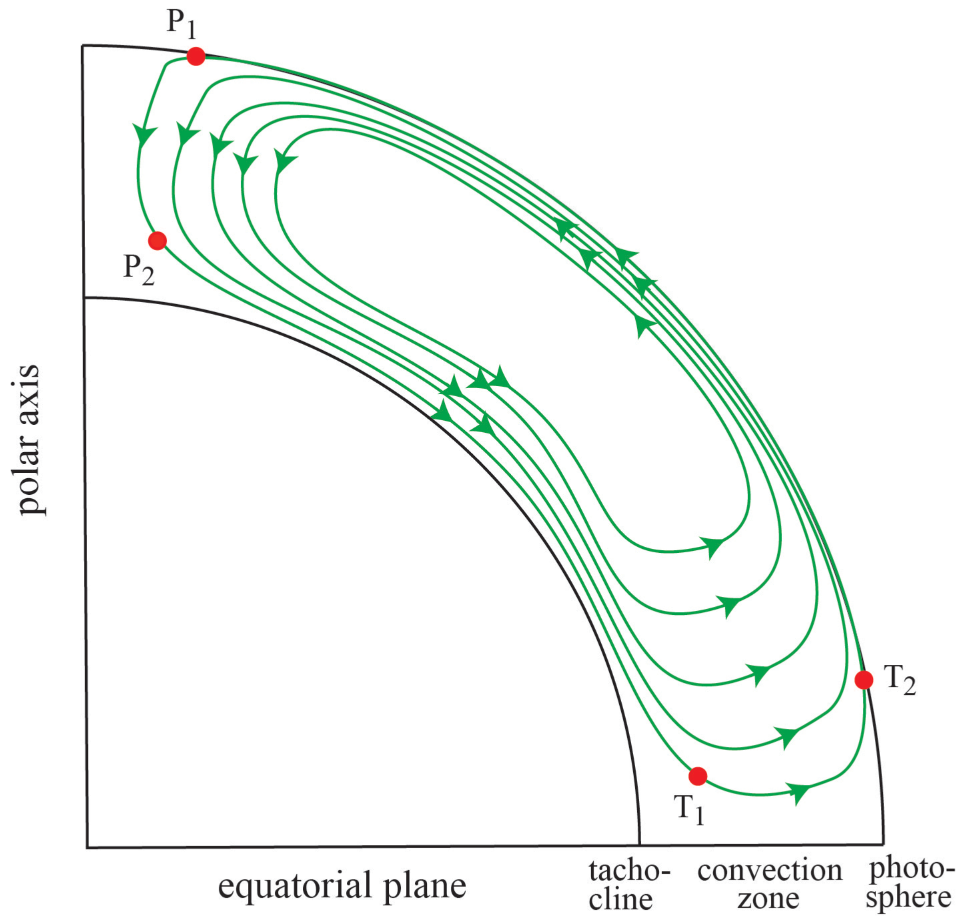

Babcock-Leighton type model
[Babcock, 1961; Leighton, 1964; 1969]

Dikpati et al. [2010]

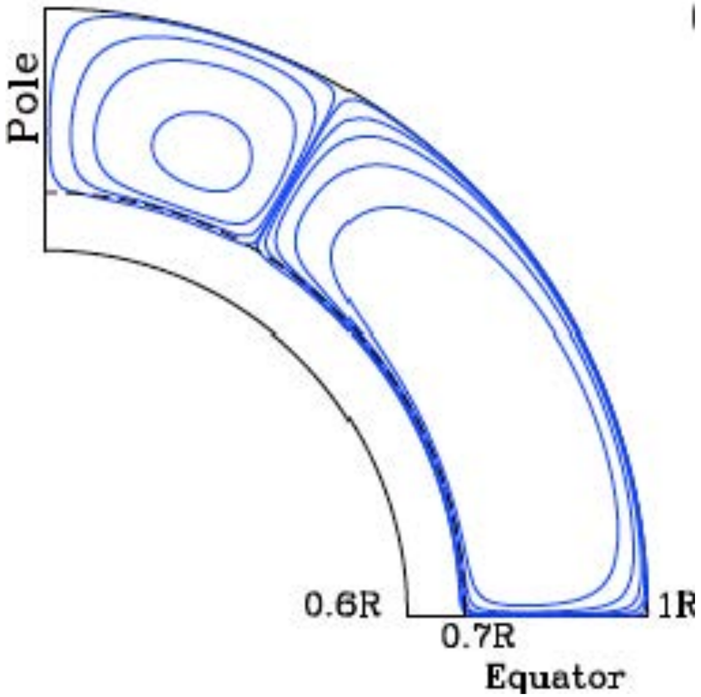

Which parameters control the polar field?

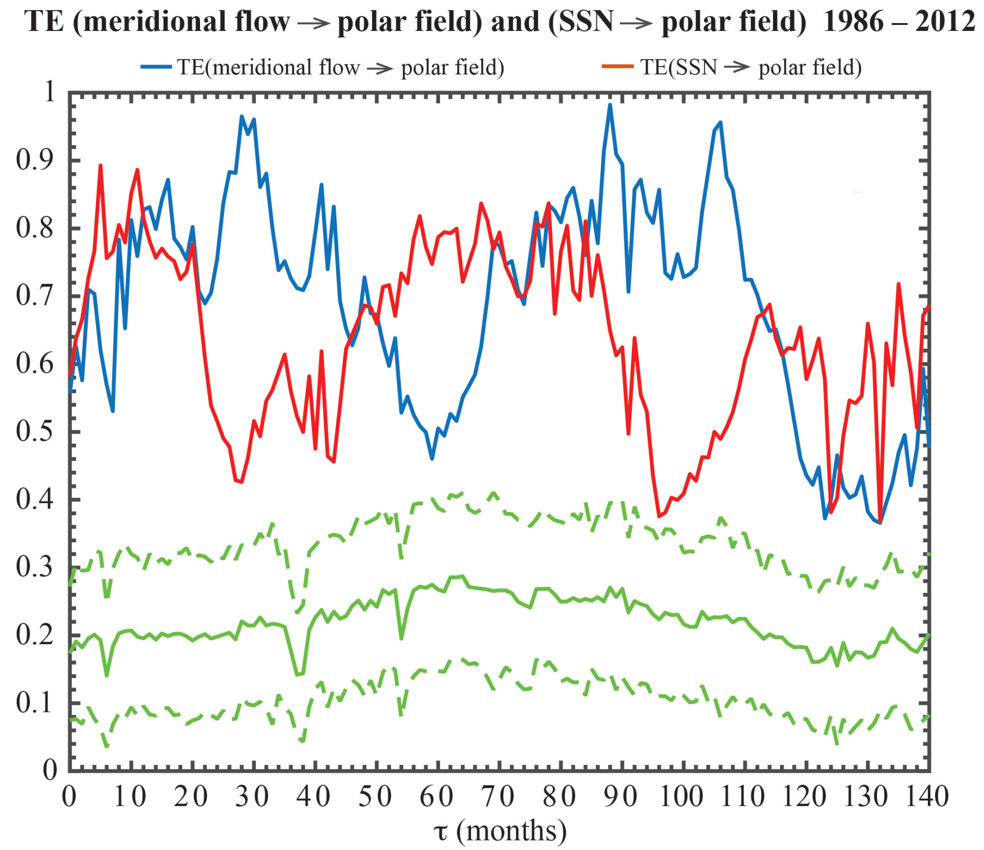

- surface flux transport models [e.g., Devore and Sheeley, 1987; Wang et al., 1989;2005] and flux transport dynamo models [e.g., Dikpati et al., 2006, Choudhuri et al., 2007]: meridional flow controls the strength of the polar field
- amount flux emergence (SSN) controls the polar field [Upton and Hathaway, 2014]
- TE(meridional flow→polar field) peaks τ~30-40 (pos corr),~90-110 months (neg corr)
- TE(SSN→ polar field) peaks τ ~50–80 months (pos corr)

Are the past n cycles important for predicting SSN?

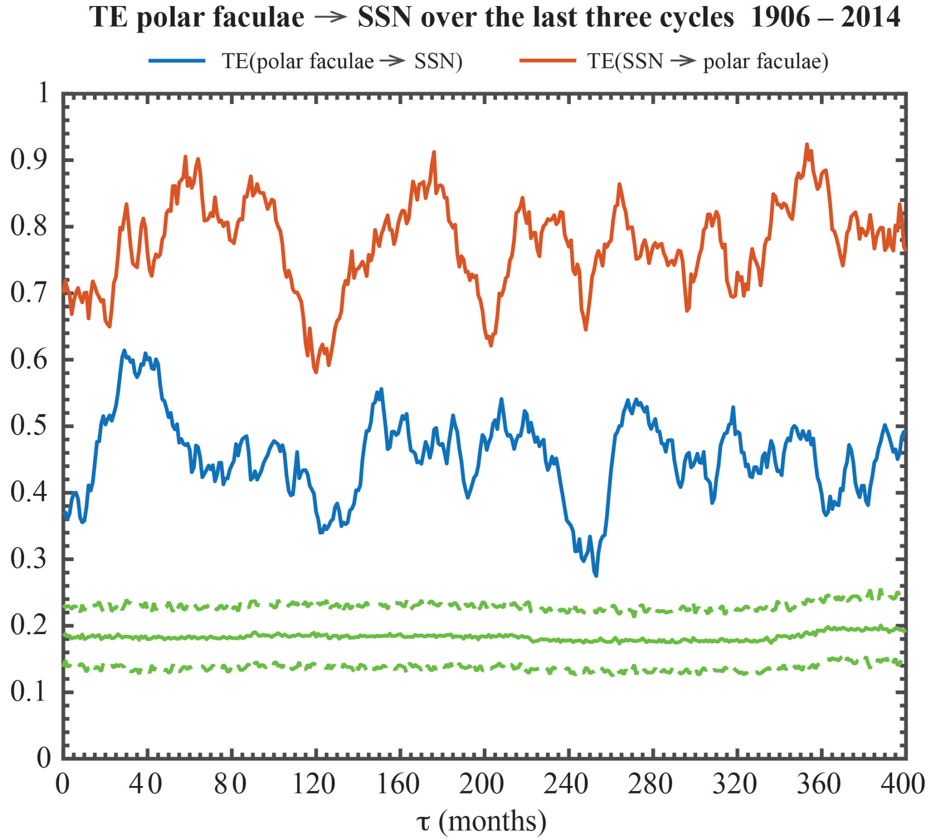

- Dikpati et al. [2004] suggested that meridional flow is slower at the bottom of the convection zone and hence the polar fields from the last 3 cycles should affect SSN (see also Charbonneau & Dikpati, 2000)
- TE(polar faculae → SSN) peaks at τ ~30-40 months but persists at a lower level thereafter for at least 400 months (~ 3 solar cycles)
- There are minima at τ ~1 and ~2 solar cycle periods

Information transfer from polar field, polar faculae,and meridional flow to SSN

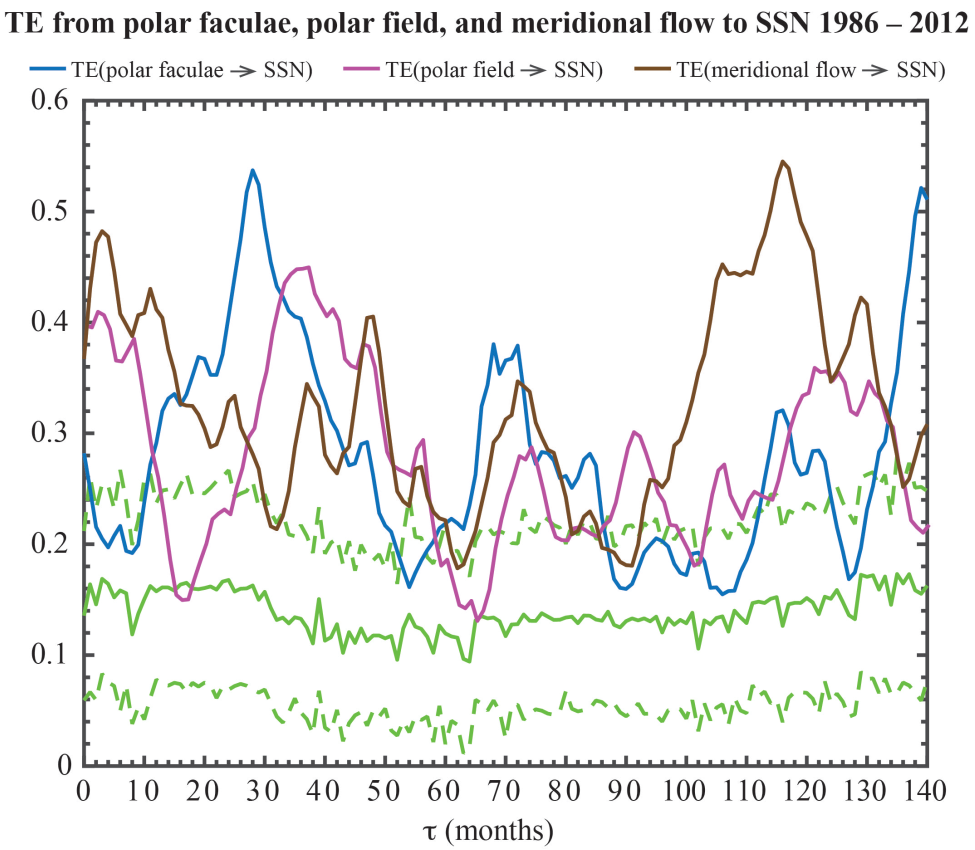

- noisy because data have shorter timespan, limited by meridional flow data
- TE([polar faculae, polar field]→SSN) > TE(meridional flow → SSN) at τ ~30–40 months, which may be consistent with Dikpati et al. [2010] model.
- TE(meridional flow → SSN) peaks around τ ~120 months (~1 solar cycle period), suggesting the meridional flow can be used to predict SSN one solar cycle period ahead

Conversion from toroidal to poloidal field is hard

Jie Jiang (Space Climate 7, 2019)

Sketch of model-based predictions

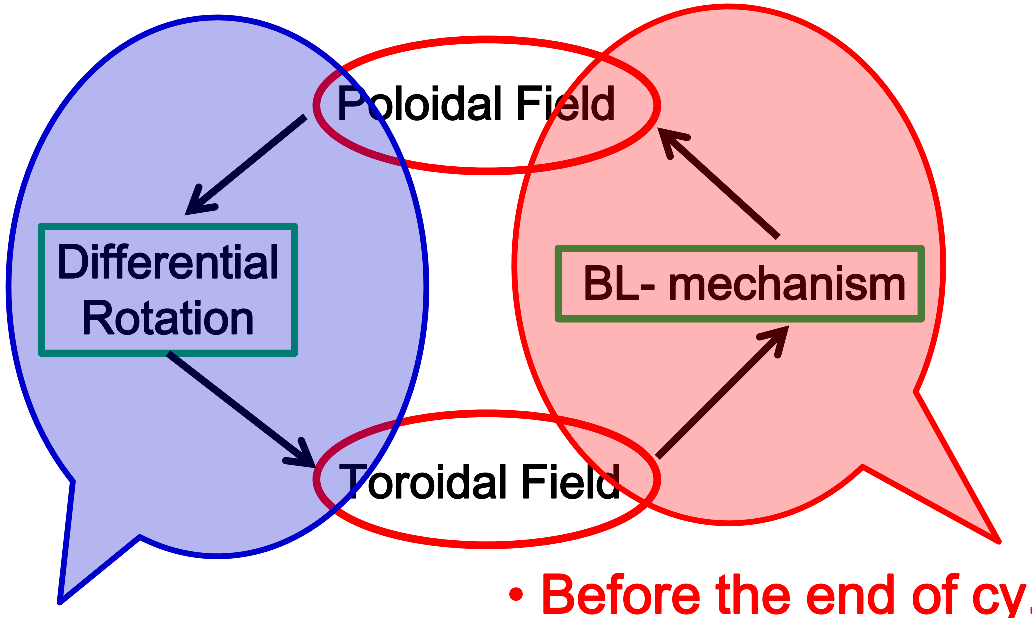

- Around the end of cy. 23
- Flux transport dynamo-based prediction
- Easy part –linear

- Before the end of cy.24
- Surface flux transport model-based prediction
- Hard part –randomness & nonlinearities

Comparing observations with Dikpati simulation

4

TE of polar field and SSN 1967 – 2014

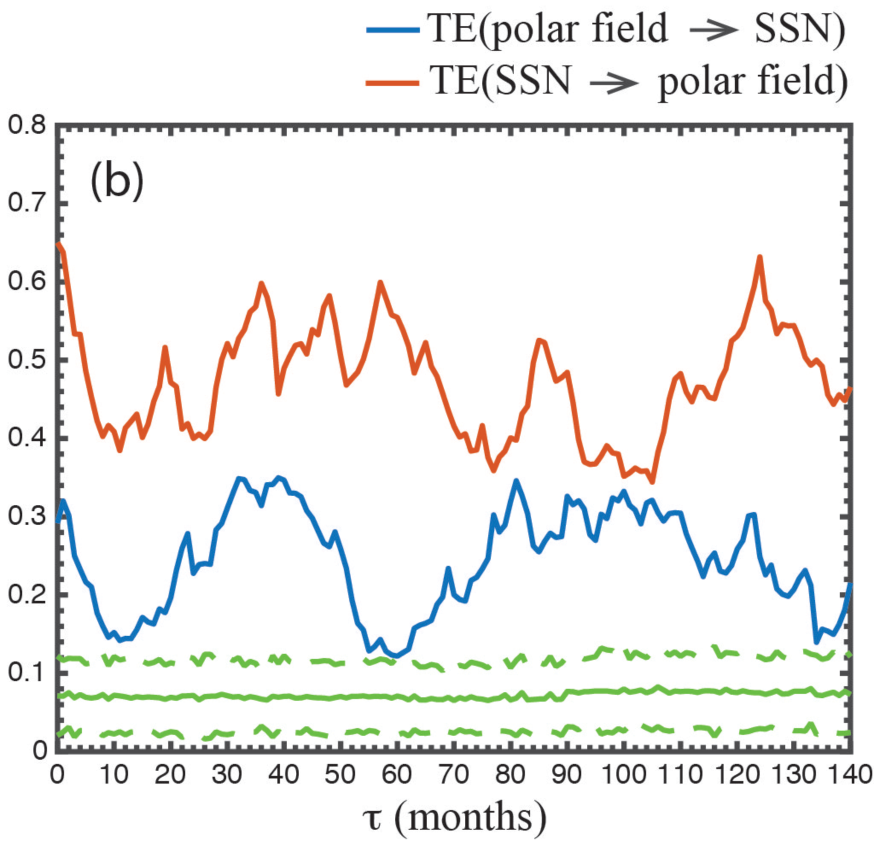

Dikpati simulation

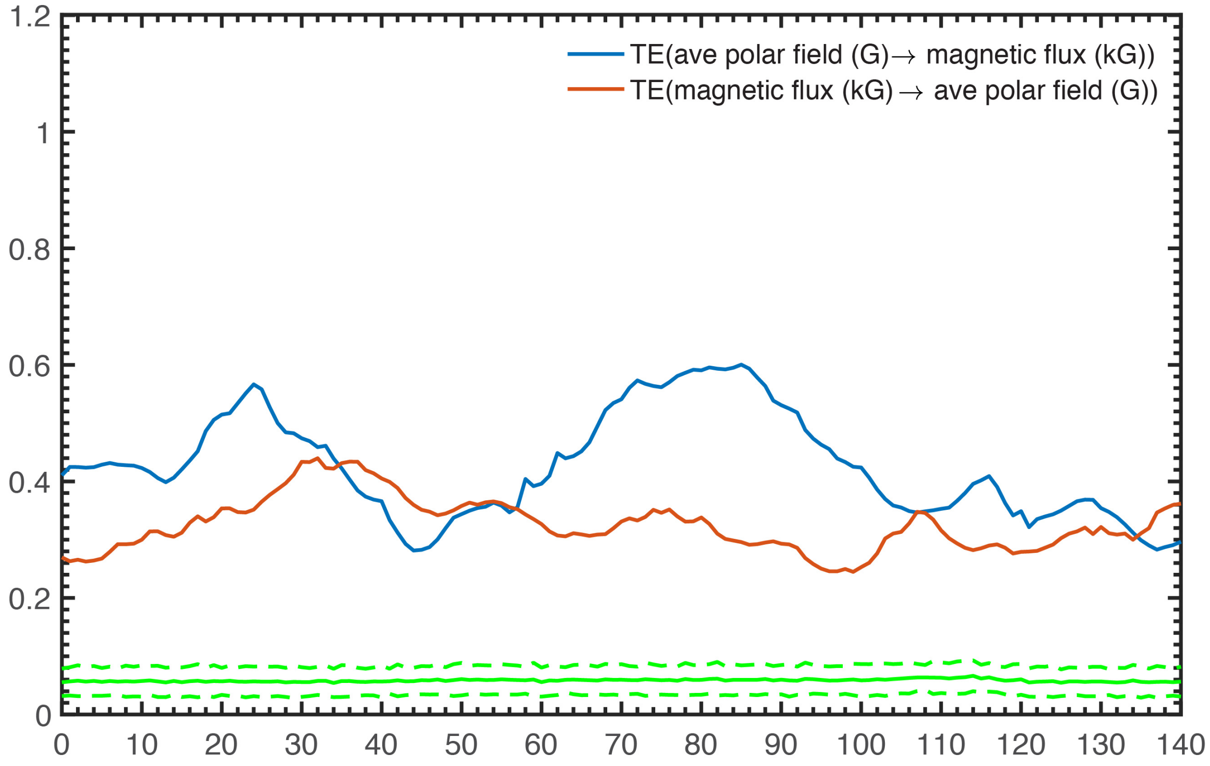

Summary

- TE(SSN → aa index) > TE(aa index → SSN)
- TE(polar field → SSN) peaks at $\tau \sim 30$–40 months (the response of SSN to polar field peaks ~3-4 years, not 5.5 years).
- TE(polar faculae → SSN) peaks at $\tau \sim 30$–40 months, but persists at lower level for at least 3 solar cycles
- Our results provide observational constraints to solar cycle models and theories

Radiation belt dynamics

1. Radiation belt dynamics

2. Solar dynamo

3. Radio waves at Saturn

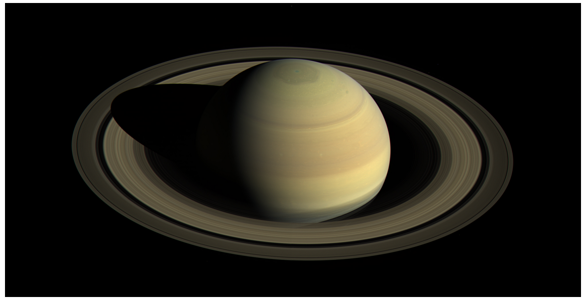

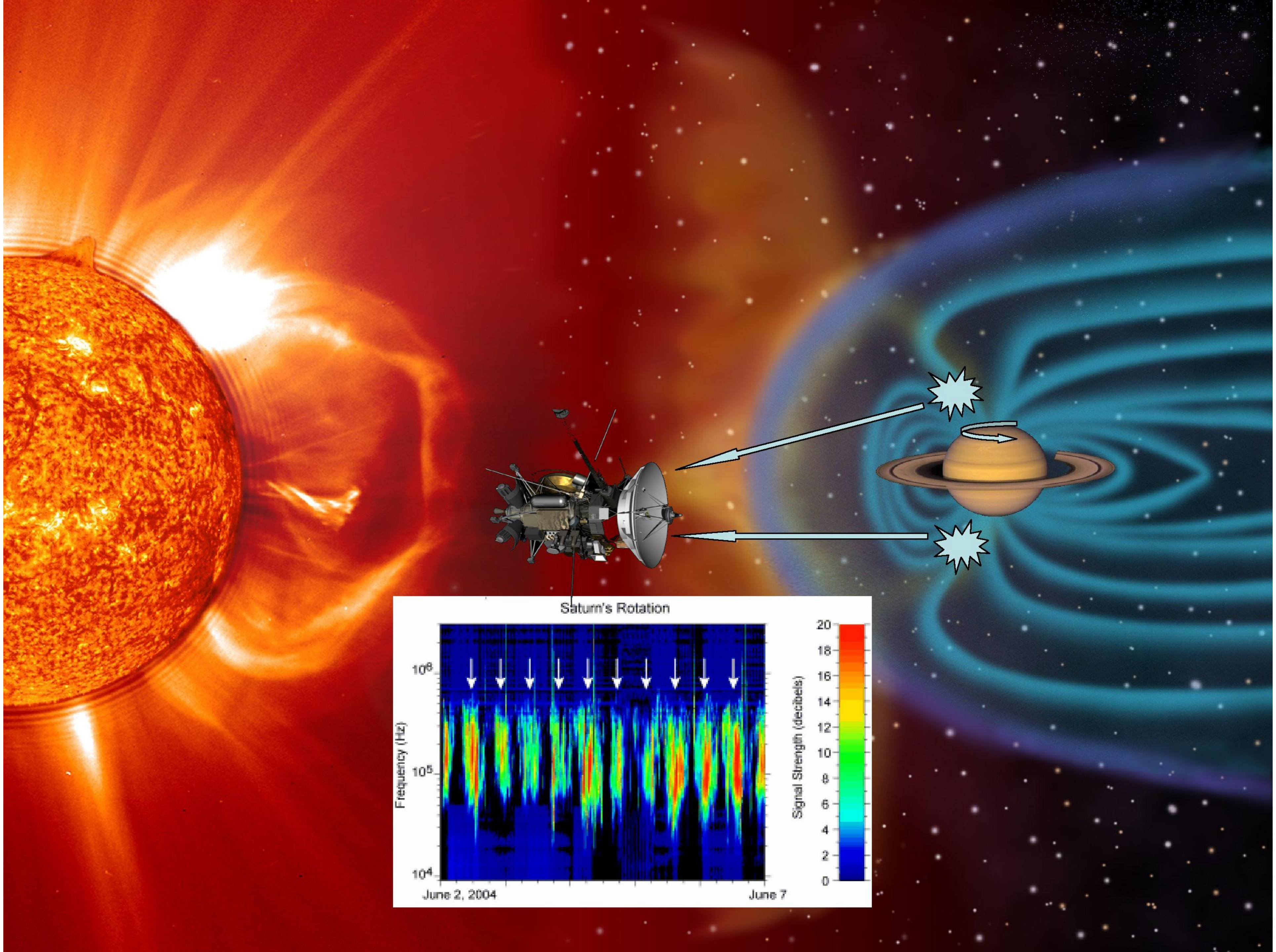
Saturn's Rotation
Frequency (Hz)
10^6
10^5
10^4
June 2, 2004
June 7
Signal Strength (decibels)
20
18
16
14
12
10
8
6
4
2
0

RPWS radio wave data

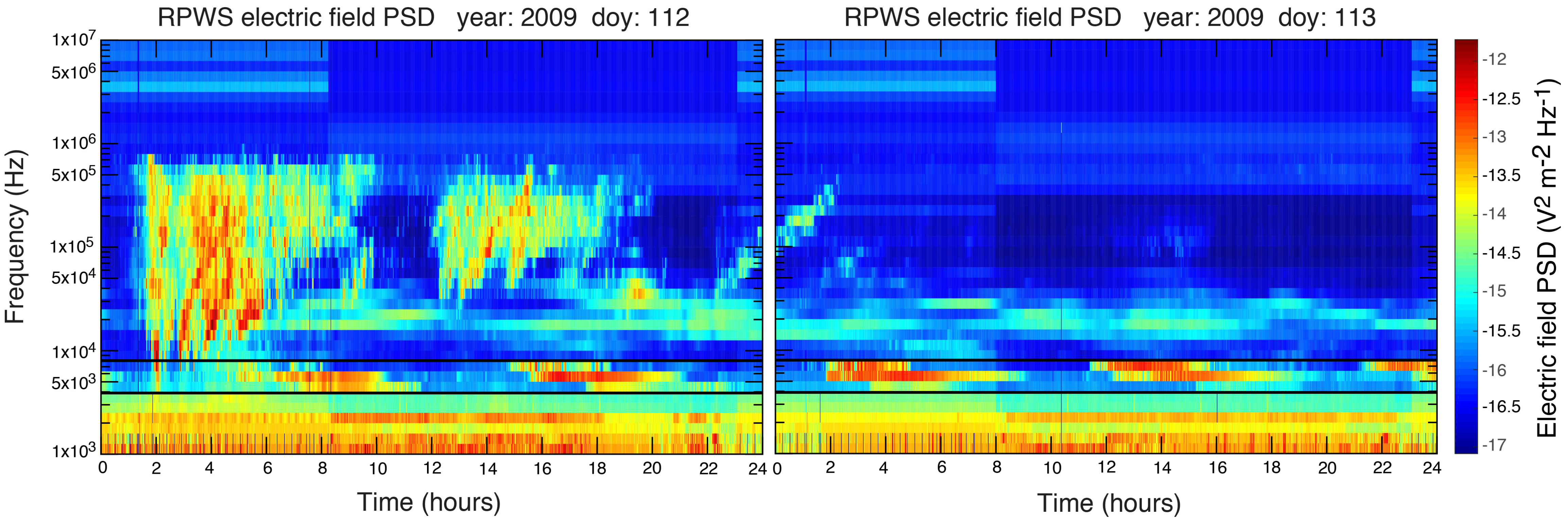

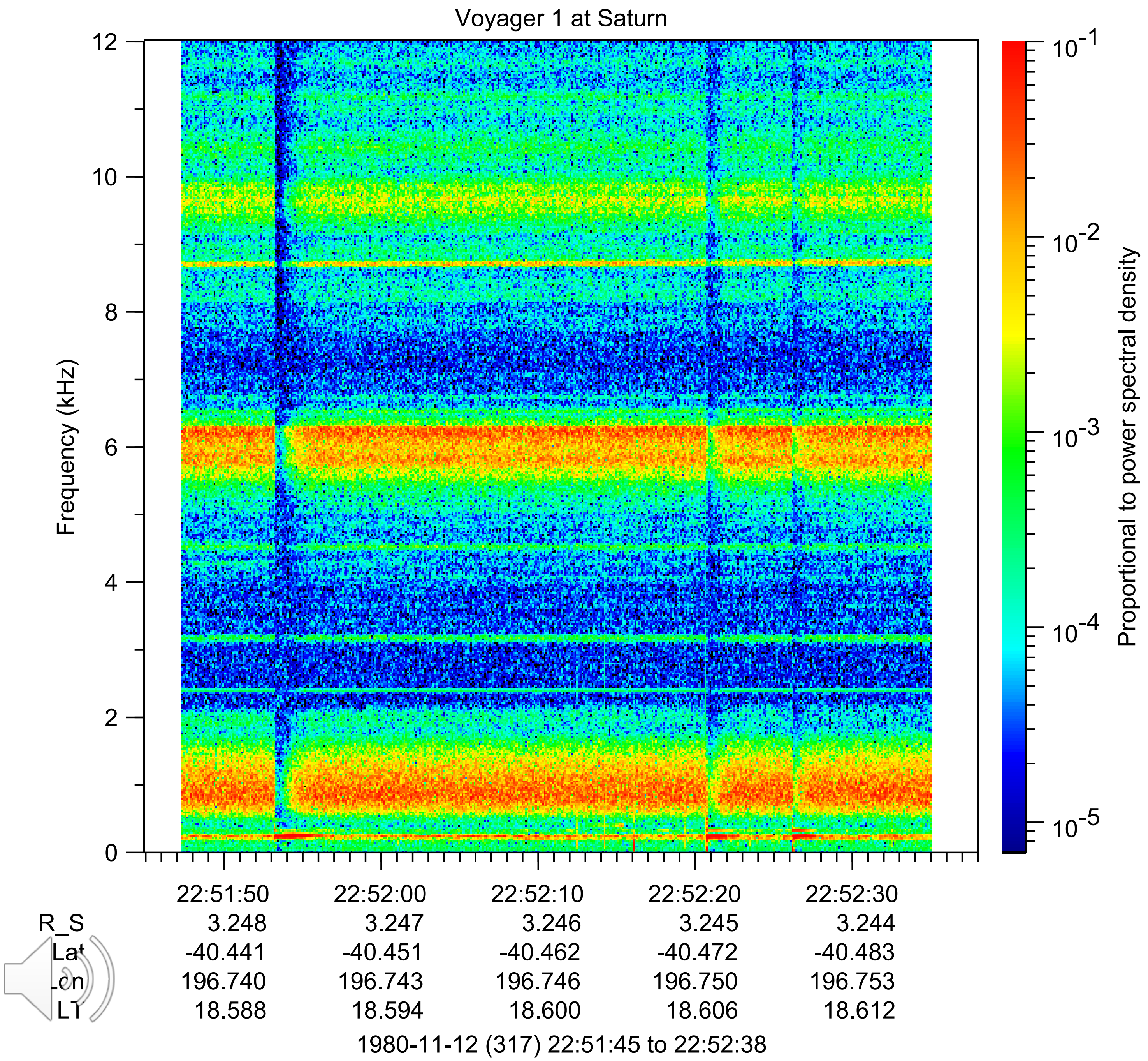

Voyager 1 at Saturn
Frequency (kHz)
12
10
8
6
4
2
0
10^-1
10^-2
10^-3
10^-4
10^-5
Proportional to power spectral density
22:51:50
22:52:00
22:52:10
22:52:20
22:52:30
R_S 3.248 3.247 3.246 3.245 3.244
Lat -40.441 -40.451 -40.462 -40.472 -40.483
Lon 196.740 196.743 196.746 196.750 196.753
LT 18.588 18.594 18.600 18.606 18.612
1980-11-12 (317) 22:51:45 to 22:52:38

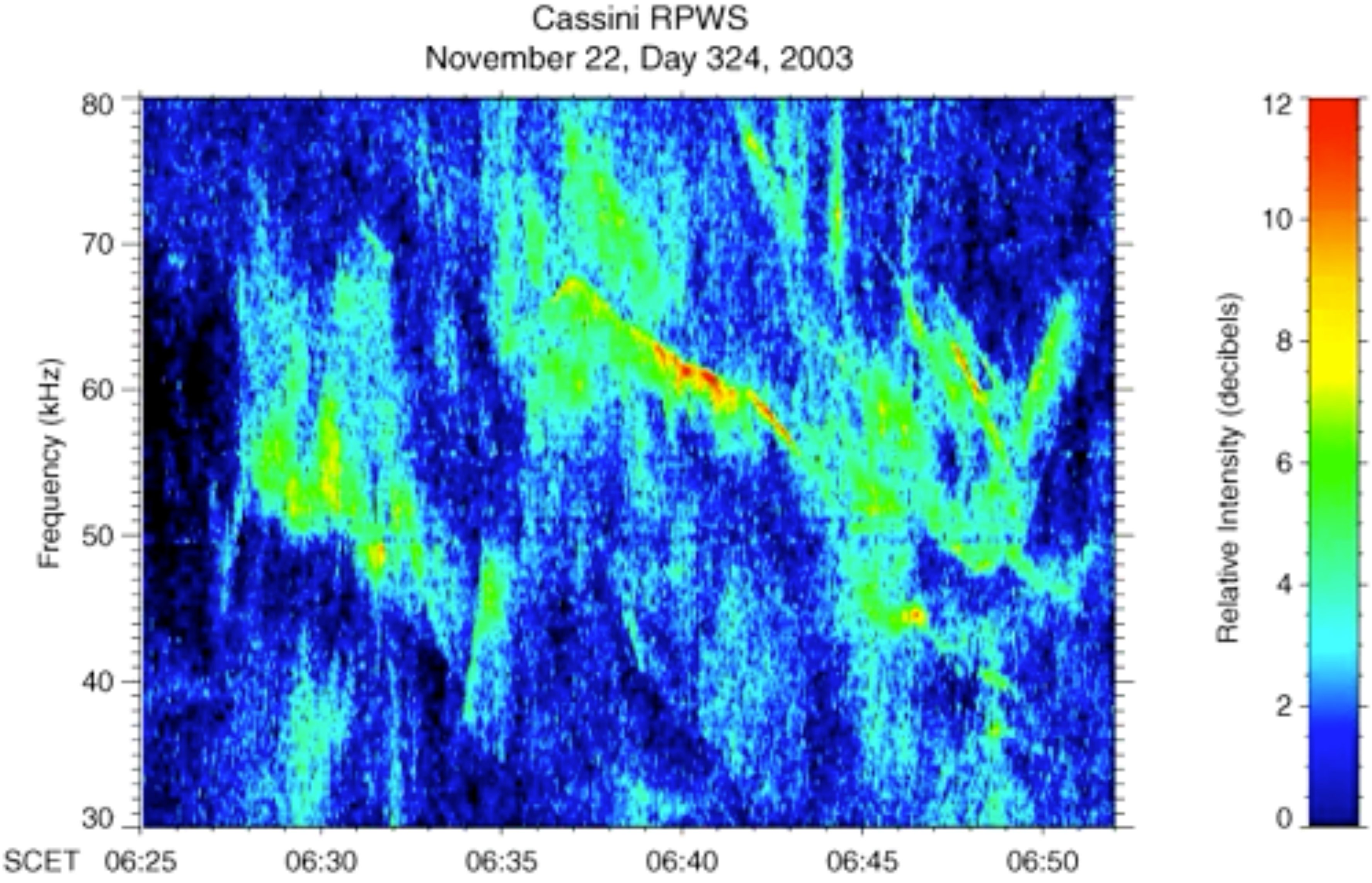
Cassini RPWS
November 22, Day 324, 2003
Frequency (kHz)
80
70
60
50
40
30
SCET
06:25
06:30
06:35
06:40
06:45
06:50
Relative Intensity (decibels)
12
10
8
6
4
2
0

Cassini INCA instrument

Cassini spacecraft

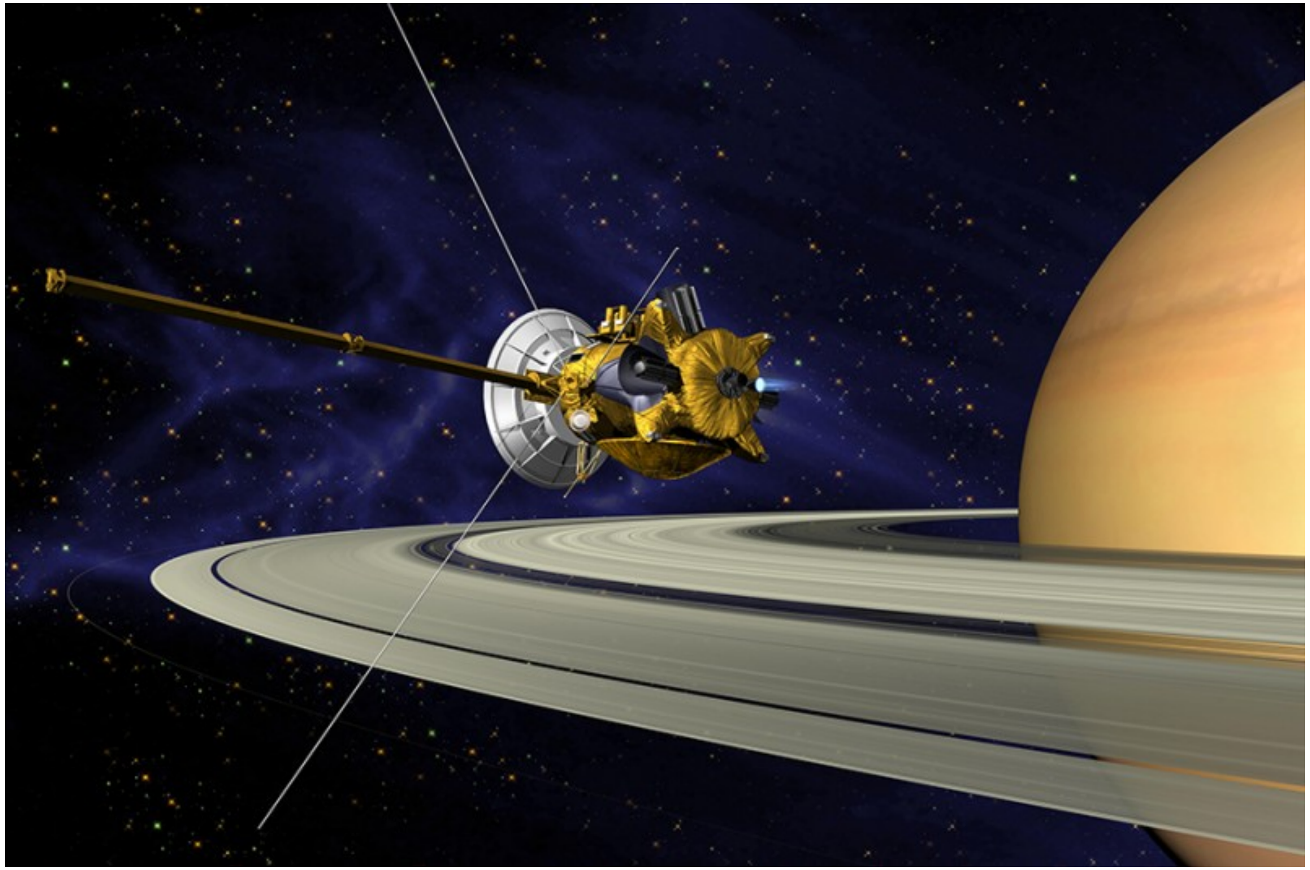

APL built the Ion and Neutral Camera (INCA) that imaged energetic neutral atoms (ENAs)

ENA Imaging

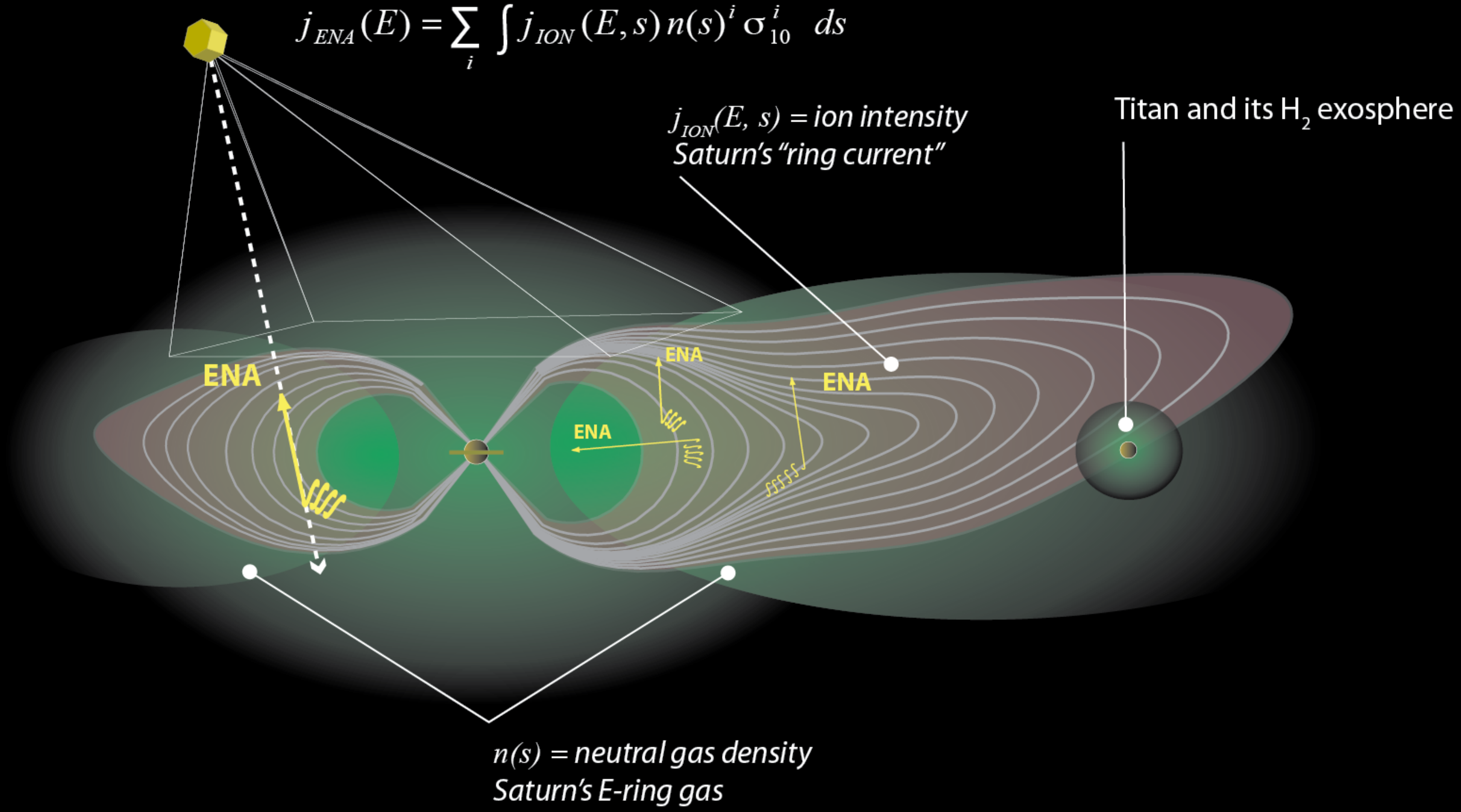

$$j_{ENA}(E) = \sum_i \int j_{ION}(E,s)\, n(s)^i\, \sigma_{10}^i \; ds$$
$j_{ION}(E, s)$ = ion intensity
Saturn's "ring current"
Titan and its H_2 exosphere
ENA
ENA
ENA
ENA
$n(s)$ = neutral gas density
Saturn's E-ring gas

Cassini INCA ENA injections

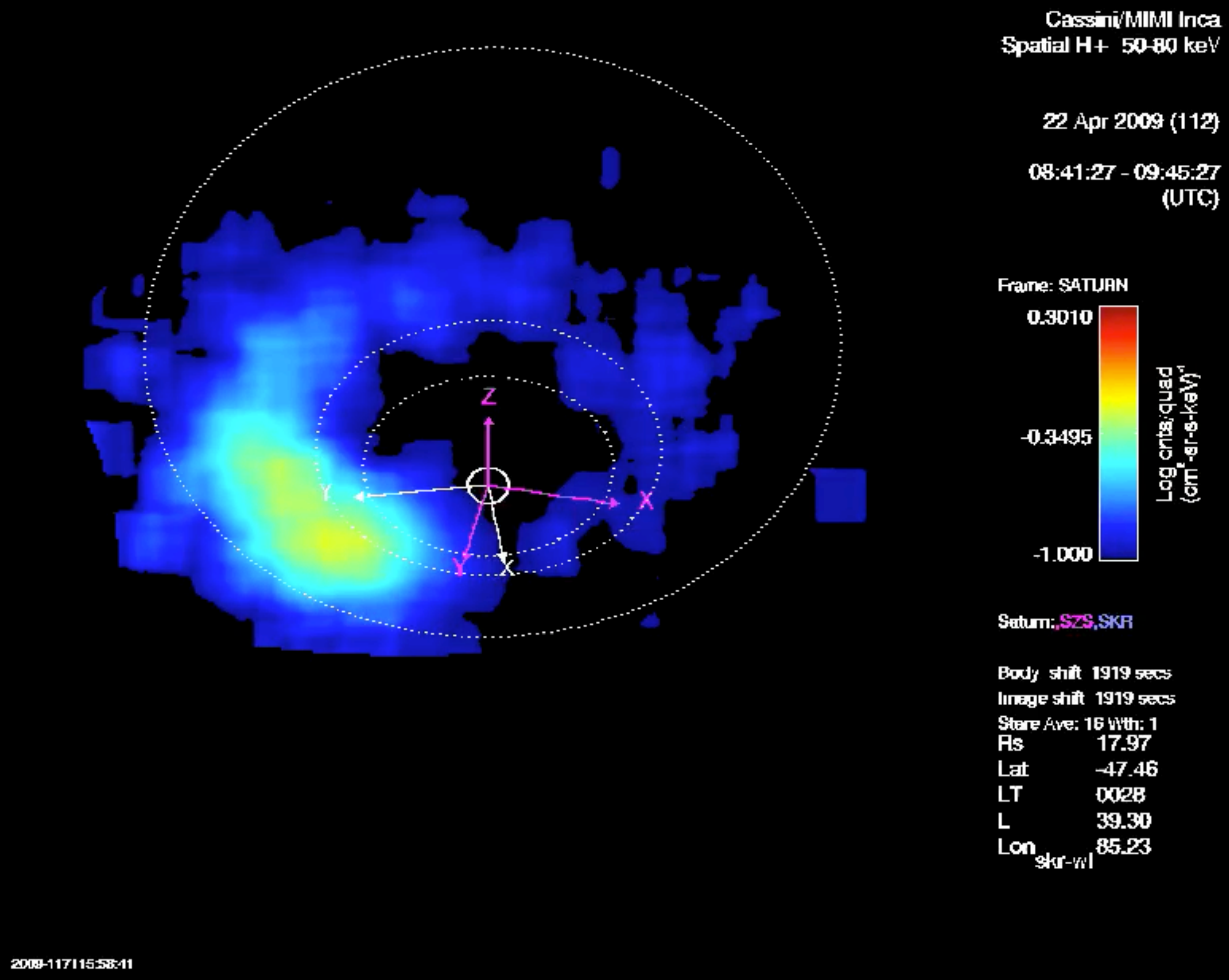

Particle injections and ENA emissions

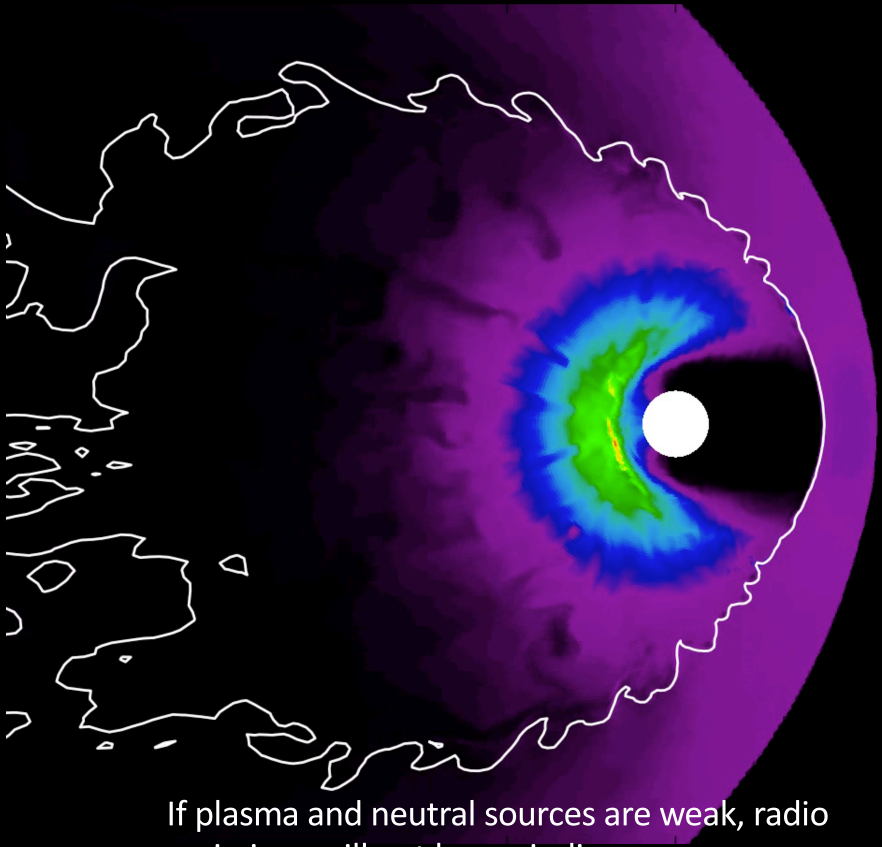

If plasma and neutral sources are weak, radio emissions will not be periodic.

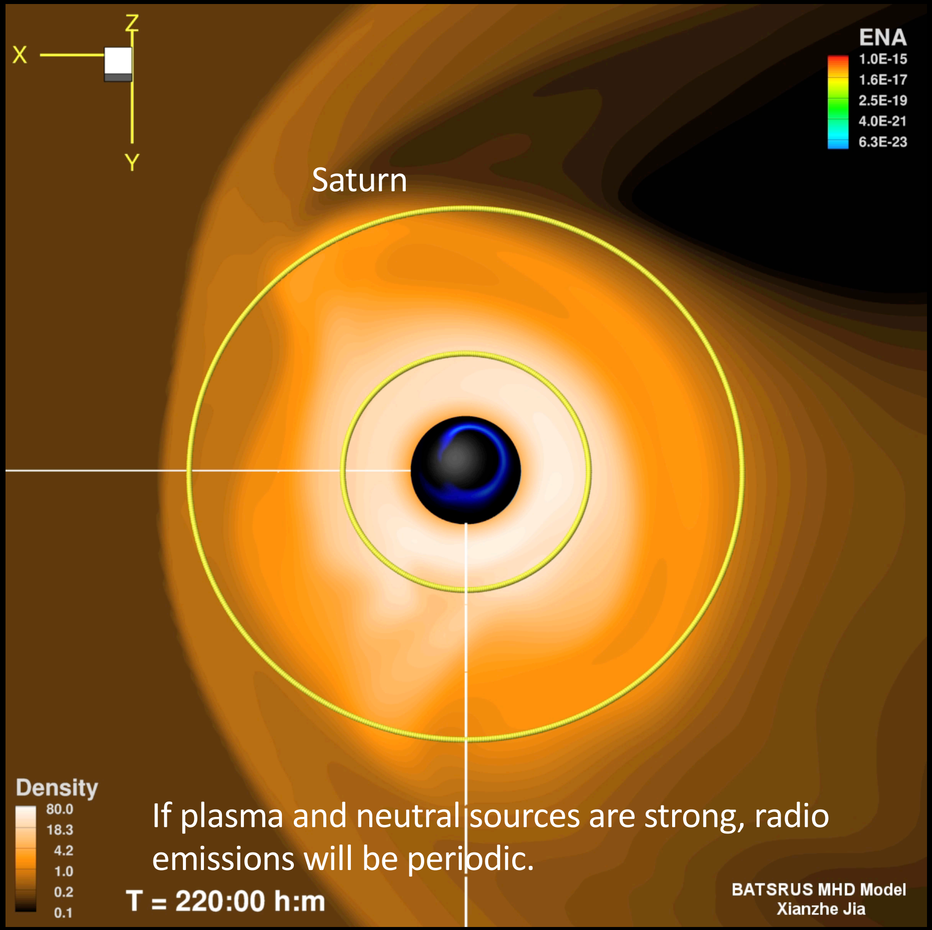

If plasma and neutral sources are strong, radio emissions will be periodic.

Type 1 and Type 2 ENA injections

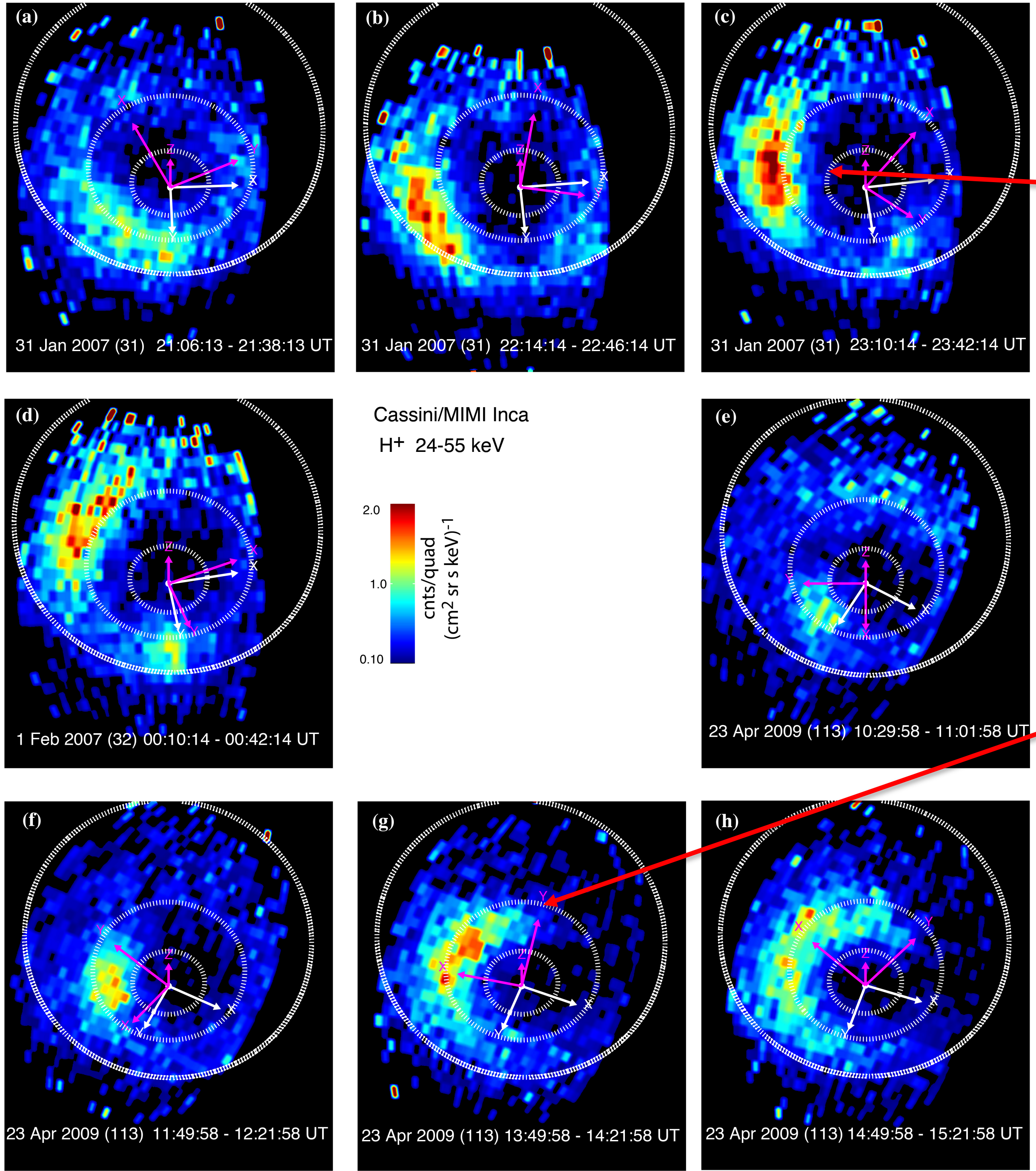

- Type 1
  - > 10–12 Rs
  - wide MLT
  - intense
  - reconnection/current sheet collapse
- Type 2
  - < 10–12 Rs
  - narrower in MLT
  - less intense
  - interchange instability

Events

event number	start time	end time	comment
1	2007 038 22:45:00	2007 039 17:25:00	
2	2007 042 02:00:00	2007 043 01:00:00	NB contaminated by SKR
3	2007 096 00:15:00	2007 096 17:22:00	
4	2008 025 14:30:00	2008 026 04:00:00	weak NB
5	2008 078 11:00:00	2008 079 21:00:00	weak NB
6	2009 012 12:45:00	2009 013 12:09:30	
7	2009 021 14:30:00	2009 023 13:45:00	
8	2009 065 06:00:00	2009 066 04:00:00	2 injections simultaneously
9	2009 112 22:20:00	2009 114 18:00:00	
10	2009 149 02:00:00	2009 149 16:00:00	
11	2009 151 00:00:00	2009 152 07:00:00	
12	2009 179 02:00:00	2009 179 17:51:00	
13	2009 181 00:00:00	2009 181 18:30:00	weak NB

- Search for type 2 injections that have RPWS wave data in ENA injection library 2007–2009
- 13 events found

ENA keogram 21-03 MLT

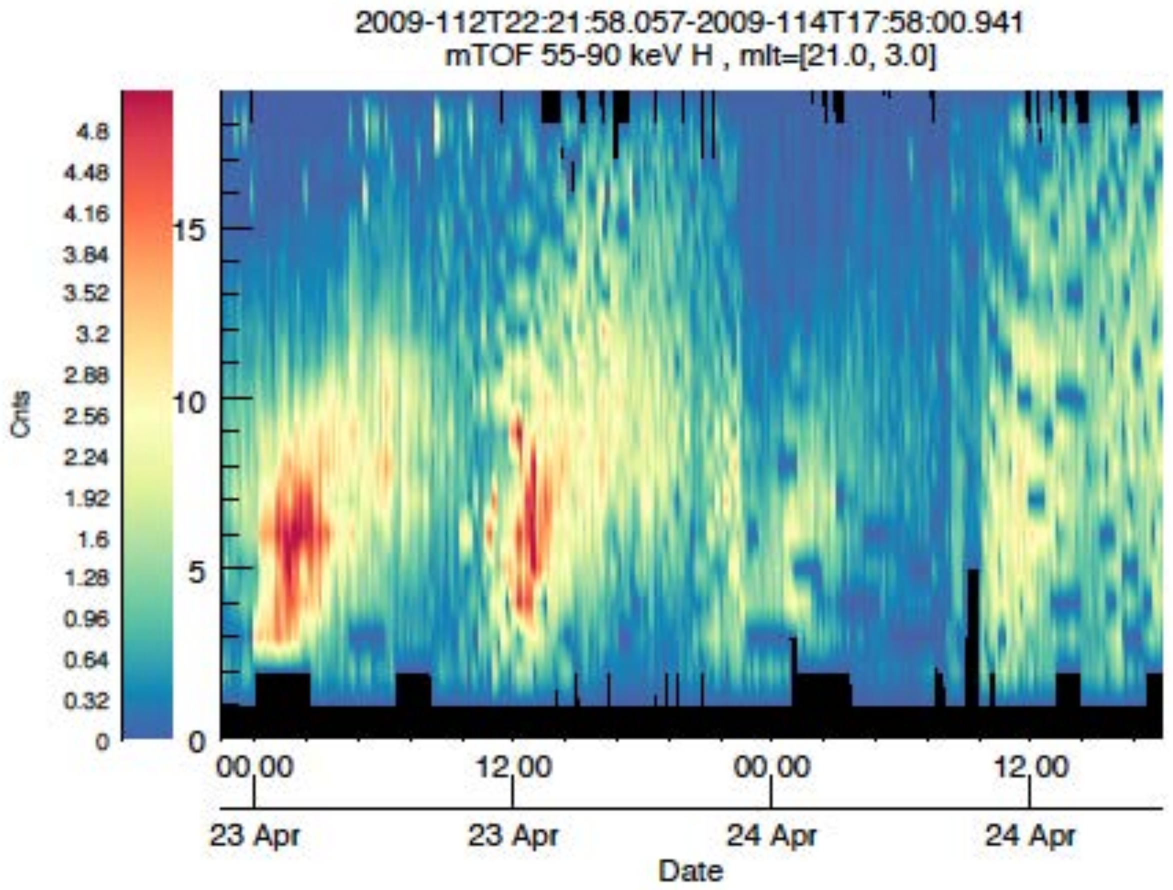

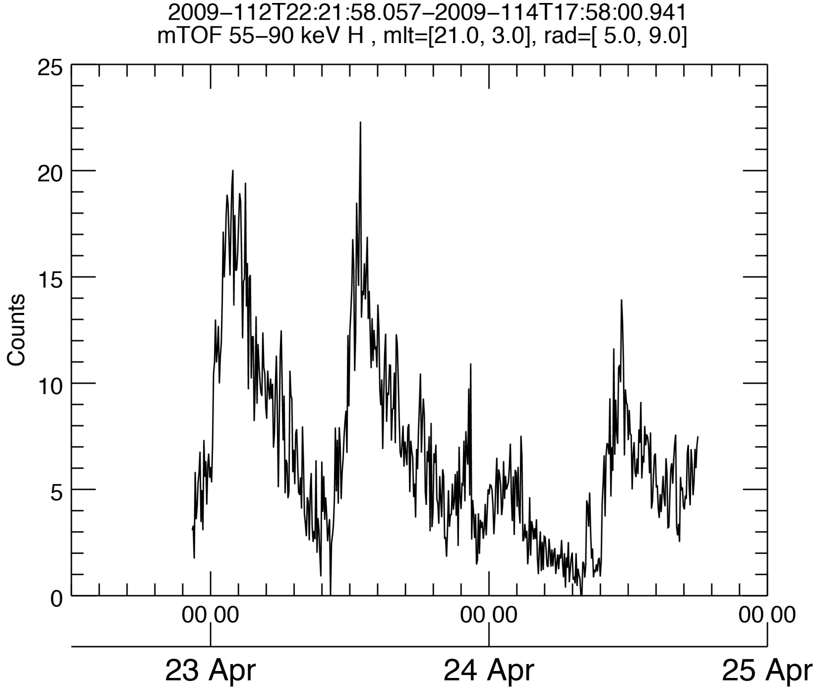

ENA time series

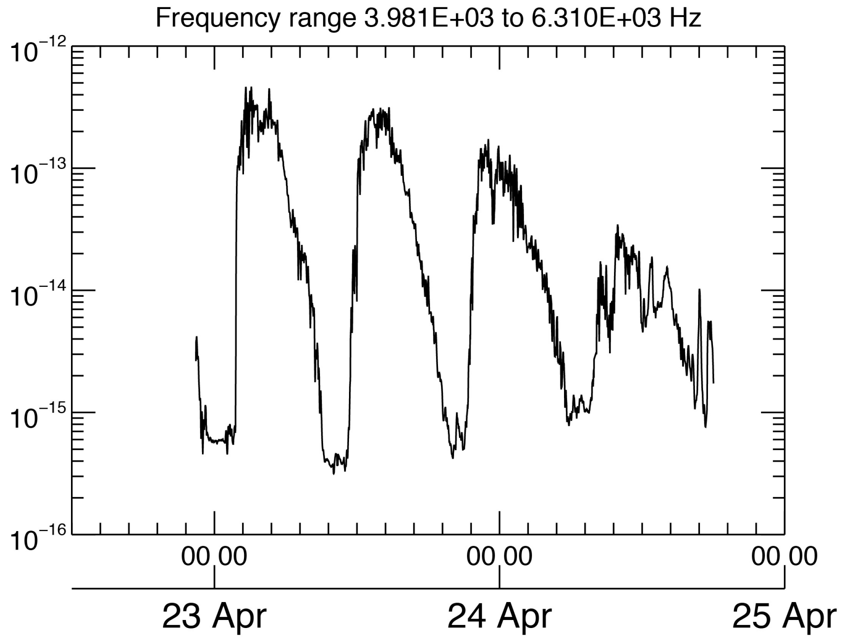

5 kHz NB time series

RPWS radio wave data

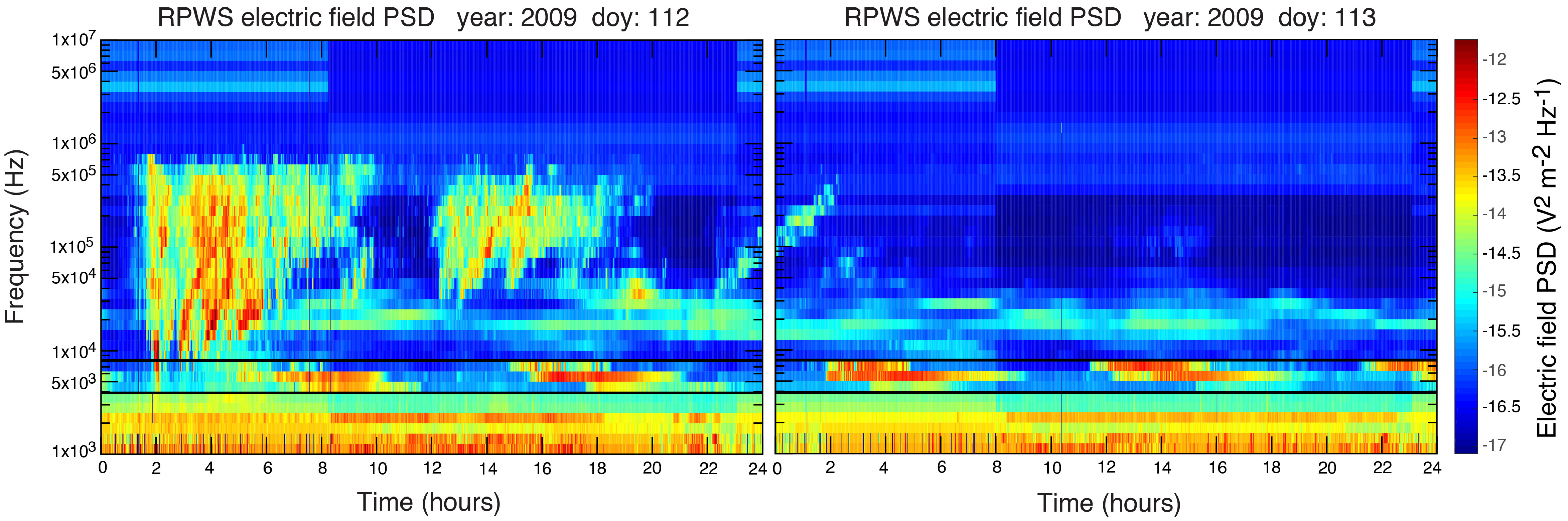

2009 Apr 22 event

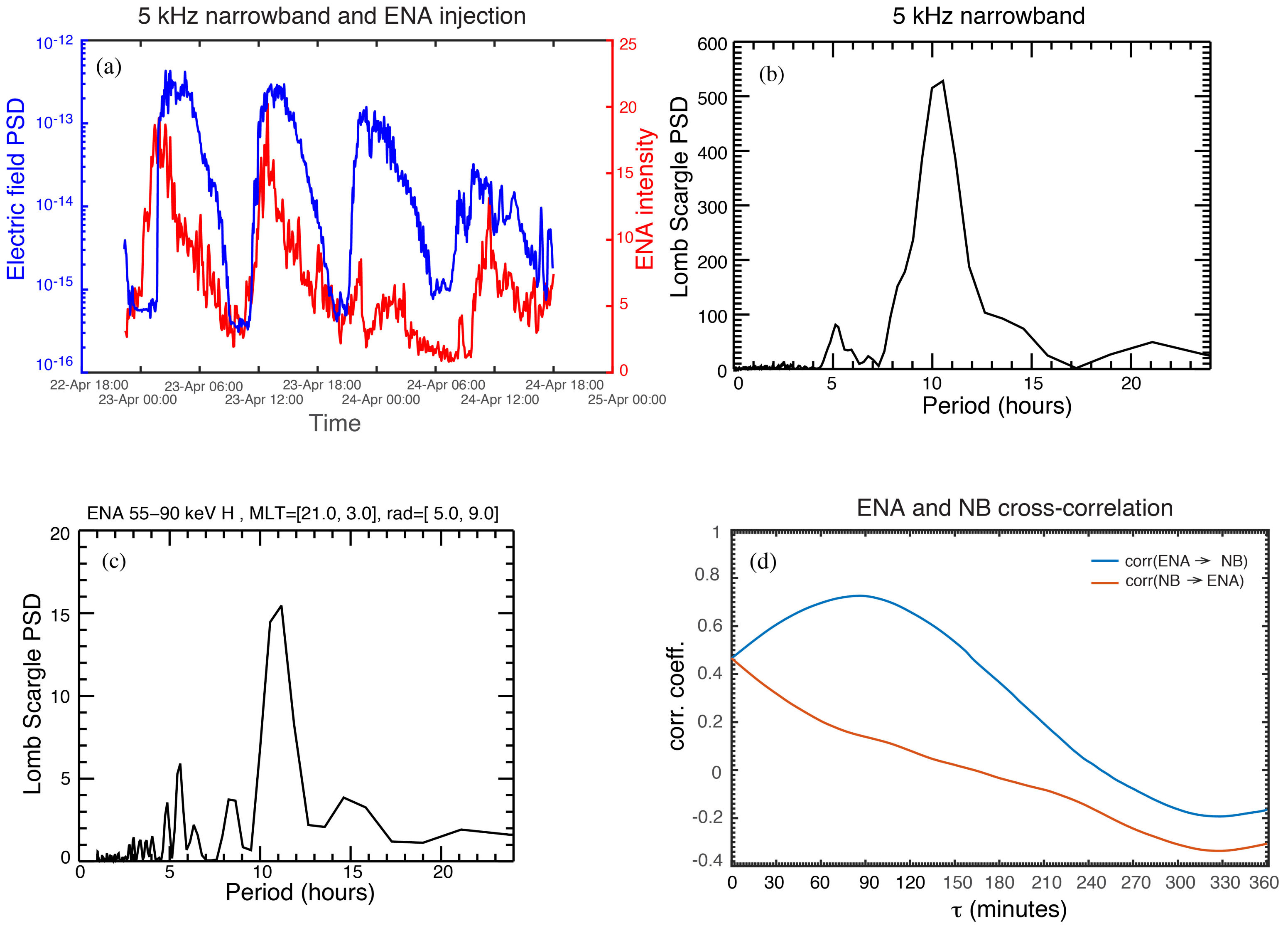

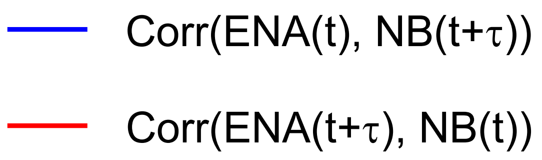

2009 Jan 21 event

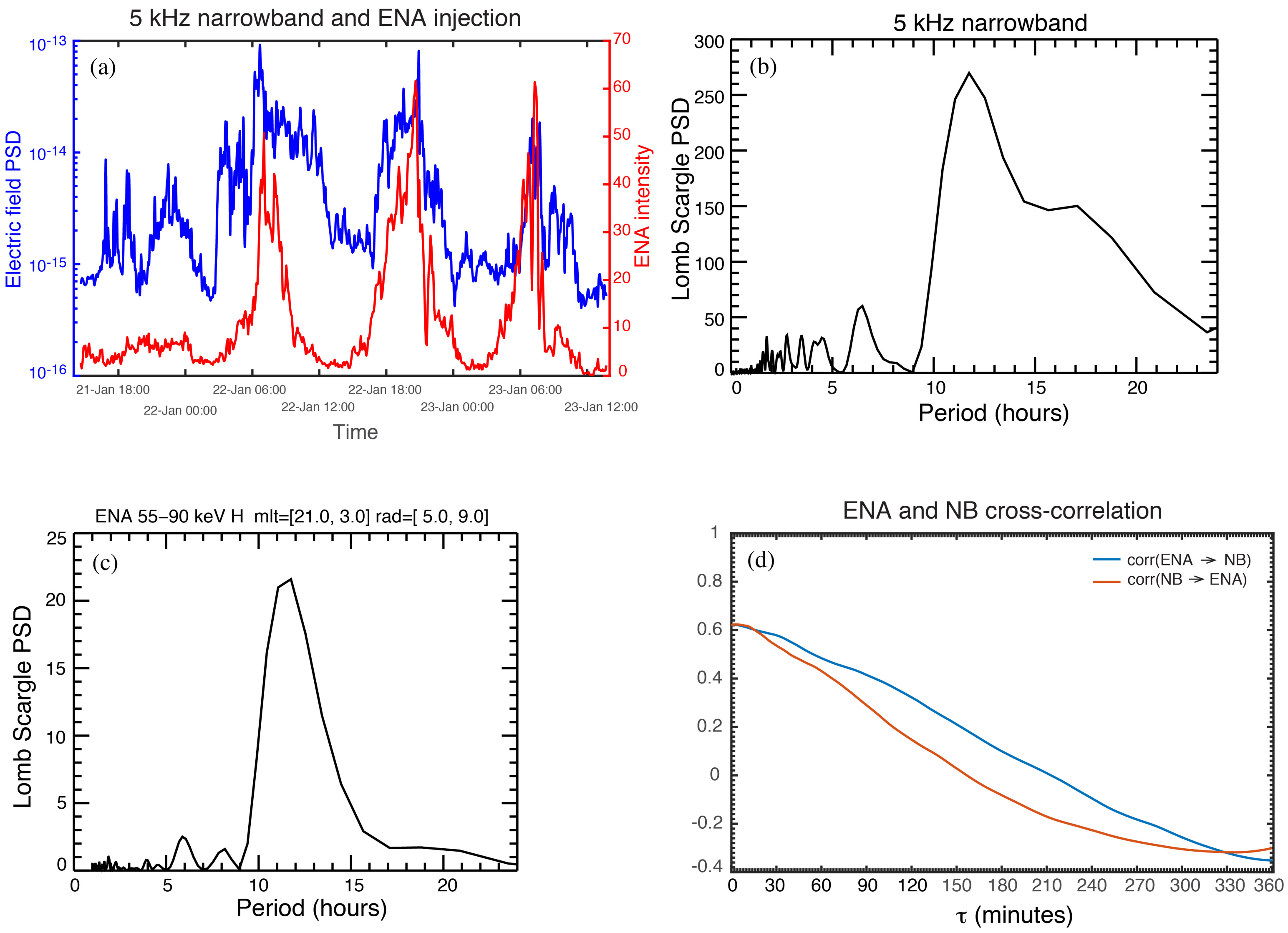

Corr(ENA(t), NB(t+τ))

Corr(ENA(t+τ), NB(t))

Correlation vs. mutual information

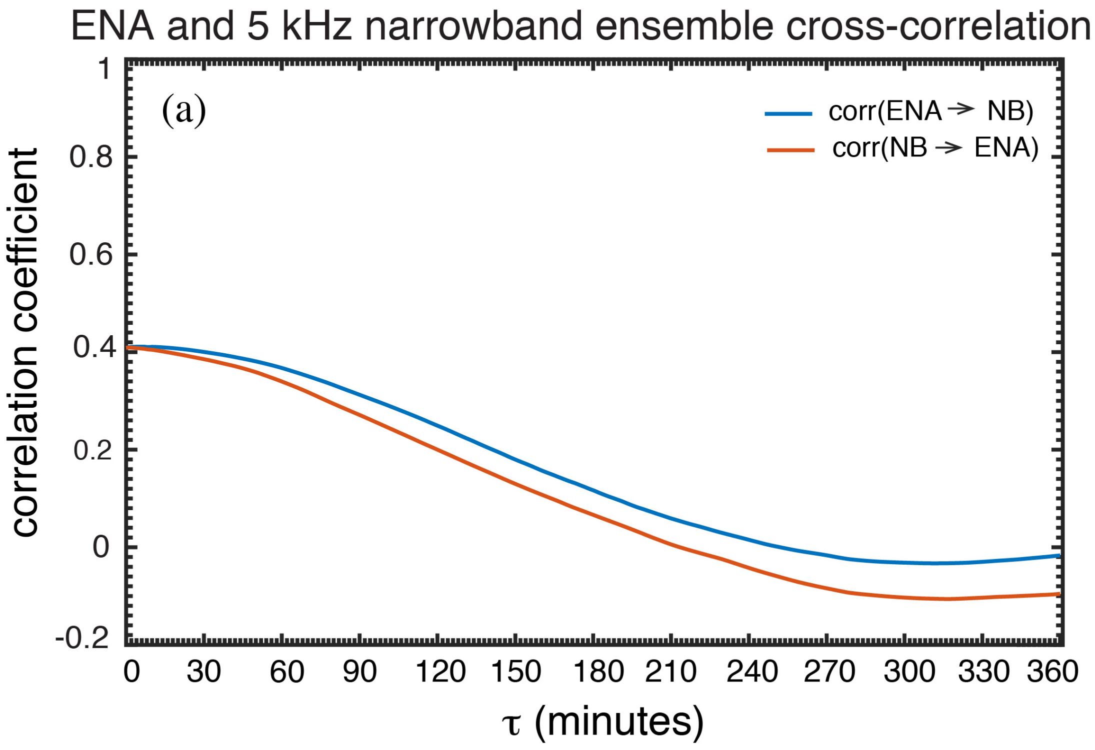

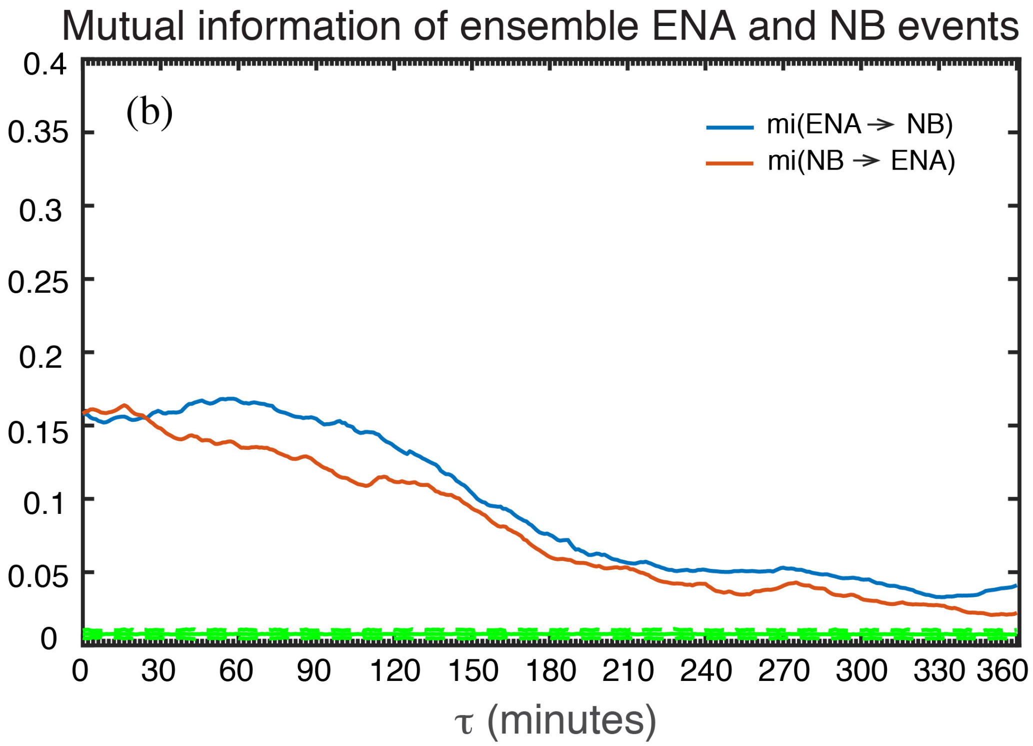

Corr(ENA(t), NB(t+τ))

Corr(ENA(t+τ), NB(t))

MI(ENA(t), NB(t+τ))

MI(ENA(t+τ), NB(t))

Particle injections and 5 kHz NB emissions

injection hot plasma → temperature anisotropy → upper hybrid waves → density gradient at Enceladus density torus → Z mode → O mode

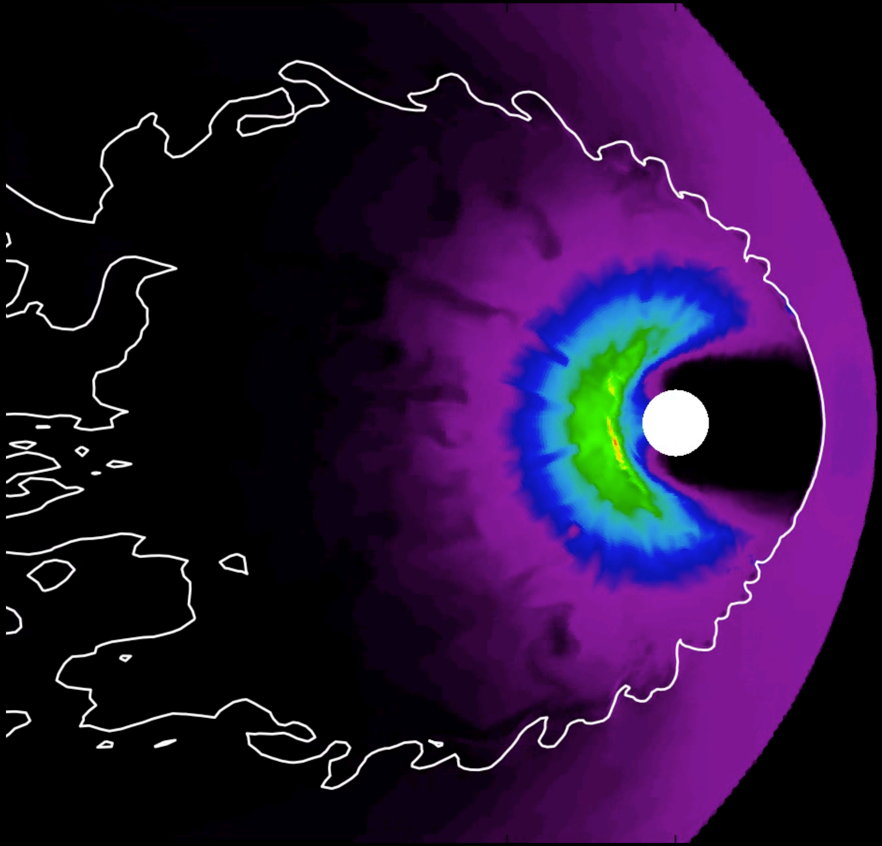

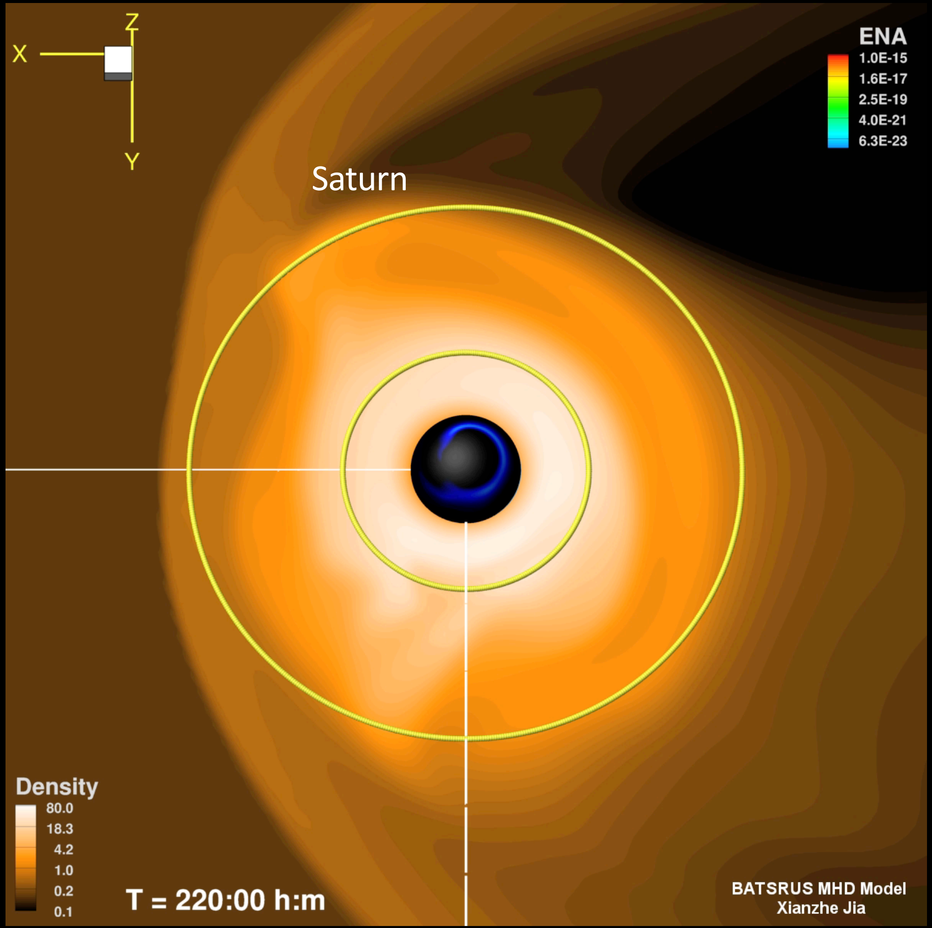

1.6 Jupiter

- Hectometric Auroral Radiation (HOM)
  - Related to “energetic events” large-scale plasma heating events in the magnetotail (Louarn+2007, Woch+1998, Krupp+1998)
- Narrowband Emissions (n-KOM)
  - Source within Io Torus (Reiner+1993)
- JUICE will provide extensive observations in 2030

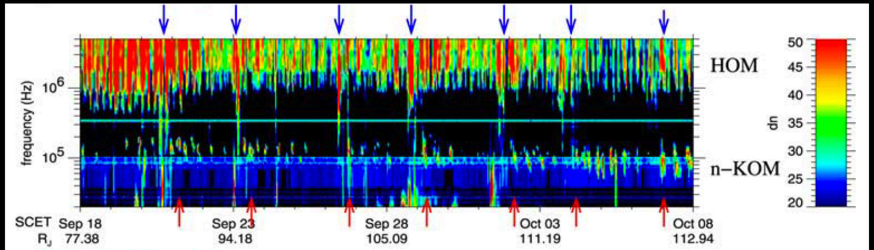

Louarn+2007

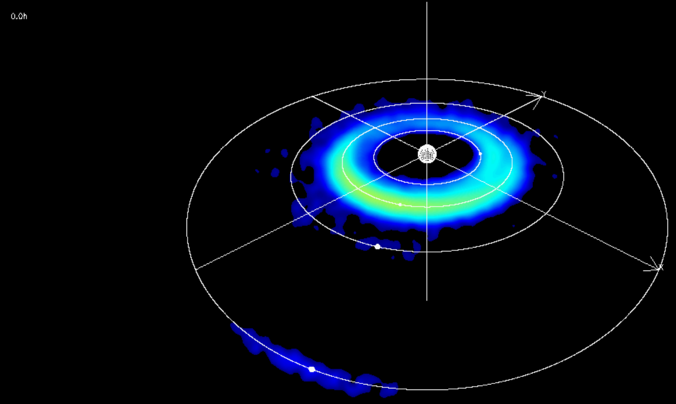

Simulated ENA image of magnetotail plasma heating at Jupiter. The ESA JUICE Mission to Jupiter will observe the system in ENAs and radio frequencies.

brown dwarfs
exoplanets

~ 10^{22} – 10^{24} stars in the visible universe

Conclusion

- The phase relation between type 2 ENA injection and 5 kHZ narrowband emission is not random.
  - The 5 kHz narrowband emission lags ENA injection by a 60–120 min.
- Injections bring hot plasma to the inner magnetosphere which increase T anisotropy, which drives upper hybrid waves, which in the presence of steep density gradient at the outer edge of Enceladus density torus, mode convert to Z mode and then to O mode (NB is an O mode).
- The variability of the NB response lag time may be attributed to the relative position of Cassini with the injections
- Implications to NB emissions at Jupiter
- Implications to brown dwarfs and exoplanets

Summary

- Apply information theory to
  - Solar wind – Radiation belt system
  - Solar dynamo
  - Radio waves at Saturn
- Information theory can be a useful tool for input-output problems
  - Establish linear and nonlinear correlations
  - Untangle the effects of input parameters that are correlated/anticorrelated with one another
- Information theory can be useful for modeling
  - Select and rank input parameters
  - Determine prediction horizons
  - Detect changes in the underlying dynamics of the systems